The Role of β-adrenergic Signalling and Natriuretic Peptide Receptors in Cardiac Myofibroblast Proliferation and Differentiation

by

Jessica E MacLean

Submitted in partial fulfilment of the requirements
for the degree of Master of Science

at

Dalhousie University

Halifax, Nova Scotia

April 2014

This thesis is dedicated to my family, friends, and everyone who has helped me along the way.

Table of Contents

List of Tables

List of Figures

Abstract

Uncontrolled proliferation of cardiac myofibroblasts (CMFs) leads to increased extracellular matrix (ECM) remodelling, resulting in cardiac fibrosis. Cardiac fibrosis occurs in many forms of heart disease and increases the risk of progression to heart failure. Treatment with atrial natriuretic peptide (ANP) was shown to decrease CMF proliferation. Chronic treatment of adult mice with a synthetic catecholamine, isoproterenol (ISO), induced cyclin dependent kinase 1 (CDK1) expression in non-cardiomyocytes. The aims of this study were to develop and characterize an *in vitro* cell culture system for adult mouse CMFs, and determine the effects of ISO treatment on the status of CDK1 expression, and proliferation and differentiation of CMFs. We also investigated the effect of genetic ablation of the atrial natriuretic peptide (ANP) receptor 1 (*Npr1*) on CMF proliferation and their sensitization to further treatment with catecholamines. Results showed that CDK1 expression, DNA synthesis and proliferation increase in adult mouse CMFs in response to ISO treatment. Analysis of cAMP levels in CMFs treated with ISO in the presence or absence of β adrenergic receptor (βAR) subtype specific blockers indicated that the β2AR response may be predominant in these cells. Consistent with this, the β2AR specific blocker ICI-118,551 and the non-selective βAR blocker carvedilol effectively blocked ISO induced CMF proliferation. ISO is also able to modulate pro-fibrotic gene expression program in CMFs by significantly increasing the transcription of genes such as collagen type 3 α1, connective tissue growth factor, α-smooth muscle actin and plasminogen activator inhibitor. Furthermore, pharmacological inhibition of CDK1 using RO-3306 effectively decreased CMF proliferation. In contrast, genetic ablation of both copies of *Npr1* significantly increased CMF proliferation compared to wild type CMFs. Unexpectedly, CMFs lacking either one or both copies of *Npr1* receptor revealed blunted mitogenic responses to ISO treatment compared to wild type cells. Collectively, these results suggest that CDK1 levels may be increased in response to the over-activated adrenergic signalling seen in heart failure. As such, it may present a possible drug target for inhibiting the expression of pro-fibrotic genes and CF proliferation. In addition, β2AR specific blockers, ANP and other synthetic *Npr1* ligands may be effective in amelioration of excessive cardiac fibrosis commonly seen with many cardiovascular diseases.

List of Abbreviations and Symbols Used

%	Percent
≈	Approximately
15d-PGJ_2	15-Deoxy-Δ12,15-Prostaglandin J2
αSMA	Alpha Smooth Muscle Actin
β	Beta
°	Degree
Δ	Delta
µL	Microliter
µm	Micrometer
µM	Micromolar
AB/AM	Antibiotic Antimycotic
AC	Adenylyl Cyclase
ACE	Angiotensin Converting Enzyme
AngII	Angiotensin II
ANOVA	Analysis of Variance
ANP	Atrial Natriuretic Peptide
AT1	Angiotensin II Receptor Type 1
βAR	β Adrenergic Receptor
BNP	B-type Natriuretic Peptide
BrdU	5-Bromo-2-Deoxyuridine
BSA	Bovine Serum Albumin
C	Celsius
Ca	Calcium
cAMP	Cyclic Adenosine Monophosphate

cGMP	Cyclic Guanosine Monophosphate
CT-1	Cardiotrophin-1
CDK	Cyclin Dependent Kinase
cDNA	Complementary DNA
CF	Cardiac Fibroblast
CITP	Collagen I Telopeptide
CMF	Cardiac Myofibroblast
CREB	cAMP Response Element Binding Protein
CTGF	Connective Tissue Growth Factor
CVF	Collagen Volume Fraction
CYC	Cyclin
dd	Double Distilled
DDR2	Discoidin Domain Receptor 2
DMEM	Dulbecco's Modified Eagle's Media
DMSO	Dimethyl Sulfoxide
DNA	Deoxyribonucleic Acid
dNTP	Deoxynucleoside Tri Phosphate
Epi	Epinephrine
ECL	Enhanced Chemiluminescence
ECM	Extracellular Matrix
ED-A	Extra Domain A
EEC	Endocardial Endothelial Cell
EGF	Epidermal Growth Factor
EGFR	Epidermal Growth Factor Receptor
ELISA	Enzyme-linked Immunosorbent Assay

EMT	Epithelial Mesenchymal Transition
EndMT	Endothelial Mesenchymal Transition
ERK	Extracellular Signal-Regulated Kinase
ET-1	Endothelin-1
FACS	Fluorescence Activated Cell Sorting
FAK	Focal Adhesion Kinase
FBS	Fetal Bovine Serum
FGF	Fibroblast Growth Factor
Fsp1	Fibroblast Specific Protein 1
g	Gram
G0	Gap 0
G1	Gap 1
G2	Gap 2
GAPDH	Glyceraldehyde 3-Phosphate Dehydrogenase
G_i	Inhibitory G Protein
G_s	Stimulatory G Protein
GPCR	G Protein Coupled Receptor
H_2O	Water
HMG-CoA	3-Hydroxy-3-Methylglutary Coenzyme A
HTRF	Heterogeneous Time Resolved Fluorescence
IBMX	3-Isobutyl-1-Methylxanthine
ICI	ICI-118,551
Ig	Immunoglobulin
IL-1β	Interleukin 1 Beta
IL-1R1	Interleukin-1 Receptor 1

IL-6	Interleukin 6
IP	Intraperitoneal
ISO	Isoproterenol
Jak/STAT	Janus-kinase Signal Transducer and Activator of the Transcription
JNK	c-Jun N-terminal Kinase
kDa	Kilo Dalton
L-TGF-β	Latent Form of TGF-β
M	Mitosis
mA	Milliamperes
MAPK	Mitogen-activated Protein Kinase
MEK	MAPK/ERK Kinase
MF20	Antibodies against Sarcomeric Myosin
MI	Myocardial Infarction
MMP	Matrix Metalloproteinase
MOI	Multiplicity of Infection
MRI	Magnetic Resonance Imaging
mRNA	messenger Ribonucleic Acid
mTBP	Mouse TATA Box Binding Protein
NADPH	Nicotinamide Adenine Dinucleotide Phosphate
NE	Norepinephrine
Nox4	NADPH Oxidase 4
NPR	Natriuretic Peptide Receptor
P	Passage
pRB	Retinoblastoma Protein
PAI1	Plasminogen Activator Inhibitor-1

PAR-1	Protease-Activated Receptor-1
PBS	Phosphate Buffered Saline
PCR	Polymerase Chain Reaction
PDGF	Platelet Derived Growth Factor
PI3K	Phosphoinositide 3-kinase
PIP	Carboxyterminal Propeptide of Collagen Type I
PKA	Protein Kinase A
PMSF	Phenylmethylsulphonyl Fluoride
PPAR	Peroxisome Proliferator Activated Proteins
QPCR	Real Time Quantitative Polymerase Chain Reaction
r-SMAD	Receptor-regulated SMAD
RAS	Renin-Angiotensin System
RNA	Ribonucleic Acid
RPM	Revolutions per Minute
ROS	Reactive Oxygen Species
S	Synthesis
SDS	Sodium Dodecyl Sulfate
SEM	Standard Error of Mean
SMAD	Small Mothers Against Decapentaplegic
$SP1_3$	Spingosine-1-Phosphate Receptor Subtype 3
TAK1	TGF-β Activated Kinase 1
TEMED	Tetramethylethylenediamine
Thr	Threonine
TIMP	Tissue Inhibitor of Matrix Metalloproteinase
TGF-β	Transforming Growth Factor Beta

Tyr	Tyrosine
V	Volts
vWF	von Willebrand Factor
X	Times

Acknowledgements

First I would like to thank my supervisor, Dr. Kishore Pasumarthi, for his guidance and the opportunity to work in his lab. I am beyond grateful for his patience, kindness, positivity and encouragement throughout my degree. I am sincerely appreciative of everything that I have learned from him and the time that he has dedicated to helping me with my research.

I would also like to thank all the members of the Pasumarthi lab, past and present, who have helped me countless times over the past few years, always answered my many questions, and been great friends along the way. I would especially like to acknowledge Sarita Chinni for her technical assistance.

Thank you to my advisory committee, Dr. Ryan Pelis and Dr. Melanie Kelly for their advice and support over the course of my degree. Thank you also to the staff of the Department of Pharmacology, Luisa Vaughan, Sandi Leaf and Cheryl Bailey for their help with administrative tasks and answering questions.

I would like to express my gratitude and appreciation to my thesis examiners, Dr. Jean Francois Legare and Dr. Chris Sinal for agreeing to review my thesis.

Finally, I would like to thank my family and friends for their support, encouragement and understanding throughout my degree.

Chapter 1: Introduction

1.1 Thesis Introduction

Cardiovascular diseases often result in cardiomyocyte death in response to injury, such as a myocardial infarction (MI). Because the adult mammalian heart has a limited capacity for cardiomyocyte regeneration (Laflamme & Murry, 2011) the dead cardiomyocytes are replaced by cardiac fibroblasts (CFs). This process results in the formation of a scar. While this scar tissue is initially intended to heal the wound, over the long term cardiac fibrosis may develop in response to pathological signalling. In chronic cases of cardiac disease, the scar impairs the ability of the heart to function effectively and can lead to heart failure and death. Much research has been focused upon the role of cardiomyocytes in heart disease, however, the role of non-myocyte cell types is also important for a more complete understanding of heart function in order to better treat cardiovascular diseases.

While cardiomyocytes occupy the largest volume of the heart, non-cardiomyocytes have been reported to represent approximately 70% of the total cell number (Baudino et al., 2006). In particular, CFs were found to represent 27% of the total cell number in the adult mouse heart as measured by fluorescence activated cell sorting (Banerjee et al., 2007). Given this, it is reasonable to assume that CFs must also have functions that are critical to maintaining cardiovascular homeostasis. Cardiac fibrosis results in part from uncontrolled proliferation of CFs. In order to effectively treat this condition, it is necessary to understand the factors involved in regulating CF

proliferation. By increasing our understanding it may be possible to modulate CF growth thereby improving the prognosis for patients with cardiovascular diseases.

1.2 Developmental Origins of Cardiac Fibroblasts

The mammalian heart develops principally from the mesodermal germ layer of the primitive embryo (Souders et al., 2009). CFs are first detected in mice at embryonic day 12.5 and are derived from mesenchymal cells originating in the embryonic proepicardium (Ieda et al., 2010; Krenning et al., 2010; Moorman & Christoffels, 2003; Norris et al., 2008). Proepicardial cells form the embryonic epicardium by migrating over the embryonic heart. The epicardium in turn gives rise to endothelial and smooth muscle cells of the coronary arteries and undergoes epithelial mesenchymal transition (EMT) to form epicardial derived cells. With the help of growth factors such as platelet derived growth factor (PDGF), fibroblast growth factor (FGF) and transforming growth factor (TGF) these cells differentiate into fibroblasts (Krenning et al., 2010; Moorman & Christoffels, 2003; Norris et al., 2008).

It has also been reported that mesangioblasts (mesodermal progenitor cells of vascular or mesodermal tissue) are able to give rise to CFs (Souders et al., 2009). Mesangioblasts are identifiable around embryonic day 10.5 in mice (Cossu & Bianco, 2003). They originate from hematopoietic stem cells of the bone marrow and studies have indicated they possess the ability to become pericytes and endothelial cells, both of which are able to differentiate into CFs (Souders et al., 2009). After birth, circulating fibroblast progenitor cells derived from adult bone marrow hematopoietic stem cells are

recruited into the ventricular myocardium and can differentiate into fibroblasts (Norris et al., 2008). The postnatal heart continues to undergo morphological changes. It must adapt to an increase in systolic pressure and does so by increasing the thickness and stiffness of the ventricular wall, which occurs due to an increase in the number of CFs. In addition, collagen fibrils form around myocytes in a network that allows signalling between cardiomyocytes and CFs. CFs and cell-extracellular matrix (ECM) contacts are also important in preparing the myocardial wall to withstand the increase in blood pressure occurring at birth (Norris et al., 2008).

1.3 The Extracellular Matrix and Cardiac Fibroblast Function

The ECM of the heart consists of the endomysium, perimysium and the epimysium. The endomysium is a network of type I and III collagen fibrils, wound around laminae, which are layers of cardiomyocytes between two and five cells thick (Baudino et al., 2006). The perimysium is in turn woven around these muscle fibres, grouping them into bundles. The epimysium is yet another layer of connective tissue surrounding the perimysium (Brown et al., 2005). CFs are interconnected in the endomysium, allowing them to contract the collagen network which can exert force on cardiomyocytes, and may affect myocardial relaxation (Kaneka et al., 1998).

The ECM of the heart is an important conductor of chemical, mechanical and electrical signals from the extracellular environment, the end results of which could be morphological, functional or phenotypical cellular changes (Kanekar et al., 1998). The ECM serves to connect and support cardiac cells. As mentioned above, the ECM consists

primarily of interstitial collagen, as well as laminin, fibronectin, elastin, proteoglycans, glycoproteins, cytokines, growth factors and proteases (Baudino et al., 2006; Porter & Turner, 2009).

CFs are responsible for maintaining the ECM through myocardial remodelling, which involves a balance between ECM synthesis and degradation. Their functions include the production of ECM components such as collagen types I and III, laminin and fibronectin. CFs also synthesize and secrete various growth factors and cytokines, and enzymes called matrix metalloproteinases (MMPs) that are responsible for degrading the ECM (Baudino et al., 2006; Goldsmith et al., 2004). In a healthy heart, levels of ECM remodelling are low. Under pathological circumstances, for example during hypertension or after MI, remodelling increases in response to stresses placed on the heart.

1.4 Cardiac Fibroblast Activation in Response to Injury

A complicated response ensues following myocardial injury. Hemostasis occurs first, followed by the arrival of both immune and inflammatory cells. Inflammatory cells in the area release reactive oxygen species (ROS), which contribute to the death of cardiomyocytes. Subsequently, the dead cardiomyocytes are removed and CFs proliferate to fill in the empty space in an attempt to maintain the structure of the myocardium (Brown et al. 2005). In response to injury, CFs become activated and differentiate into a more active cell type, called a cardiac myofibroblast (CMF).

CMFs have increased secretion, migration and proliferation capabilities compared to CFs. In response to injury, they migrate towards damaged tissue and are important for closing the wound and maintaining the structure of healing scars (Hinz et al., 2007; Brown et al., 2005). As discussed above, remodelling occurs in response to stresses placed on the heart during disease states. During heart disease, the signalling pathways controlling myocardial remodelling become dysregulated resulting in an imbalance between ECM degradation and synthesis. The early phase of pathological remodelling consists mainly of degradation while the later stages favour synthesis, leading to formation of a fibrotic scar which results in cardiac fibrosis. Fibrosis can be reparative, when CFs replace dead cardiomyocytes, or reactive, when ECM deposition occurs at sites distant from the point of myocardial injury and is not associated with cardiomyocyte death (Brown et al., 2005; Takeda & Manabe 2011).

CMFs modulate the balance between ECM synthesis and degradation by increasing collagen secretion and shifting the levels of MMPs and tissue inhibitors of MMPs (TIMPs) in an attempt to repair the damaged tissue and maintain myocardial structure (Tomasek et al. 2002; Hinz 2010).

1.5 Cardiac Fibroblast Markers

There is no single unique marker for CFs due to expression overlaps with other cell types, which is problematic when trying to distinguish them. The discoidin domain receptor 2 (DDR2) is expressed in CFs, but also detected in fibrocytes (bone marrow derived cells), smooth muscle cells, liver cells and endothelial cells (Goldsmith et al.,

2004; Krenning et al., 2010). Fibroblast specific protein 1 (Fsp1) is another CF marker but it is also expressed in cancer cells and smooth muscle cells (Krenning et al., 2010). CFs also have high levels of the intermediate filament vimentin, which again is also expressed in endothelial cells, smooth muscle cells, pericytes and myoepithelial cells (Krenning et al., 2010). CFs have also been found to express embryonic smooth muscle myosin heavy chain (SMemb) in the post-MI region of dog and rat hearts, as well as in culture (Frangogiannis et al., 2000; Shiojima et al., 1999). Expression of spingosine-1-phosphate receptor subtype 3 ($SP1_3$) was found to be higher in CFs, however it is also present in cardiomyocytes, aortic smooth muscle cells and endothelial cells in the vasculature (Means & Brown, 2009). Thymus cell antigen-1 (Thy-1) expression has also been found in areas of interstitial fibrosis and in cultured CFs and CMFs, however it is also expressed in leukocytes, endothelial cells and certain types of progenitor cells (Hudon-David et al., 2007; Krenning et al., 2010).

CMFs express the same markers as CFs, however, due to their increased contractile ability, CMFs can be distinguished from CFs by expression of the contractile protein α-smooth muscle actin (αSMA). As is the case with the makers listed above, αSMA is also expressed in smooth muscle cells, pericytes and myoepithelial cells (Krenning et al., 2010). Stimulation of fibroblasts from skin or fascia with TGF-β resulted in synthesis of the extra domain A (ED-A) splice variant of fibronectin, which binds focal adhesions allowing interaction between myofibroblasts and the ECM (Serini et al., 1998). ED-A fibronectin synthesis occurred prior to expression of αSMA, and the extent of phenoconversion in fibroblasts from different sources was shown to be proportional to the quantity of ED-A fibronectin produced.

Because they lack a unique marker, using a combination of marker proteins would seem to present the best option for identifying CFs. Marker proteins are presented in Table 1.1.

Table 1.1: Markers routinely used to identify cardiac fibroblast or cardiac myofibroblast cell types.

Marker	Other cell types	References
DDR2	Fibrocytes, smooth muscle, liver and endothelial cells	(Goldsmith et al., 2004; Krenning et al., 2010)
Fsp1	Cancer and smooth muscle cells	(Krenning et al., 2010)
Vimentin	Pericytes, endothelial, smooth muscle and myoepithelial cells	(Krenning et al., 2010)
SMemb	Dedifferentiated and embryonic smooth muscle cells	(Frangogiannis et al., 2000; Shiojima et al., 1999)
$SP1_3$	Cardiomyocytes, aortic smooth muscle and vascular endothelial cells	(Means & Brown, 2009)
Thy-1	Leukocytes, endothelial cells and some progenitor cells	(Hudon-David et al., 2007; Krenning et al., 2010)
αSMA (cardiac myofibroblast marker)	Pericytes, myoepithelial and smooth muscle cells	(Krenning et al., 2010)

1.6 Phenoconversion of Cardiac Fibroblasts to Myofibroblasts

Given the presence of the wide variety of signalling molecules in the myocardium following injury, it follows that the mechanisms governing the transition from fibroblast to myofibroblast are complex and therefore have not been fully elucidated. The two best known participants in this phenotypic transition are transforming growth factor β (TGF-β) and mechanical stress due to changes in the ECM (Hinz et al., 2007; Tomasek et al., 2002).

Angiotensin II (Ang II, a well-known pro-fibrotic factor) induces TGF-β mRNA and protein expression in cardiomyocytes and CFs through the angiotensin II type 1 (AT1) receptor (Campbell & Katwa, 1997; Lee et al., 1995). CFs are able to produce TGF-β, and TGF-β is able to induce expression of its own mRNA thereby increasing its secretion, allowing pro-fibrotic stimuli to continue after the injury response has subsided (Hattori et al., 1990; Tomasek et al., 2002). In addition, TGF-β can stimulate expression of the AT1 receptor via SMADS, the p38 mitogen-activated protein kinase (MAPK), c-Jun N-terminal kinase (JNK), and phosphoinositide 3-kinase (PI3K) pathways (Leask, 2010).

TGF-β is released in a latent form (L-TGF-β) that binds to the L-TGF-β binding factor in the ECM. In order to be activated and interact with receptors, L-TGF-β must be cleaved from the binding factor by proteases such as thrombospondin-1 (which is proposed to be induced by Ang II) or plasmin (Leask, 2007; Tomasek et al., 2002). When TGF-β binds to its type II receptor it complexes with the type I receptor. This complex subsequently phosphorylates receptor-regulated small mothers against

decapentaplegic (r-SMADs) 2 and 3 which are able to bind co-SMADs (SMAD 4), allowing translocation to the nucleus and activation of transcription of target genes (Leask, 2007; Santibañez et al., 2011). The CMF marker αSMA is a well-known target of downstream TGF-β signalling (Leask, 2010).

With respect to differentiation to a CMF phenotype, a variety of signalling molecules have been found to interact with TGF-β induced SMAD 2/3 activation. In human CFs, an increase in ROS derived from the NAD(P)H oxidase 4 (Nox4) was found to increase TGF-β-mediated activation of SMADs 2/3, and subsequently the expression of αSMA. In turn, TGF-β stimulation up-regulated expression of Nox4 mRNA. This indicates that Nox4 is involved in the differentiation of CFs to CMFs (Cucoranu et al., 2005). Mouse embryonic fibroblasts treated with the glycoprotein Wnt3a exhibited characteristics of myofibroblasts, including an increase in αSMA expression and an increased contractile ability. The ability of Wnt3a to induce differentiation to a myofibroblast phenotype was dependent on β-catenin, indicating a role for the canonical Wnt signalling pathway in fibroblast differentiation. Wnt3a-induced phenoconversion occurred via an up-regulation of TGF-β and subsequent SMAD2 signalling (Carthy et al., 2011).

TGF-β is also able to activate signalling pathways other than SMADs, and in the context of fibrosis has been reported to activate focal adhesion kinase (FAK) signalling cascades (Leask, 2007). A study conducted with embryonic mouse fibroblasts determined that FAK and JNK were both required for TGF-β-induced differentiation to myofibroblasts (S. Liu et al., 2007). In lung fibroblasts, TGF-β induction of ET-1 occurred via activation of JNK, and it was shown that ET-1 is able to act via the ET-A/B

receptors to initiate rac/Akt/PI3K signalling resulting in expression of αSMA (Leask, 2010). TGF-β activated kinase 1 (TAK1) was implicated downstream of FAK and was required for activation of JNK (Shi-wen et al., 2009). A summary of the signalling pathways involving TGF-β-stimulated phenoconversion of CFs to CMFs is presented in figure 1.1

Expression of the homeobox genes Meox1 and 2 was found to decrease during differentiation from CFs to CMFs.; this was due to increased levels of Zeb2, a transcriptional repressor of Meox2, during CMF differentiation. A negative regulator of TGF-β, Ski, was able to supress Zeb2, resulting in de-repression of Meox2, which reversed the CMF phenotype (Cunnington et al., 2011).

In addition to Ski, the hormone relaxin was also found to be capable of reversing the CF to CMF phenoconversion *in vitro* in rat, as indicated by a decrease in αSMA and collagen expression (Samuel et al., 2004). Also, increased intracellular cAMP has been shown to be capable of reversing phenoconversion. Treatment of adult rat CMFs with the AC activator forskolin, overexpression of AC, or pharmacological activation of PKA, all of which increase cAMP, resulted in a reduction of TGF-β stimulated αSMA expression and collagen synthesis (Swaney et al., 2005).

Mechanical tension has also been shown to regulate fibroblast to myofibroblast differentiation. In response to mechanical tension, production of Ang II occurs, which would allow subsequent activation of TGF-β signalling (Baudino et al., 2006). In neonatal rat CFs, application of mechanical tension was found to result in expression of αSMA. This was due to phosphorylation of ERK, implicating activation of the MAPK

signalling cascade in this process (Wang et al., 2003). In addition, an *in vivo* study on rat granulation tissue (connective tissue produced as part of the healing process) demonstrated that αSMA expression was positively correlated with the amount of mechanical tension the tissue was subjected to. Mechanical tension was also able to increase expression of ED-A fibronectin *in vivo* (Hinz et al., 2001). When biopsies from human burn scars were subjected to mechanical tension an increase in dermal myofibroblast number was observed, as indicated by expression of αSMA (Junker et al., 2008).

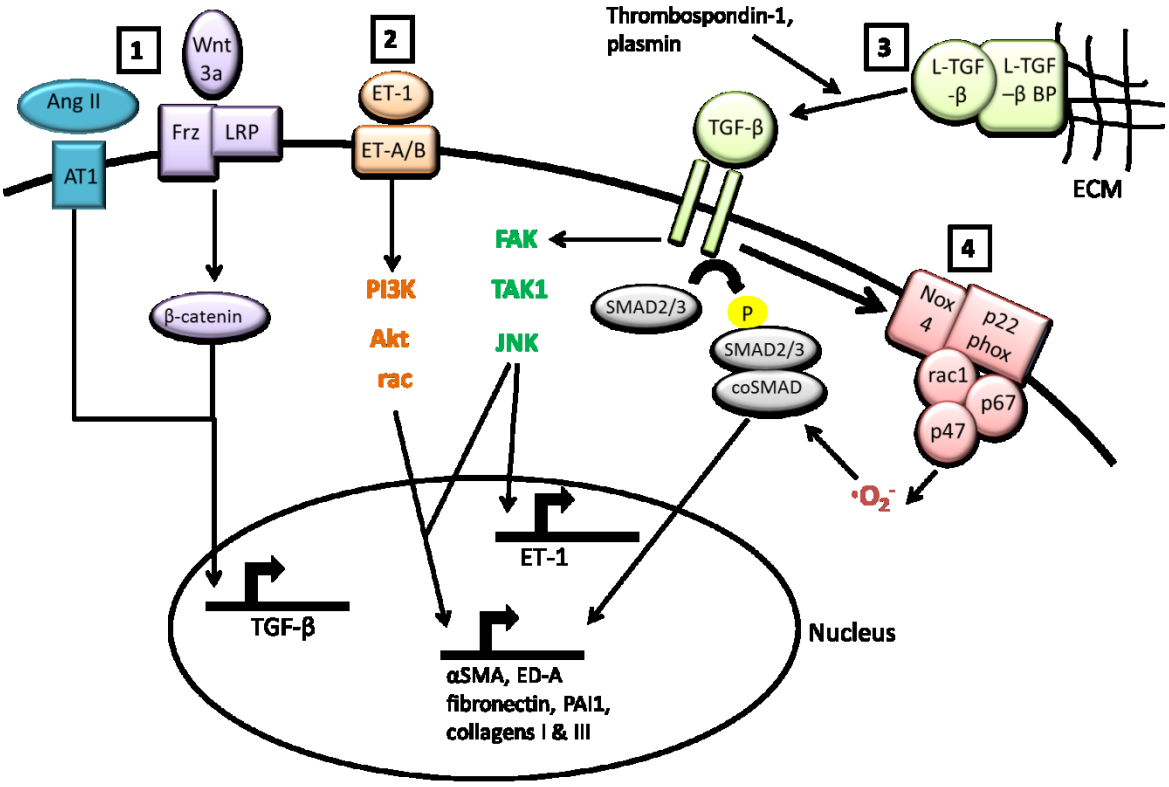

Figure 1.1 Summary of pathways involving TGF-β-mediated regulation of cardiac fibroblast phenoconversion. 1) Ang II induces expression of TGF-β via the AT1 receptor in CFs. Wnt3a activates the frizzled (Frz) receptor, resulting in activation of the co-receptor low density lipoprotein related receptor-related protein (LRP). Wnt3a activation of TGF-β expression in this case is dependent on the downstream actions of β-catenin. **2)** ET-1 acts via the ET A/B receptors to activate a PI3K-Akt-rac pathway resulting in expression of αSMA. **3)** TGF-β is released as latent-TGF-β (L-TGF-β) and bound to L-TGF-β binding protein (L-TGF-β BP) in the ECM. L-TGF-β is cleaved and activated by proteases like thrombospondin-1 and plasmin. TGF-β binds to its type II receptor, which complexes with the type I receptor resulting in phosphorylation of SMADs. Activated SMADs then bind to a co-SMAD allowing translocation to the nucleus and activation of TGF-β target genes like αSMA, ED-A fibronectin, PAI1, and collagens type I and II. Aside from signalling via SMADs, TGF-β can also activate a FAK-TAK1-JNK signalling cascade in order to stimulate target genes. **4)** TGF-β increases Nox4 levels, and reactive oxygen species produced from Nox4 and its associated proteins increase TGF-β-mediated activation of SMADs. Figure adapted from Leask (2007), Liu et al. (2007), and Rocic and Lucchesi (2005).

1.7 Alternative Sources of Fibroblasts During Injury Response

In addition to the traditional view of resident CFs as the source of CMFs, reviewed above, studies have shown that they can be generated from other sources of cells activated in response to myocardial injury. In a model of cardiac fibrosis produced by aortic banding, TGF-β was implicated in inducing endothelial mesenchymal transition (endMT), causing endothelial cells to undergo endMT and become CFs (Zeisberg et al., 2007). During embryonic development, TGF-β is also involved in the differentiation of endothelial cells through endMT into cells that will form the heart valves and septa, and endMT is known to occur during fibrosis of other tissues (Goumans et al., 2008). During endMT, loss of endothelial markers such as vascular endothelial cadherin and CD31 occurs and cells start to express mesenchymal (and fibroblast) markers such as αSMA, vimentin, and Fsp-1 (Goumans et al., 2008). In addition to TGF-β, ET-1 was also implicated in inducing endMT during diabetes mellitus-induced cardiac fibrosis (Widyantoro et al., 2010).

Pericytes from the vasculature of the heart may also contribute as they were demonstrated to have an ability to secrete collagen in models of dermal scarring and were shown to be present in fibrotic kidneys (Krenning et al. 2010). In an Ang II mouse model of cardiac fibrosis, investigation of infiltrating cells in the myocardium revealed that a population of cells expressing αSMA also expressed hematopoietic progenitor cell (CD133) and mesenchymal (SMA) markers. This indicates a potential for cells of a hematopoietic origin, termed fibrocytes, to differentiate into CMFs (Sopel et al., 2011). Other studies have demonstrated the contribution of hematopoietic derived progenitor cells to the CMF population in models of cardiac fibrosis, however these cells do not

persist in high numbers in the fibrotic scar after 14 days (Kania et al., 2009; van Amerongen et al., 2008). Monocytes present another possible pool of cells able to differentiate into myofibroblasts in response to injury. Myofibroblast-like cells were found to express markers of both monocytes and myofibroblasts, and in addition to this when recruitment of monocytes was inhibited both remodelling and the number of CFs present following MI was decreased (Haudek et al., 2006; van Amerongen et al., 2007).

1.8 Gene Expression Changes in Response to Cardiac Fibrosis

Increased deposition of collagen is a hallmark of cardiac fibrosis. Collagen is synthesized by CFs as a precursor (procollagen) which is then secreted and cleaved by proteinases into its mature form (Díez et al., 2001). Following MI, mRNA expression of collagen types I and III increases in the infarct border zone and scar regions, and collagen protein is increased throughout the heart (Dean et al., 2005, Sun et al., 2000).

In addition to the up-regulation of collagen, increased levels of connective tissue growth factor (CTGF) are also associated with the fibrotic response. TGF-β is able to activate a response element in the CTGF promoter (Leask, 2007), and CTGF mRNA and protein expression is up-regulated in failing compared with normal control rat hearts. The increase in mRNA was localized to cells resembling fibroblasts located in the scar tissue of the myocardium (Ahmed et al., 2004). Rat CFs treated *in vitro* with Ang II had increased levels of CTGF mRNA and protein, and *in vivo* treatment with the AT1 receptor blocker Losartan was able to decrease CTGF mRNA levels in the heart, indicating that Ang II is involved in stimulating expression of CTGF (Ahmed et al.,

2004). In addition, mice treated with Ang II i*n vivo* had increased CTGF mRNA and protein levels. This increase occurred via activation of SMAD-2, implicating TGF-β signalling upstream of this. Treatment of fibrocytes (reviewed above in section 1.7) with CTGF increased their proliferation and the expression of collagen type 1 α1, indicating that CTGF is able to cause differentiation of fibrocytes to a more CMF-like cell type (Rosin et al., 2013).

Increased CTGF expression has been found concurrently with increased expression of fibronectin in human CFs (Chen et al. 2000). In a rat model of cardiac fibrosis, cells in the scar region had increased fibronectin mRNA expression. Losartan was able to decrease expression of fibronectin, indicating that Ang II signalling is likely involved in inducing fibronectin in the injured heart (Crawford et al. 1994).

Plasminogen activator inhibitor-1 (PAI1) is another protein associated with fibrosis. PAI1 prevents MMP activation and also activation of plasmin (which degrades fibronectin and collagens) from its precursor plasminogen (Takeshita et al., 2004). Interfering with these enzymes decreases ECM degradation. In a study in mice 4 weeks post-MI, PAI1 mRNA was increased in the infarct border, and PAI1 null mice developed less extensive cardiac fibrosis compared with wild type (Takeshita et al., 2004). In contrast, another study using aged PAI1 null mice found that they had accumulation of macrophages and an increase in cardiac fibrosis compared with control, suggesting that a lack of PAI1 causes cardiac fibrosis, indicating it may be anti-fibrotic under certain circumstances (Moriwaki et al., 2004). Moriwaki et al. (2004) explain this conflict by stating that a lack of PAI1 could have different effects in injured versus non-injured hearts. They reason that PAI1 could be pro-fibrotic in the case of myocardial injury yet

have anti-fibrotic effects in a non-injured heart. In mice subjected to a combination of Ang II infusion and a high salt diet, pharmacological inhibition of PAI1 and PAI1 null mice exhibited decreased Ang II-induced aortic remodelling and increased cardiac fibrosis. In explanation of these findings, Weisberg et al. (2005) suggest that the decrease in aortic remodelling may occur due to PAI1 inhibition resulting in increased plasmin, which degrades fibronectin and collagen, and activates MMPs. They propose that in the heart PAI1 inhibition of uPA or plasmin may prevent activation or release of growth factors leading to decreased inflammation or infiltration of cells, resulting in increased fibrosis. However, PAI1 has been reported to serve as a pro-fibrotic factor in other tissues such as lung, liver and kidney (Ghosh & Vaughan, 2012). Thus, while it is evident that changes in PAI1 occur in cardiac fibrosis and that it is a fibrotic mediator, the exact role that it plays during this process remains to be investigated.

1.9 Regulation of Cardiac Fibroblast Proliferation

Due to the important role of CF proliferation in initiating cardiac fibrosis, much work has been done to characterize the response of these cells to neurohumoral and cytokine factors that circulate in the heart following injury. Following is a review of some of the most well-known regulators.

1.9.1 Angiotensin II

The renin-angiotensin system (RAS) helps to maintain homeostasis of the kidneys and the cardiovascular system. Activation of RAS also occurs during cardiac fibrosis,

and angiotensin II (Ang II) is known to promote fibrosis. Ang II plays many roles in cardiac fibrosis, including stimulating secretion of collagen, fibronectin, laminin, and expression of TGF-β, ET-1 and interleukin 6 (IL-6). It has also been shown to regulate CF proliferation. In the heart, Ang II is produced by CFs, CMFs and inflammatory cells located at the site of myocardial injury (Chen & Frangogiannis, 2013). In CFs, binding of Ang II to the AT1 receptor was able to activate the ERK, Src tyrosine kinase, Shc, Grb2, Ras and Raf-1 kinase pathway (Zou et al., 1998). In neonatal rat non-myocyte cultures, Ang II acted through the AT1 receptor to increase DNA and protein synthesis as well as cell number (Sadoshima & Izumo, 1993). In human CFs, Ang II was also found to increase DNA synthesis, activate MAPK activity and increase proliferation (Kawano et al., 2000).

1.9.2 Endothelin-1

ET-1 levels are increased in the myocardium of patients with heart failure (Motte et al., 2006). Both ET-A and ET-B type receptors are expressed in CFs, however the effects of ET-1 on CF proliferation have differed in various studies. In human CMFs, ET-1 stimulated collagen synthesis, but was not able to stimulate proliferation and was in fact shown to decrease DNA synthesis (Hafizi et al., 2004; Turner et al., 2004). In neonatal and adult rat CFs, ET-1 was able to stimulate CF proliferation via the ET-A receptor (Piacentini et al., 2000; Ogata et al., 2004; Kuruvilla et al., 2007). Kuruvilla et al. (2007) identified ET-1 as the factor stimulating neonatal rat CF proliferation in media conditioned by porcine endocardial endothelial cells (EEC). Inhibition of PKC and MAPK/ERK kinase (MEK) were both able to prevent the increase in CF proliferation due to EEC-conditioned media, implicating PKC and MAPK signalling in ET-1 induced CF

proliferation. In support of these findings, inhibition of PKC abrogated ET-1 stimulated neonatal rat CF proliferation, and treatment with ET-1 increased phosphorylation of ERK1/2 and cAMP response element binding protein (CREB; Piacentini et al., 2000).

1.9.3 Cytokines

Proinflammatory cytokines play an important role in the pathophysiology of heart disease. Levels of interleukin 1β (IL-1β), IL-6 and tumor necrosis factor-α are increased following MI. Cytokines are known to modulate CF migration, and have also been found to affect proliferation. Treatment of CFs with IL-1β was able to decrease DNA synthesis and prevent proliferation *in vitro* via the IL-1 receptor 1 (IL-1R1) subtype (Palmer et al., 1995). Conversely, an *in vivo* study revealed a decreased fibrotic response post-MI in IL-1R1 knockout mice, as well as a decrease in pathological cardiac remodelling (Bujak et al., 2008). These studies indicate that the role of IL-1 in CFs warrants further investigation.

Cardiotrophin-1 (CT-1) is a member of the IL-6 family of cytokines. It is a known hypertrophic factor in CMs and is increased in the serum of patients with heart disease (Freed et al., 2005). Treating adult rat CFs with CT-1 activated protein synthesis and proliferation. The Janus-kinase signal transducer and activator of the transcription (Jak/STAT), ERK1/2 and Akt pathways, which are known to be involved in promoting proliferation, were activated by CT-1 induced phosphorylation of glycoprotein 130, and the CT-1 mediated increases in DNA and protein synthesis were dependent on activation of these proliferative pathways (Freed, Borowiec et al., 2003; Freed, Moon, et al., 2003). An *in vitro* study done with adult canine CFs demonstrated that CT-1 was able to

stimulate DNA synthesis in CFs through activation of glycoprotein 130/leukemia inhibitory factor receptor (known to be involved in cell proliferation) and ET receptor activation (Tsuruda et al., 2002). The increase in protein synthesis and CF proliferation was attenuated by an antibody that blocked gp130 as well as an ET-1 receptor antagonist (Freed et al., 2005).

1.9.4 Peroxisome Proliferator Activated Proteins

Peroxisome proliferator activated proteins (PPARs) are nuclear receptors that act as transcription factors and have been implicated in decreasing CF proliferation. The PPARδ isoform was found to be the most numerous in CFs and CMFs. PPARδ activation reduced CF and CMF proliferation and treatment with a PPARδ ligand (GW501516) was able to decrease expression of αSMA, indicating decreased differentiation to the CMF phenotype (Teunissen et al., 2007). The PPARα activator fenofibrate was found to decrease DNA synthesis in neonatal rat CFs both at the basal level and in ET-1 stimulated cultures (Ogata et al. 2004). In addition, an *in vivo* study demonstrated that cardiac fibrosis was prevented in pressure-overloaded rats by fenofibrate and this occurred via suppression of the endothelin-1 (ET-1) gene (Ogata et al., 2002), ET-1 has been shown to stimulate CF DNA synthesis via a pathway involving cGMP (Fujisaki et al., 1995). PPAR γ and α activators were also found to decrease the size of MI in rats (Wayman et al., 2002).

1.9.5 Natriuretic Peptides

Natriuretic peptides are important hormonal regulators of many processes and are modulated during pathophysiologic conditions in heart disease. In particular, atrial

natriuretic peptide (ANP) is known to be antifibrotic in the heart. All three natriuretic peptides (ANP, brain natriuretic peptide (BNP) and c-type natriuretic peptide) were found to decrease growth factor stimulated CF DNA synthesis and cell proliferation (Cao & Gardner, 1995). A study using neonatal rat CFs demonstrated that ANP is able to inhibit CF proliferation by decreasing phosphorylation of the transcription factor GATA4, which decreased ET-1 promoter activity and gene expression (Glenn et al., 2009). Another study demonstrated that ANP and BNP were both able to decrease ET-1 mRNA expression and concomitantly decrease DNA synthesis. An inhibitor of soluble guanylate cyclase and a derivative of cGMP were also able to decrease ET-1 mRNA and DNA synthesis (Cao & Gardner, 1995; Fujisaki et al., 1995). In addition, in an *in vivo* study using mice with targeted disruption of BNP, the mice had ventricular fibrosis. As well, when subjected to pressure overload the fibrosis increased, suggesting BNP may have protective effects with respect to developing cardiac fibrosis (Tamura et al., 2000).

1.9.6 Platelet Derived Growth Factor

PDGF is a receptor tyrosine kinase that is able to activate the MAPK signalling pathway. There are three biologically active forms of PDGF: PDGF-AA, PDGF-BB and PDGF-AB, resulting from different combinations of its A and B chains. Both the PDGF receptor type α and β were found to exist in rat CFs. PDGF-AA was found to be a strong stimulator of adult rat CF proliferation, as was PDGF-BB; both elicited similar growth responses in these cells as measured by cell number, and seem to act downstream via the MAPK pathway (Simm et al., 1997). Human CF proliferation was stimulated by PDGF-AB as measured by DNA synthesis. This effect was attenuated by inhibitors of

ERK and PI3K, implicating these signalling proteins in the proliferative response of CFs to PDGF (Hafizi et al., 1999).

1.9.7 Natural and Synthetic Catecholamines

Chronic adrenergic signalling is an important feature of many forms of heart disease and has therefore been studied with respect to its effects on CFs. The endogenous catecholamine norepinephrine (NE) induced proliferation in CFs and activated ERK1/2, and treatment with the non-selective βAR antagonist carvedilol was able to normalize these effects (Leicht et al., 2000). Following NE stimulation, increased levels of cGMP and L-type Ca^{2+} channel blockers were also able to inhibit DNA synthesis (Calderone et al., 1998). The non-selective β adrenergic receptor (βAR) agonist isoproterenol (ISO) has been found to positively regulate CF proliferation, and this is believed to occur mainly through the β2AR and to involve production of a heat sensitive growth factor that acts on the CF in an autocrine manner (Turner et al., 2003). ISO was found to increase DNA synthesis in both adult rat and neonatal rat CFs (Colombo et al., 2003; Colombo et al., 2001; Kim et al., 2002) and also stimulated protein synthesis and proliferation in CFs (Turner et al., 2003). Activation of the ERK1/2 pathway has been implicated in ISO mediated CF proliferation (Colombo et al., 2003; Colombo et al., 2001; Kim et al., 2002; Turner et al., 2003) and consequently inhibition of MEK1/2 upstream of ERK1/2 was able to attenuate ISO stimulated DNA and protein synthesis (Colombo et al., 2001). Activation of PI3K has also been shown to play a role in regulating CF proliferation in response to ISO and inhibition of MEK1/2 (MAPK kinases responsible for the activation of ERK1/2) also attenuated PI3K activity in both human and rat CF cultures (Colombo et al., 2003, 2001; Hafizi et al., 1999; Kim et al., 2002). An *in vivo* study with two weeks of

chronic ISO treatment showed that βAR antagonists were able to significantly decrease ISO induced left ventricular fibrosis in rats (Brouri et al., 2004).

A study in adult rat CFs (Kim et al., 2002) investigating the mechanism of βAR stimulation resulting in DNA synthesis determined that ISO stimulated induction of ERK activity and DNA synthesis was abrogated by inhibitors of Src tyrosine kinase (a proto-oncogene). In addition, inhibition of the epidermal growth factor receptor (EGFR) abrogated ERK activation. MMPs and the soluble, mature form of heparin-bound epidermal growth factor (EGF) were also implicated in induction of ERK activity and DNA synthesis (Kim et al., 2002). Another investigation revealed that activation of the protease-activated receptor-1 (PAR-1) by thrombin, which is generated at injury sites in the vasculature, resulted in cardiac fibroblast DNA synthesis and activation of ERK, p38 MAPK and protein kinase B. This was found to be due to PAR-1 increasing levels of Src which then resulted in the transactivation of the EGFR. Stimulation of βARs by ISO was found to cause MMP-13 to activate PAR-1, which in turn activated the Gαq and EGFR pathway in neonatal rat CFs (Jaffré et al., 2012; Sabri et al., 2002).

The specific effects observed and proposed mechanisms of βAR induced CF proliferation are reviewed in further detail in table 1.2 and figure 1.2.

Table 1.2. Summary of studies relating to β-adrenergic receptor stimulated cardiac fibroblast proliferation.

Cardiac fibroblast type	Agents(s) + dose	Effect on growth	Duration of treatment	βAR implicated	Proposed mechanism	Reference
Human right atrial appendage	0.1 nM, 10 nM, 1 μM ISO	Dose dependent ↑ in cell number	6 days	β2AR	↑ cAMP, ERK1/2 activation, production of heat sensitive autocrine agent	(Turner et al., 2003)
Adult rat ventricle	10 μM NE	No effect	48 hours	β2AR	Comitogenic (serum required), activation of ERK1/2 phosphorylation of CREB	(Leicht et al., 2000)
	10 μM NE + 10% serum	↑ in cell number				
	1-10^5 nM ISO	Dose dependent ↑ in cell number				
	10 μM NE + carvedilol	No ↑ in cell number				
	10 μM NE + propranolol	No ↑ in cell number				
	10 μM NE + metoprolol	No effect				
	10 μM NE + ICI 118,551	No ↑ in cell number				
Neonatal rat	1 μM ISO	Dose dependent ↑ in DNA synthesis	24 hours	β2AR	Involves activation of PI3K and mTOR/p70S6K	(Colombo et al., 2003)
Neonatal rat	1 μM NE	↑ in DNA synthesis	24 hours	-	-	(Calderone et al., 1998)
	NE + propranolol	No ↑ in DNA synthesis				
Adult rat	1 μM ISO	↑ in DNA synthesis	48 hours	β2AR	Activation of ERK via EGFR, Src, and PI3K	(Kim et al., 2002)

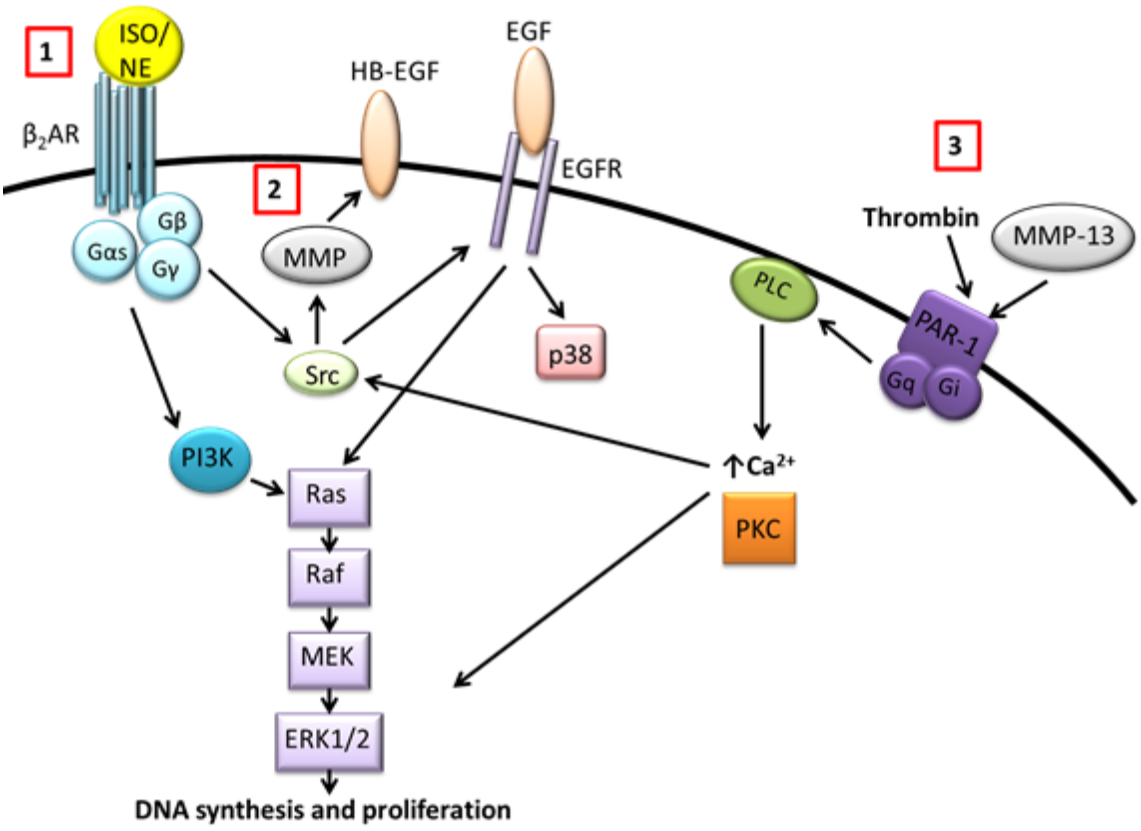

Figure 1.2: Schematic of factors involved in βAR-mediated cardiac fibroblast DNA synthesis and proliferation. 1) Binding of the β2AR by ISO or NE results in activation of G proteins. Stimulation of the β2AR was associated with an increase in PI3K which contributes to activation of the MAPK signalling cascade. **2)** The Src kinase was required for ISO-mediated ERK activation and is proposed to activate MMPs. MMPs are then able to cleave heparin bound epidermal growth factor (HB-EGF) allowing EGF to bind to the EGFR which activates the MAPK signalling cascade and has also been associated with activation of p38 MAPK in CFs. **3)** Protease-activated receptor-1 (PAR-1) is activated by thrombin released in response to injury, and was also activated by MMP-13. PAR-1 coupling to Gi and Gq proteins activated phospholipase C (PLC). PLC cleaves PIP2 into DAG and IP3, resulting in increased levels of intracellular Ca^{2+}. Protein kinase C is also predicted to be activated. It is currently unclear which messengers downstream of PAR-1 result in activation of MAPK signalling and Src kinase. Figure adapted from Sabri et al. (2002) and Kim et al. (2002).

1.10 Overview of βAR Subtypes in the Heart

βARs are members of the G protein coupled receptor (GPCR) family and as such, they have the characteristic seven transmembrane domains. The mammalian heart contains all three subtypes of βARs, β1, β2, and β3, however, the β1 and β2 subtypes are predominant (Lohse et al., 2003).

Both β1 and β2ARs are coupled to adenylyl cyclase (AC) through the stimulatory G protein, G_s, subsequently leading to increased levels of the second messenger cAMP which is able to activate protein kinase A (PKA). However, β2ARs are also able to interact with the inhibitory G protein (G_i), thereby creating a potential for interactions with other pathways including the MAPK signalling pathway (Lefkowitz et al., 2000). Cardiomyocytes express mainly the β1 subtype, whereas non-cardiomyocytes including CFs are reported to express more of the β2 subtype (Leicht et al. 2000; Gustafsson et al. 2000; Lau et al. 1980).

1.11 Comparison of βAR Ligand Affinities

The βAR receptor subtypes differ in their affinities for their ligands. β1ARs have the greatest affinity for binding the synthetic catecholamine isoproterenol (ISO; $K_i \approx 220$ nM), followed by the endogenous catecholamines norepinephrine (NE; $K_i \approx 3{,}500$ nM) and epinephrine (Epi; $K_i \approx 4{,}000$ nM), whereas β2ARs have the greatest affinity for binding ISO ($K_i \approx 460$ nM), followed closely by Epi ($K_i \approx 740$ nM), and very low affinity

for NE (K_i≈26,000 nM). This study was conducted in Chinese hamster ovary cells expressing the βAR subtypes (Hofman et al., 2004).

1.12 ISO Induced Cardiac Fibrosis Model

Chronic catecholamine stimulation is detrimental to the heart and contributes to heart failure. It has been shown to result in apoptosis, which was linked to interactions with the β1 receptor (Lefkowitz et al. 2000). A study measuring cardiac NE release in patients with and without hypertension revealed that increased plasma levels of NE were related to increased left ventricular mass (Kelm et al., 1996). Increased sympathetic activity is also related to an increase in left ventricular hypertrophy, and plasma levels of NE are related to risk of death from chronic congestive heart failure (Cohn et al., 1984; Schlaich et al., 2003).

ISO is a synthetic catecholamine and is able to bind to both β1 and β2 receptors. Chronic ISO stimulation is known to result in the death of cardiomyocytes, cardiac hypertrophy and fibrosis and is a well-established animal model of cardiac fibrosis (Benjamin et al., 1989; Boluyt et al., 1995; Kudej et al., 1997). Chronic ISO treatment results in increased deposition of collagen fibers characteristic of cardiac fibrosis, and the amount of cardiac fibrosis is directly related to the dose of ISO used (Benjamin et al., 1989; Pick et al., 1989). In response to βAR stimulation, oxygen consumption in the heart increases leading to ischemia and increased oxidative stress, which results in cardiomyocyte death and subsequent cardiac fibrosis (Benjamin et al., 1989; Bos et al., 2004). βAR stimulation may also result in myocardial collagen synthesis, contributing to

the development of fibrosis (Bos et al., 2004). Bos et al (2004) suggest that in ISO-induced cardiac fibrosis increased sympathetic activity results in production of renin, which ultimately leads to increased aldosterone and further activation of the RAS. They propose that aldosterone may decrease the uptake of catecholamines from the extracellular environment, resulting in their increased activity. Compared with NE and Epi, ISO is a more potent βAR agonist, and therefore often used for experimental purposes.

1.13 Cardiac Fibrosis and Heart Function

Cardiac fibrosis occurs in many forms of heart disease and ultimately contributes to the development of heart failure. The location of fibrosis in the myocardium depends on the pathology that caused the fibrosis (Mewton et al., 2011). The amount of fibrosis in the myocardium is associated with the severity of diastolic dysfunction (abnormal ventricular filling which can lead to pooling of blood in the lungs) in many cardiac pathologies (Moreo et al., 2009). The increase in interstitial collagen during fibrosis causes a stiffening of the myocardium, particularly during diastole, which can progress to systolic dysfunction. An increase in the amount of collagen in the heart (collagen volume fraction, or CVF) by two to three fold has been shown to negatively affect diastole due to an increase in stiffness, and a fourfold increase in CVF leads to a further increase in diastolic and systolic dysfunction (Díez et al., 2001).

In addition, the increase in ECM secretion during fibrosis interrupts the electrical connections between cardiomyocytes which disrupts the coordinated contractions of the

myocardium and can result in arrhythmias (Brown et al., 2005; Berk et al., 2007). Fibrosis around the vasculature of the heart decreases the amount of oxygen available for cardiomyocytes which worsens ischemia and perpetuates cardiomyocyte death (Brown et al., 2005).

1.14 Clinical Strategies to Diagnose Cardiac Fibrosis

Pro-collagens are synthesized in CFs and secreted into the ECM where they are cleaved into their mature forms. The carboxy-terminal propeptide (PIP) is one of the pieces cleaved from type I procollagen. PIP is released into the circulation and is removed by the liver (Querejeta et al., 2000). It is possible to use serum levels of PIP as a measure of collagen synthesis. Confirmation in patients with hypertensive heart disease revealed that levels of PIP in the serum correspond to the amount of collagen in the tissue (Querejeta et al., 2000). To detect collagen degradation, levels of collagen I telopeptide (CITP) can be assessed (Zile & Baicu, 2013). It is also possible to indirectly measure ECM metabolism by assessing concentrations of MMP-13 and TIMPs in the serum using enzyme-linked immunosorbent assay (ELISA) (Brown et al. 2005; Zile & Baicu, 2013).

Endomyocardial biopsy is another method used for the assessment of cardiac fibrosis. Examination of cardiac tissue occurs after Masson Trichrome staining which allows for qualitative assessment of collagen content. In order to quantify the amount of collagen present, picro Sirius red fast green staining can be done. This technique stains collagen fibers red and healthy myocardium green. However, depending on where the

samples are taken from, it may be difficult to obtain an accurate idea of the extent of cardiac fibrosis (Mewton et al., 2011).

Another method of assessing cardiac fibrosis is magnetic resonance imaging (MRI). This allows simultaneous assessment of cardiovascular function and anatomy. MRI using late gadolinium enhancement (an extracellular contrast agent) is able to show cardiac fibrosis, and has been used to diagnose fibrosis stemming from various kinds of cardiomyopathies (Mewton et al., 2011; Zile & Baicu, 2013).

1.15 Current Treatments Available for Cardiac Fibrosis

Many drugs currently used to treat cardiovascular conditions co-occurring with cardiac fibrosis have been shown to have off-target effects on fibrosis, as reviewed below.

Ang II is a key player in cardiac fibrosis, therefore it follows that drugs targeting its actions may be of use in treating cardiac fibrosis. Two types of drugs have been investigated in this respect, Ang II receptor blockers and angiotensin converting enzyme (ACE) inhibitors. These drugs are commonly used to treat hypertension, and act on the renin-angiotensin system (RAS) to decrease peripheral vascular resistance. Treatment with the AT1 receptor blocker, losartan, for two months was able to decrease interstitial fibrosis in hamsters with cardiomyopathy (De Mello & Specht, 2006). In addition, losartan was able to decrease collagen content in hypertensive patients and decrease myocardial fibrosis and stiffness after one year of treatment (Diez et al. 2002). The ACE

inhibitor lisinopril was administered to patients with hypertension over a period of six months, and a decrease in collagen content concurrent with an improvement in left ventricular diastolic function was observed (Brilla et al. 2000). Another ACE inhibitor, enalapril, was able to decrease both atrial fibrosis and atrial fibrillation in a canine model of congestive heart failure (Shi et al., 2002).

In addition to drugs acting on the RAS, statins have shown promise. Statins are anti-hyperlipidemics used to inhibit the enzyme 3-hydroxy-3-methylglutaryl coenzyme A (HMG-CoA) reductase which is involved in cholesterol synthesis. Increased levels of low density lipoproteins are a risk factor for heart disease, and statins are often prescribed to help reduce cholesterol. Treatment with statins has been shown to decrease both the remodelling and interstitial fibrosis that occurs post MI (Chen & Frangogiannis, 2013). In mice subjected to MI, treatment with Fluvastatin for four weeks was able to increase survival and decrease interstitial fibrosis. Treatment with Fluvastatin also prevented the increased expression of MMPs associated with MI, indicating that it is able to decrease myocardial remodelling post-MI (Hayashidani et al. 2002). In addition, statins have been shown to prevent CF growth and migration, differentiation into CMFs, and ECM remodelling. An explanation for this is that statins inhibit HMG-CoA reductase, thereby preventing formation of mevalonate from HMG-CoA during cholesterol synthesis. This in turn prevents production of intermediates in the cholesterol synthesis pathway, such as farnesyl pyrophosphate and geranylgeranyl pyrophosphate, which are required for post-translational modification of small G-proteins, including Ras, Rho, and Rac. In this way, statins are able to interfere with many downstream signalling pathways (Porter & Turner, 2009).

In keeping with the anti-proliferative effects of β-blockers on CFs, a study conducted on rats subjected to aortic banding revealed that treatment with carvedilol decreased deposition of the ECM components collagens type I and III, laminin and fibronectin. In addition, when carvedilol treated CFs from pressure-overloaded hearts were examined *in vitro*, they were found to have decreased proliferation. Treatment with the selective β1 blocker metoprolol did not have the same affect (Grimm et al., 2001) Carvedilol was also shown to have effects on ECM proteins in another study using rats that underwent left coronary artery ligation, as rats treated with carvedilol had decreased collagen in the myocardium. Metoprolol again did not affect levels of collagen protein (Wei et al. 2000).

The PPAR-γ ligands rosiglitazone and 15-deoxy-$\Delta^{12,15}$-prostaglandin J_2 (15d-PGJ_2) were found to decrease Ang II stimulated CF proliferation *in vitro*. In addition, they reduced Ang II-induced expression of the ECM proteins PAI1, collagen types I and III and fibronectin. A decrease in PAI1, collagen and fibronectin was also seen *in vivo* with rosiglitazone (Hao et al., 2008). Rosiglitazone decreased cardiac fibrosis in rats with type 2 diabetes, and this is suggested to have occurred via decreased expression of CTGF (Ihm et al., 2010). When rat CFs were treated with pioglitazone (a PPAR-γ ligand) before being subjected to anoxia-reoxygenation it attenuated the increase in collagen type I and MMP-1 levels (Chen et al. 2004).

Table 1.3. Summary of current therapeutics with known effects on cardiac fibrosis.

Agent	Activity	Effect on CFs	References
Statins	Inhibit HMG coA reductase	↓proliferation, ↓differentiation, ↓migration, ↓ECM turnover	(Chen & Frangogiannis, 2013; Hayashidani et al., 2002; Porter & Turner, 2009)
ACE inhibitors and AR blockers	Prevent Ang II signalling	↓proliferation, ↓differentiation, ↓ECM turnover, ↓secretion of profibrotic growth factors and cytokines	(Benson et al., 2008; Porter & Turner, 2009; Yu et al., 2001)
β blockers	Prevent profibrotic signalling via βARs	↓proliferation, ↓expression of colllagen I, collagen III, laminin and fibronectin	(Grimm et al., 2001)
Thiazolidinediones	PPARγ agonists	Inhibits Ang II stimulated proliferation, ↓expression of collagen and fibronectin, ↓secretion of profibrotic proteins, ↑secretion of antifibrotic proteins	(Chen et al., 2004; Chen & Mehta, 2006; Chintalgattu et al., 2007; Hao et al., 2008; J. Li et al., 2008; Makino et al., 2006)

1.16 Mammalian Cell Cycle Overview

The mammalian cell cycle consists of four phases: Gap 1 (G1), Synthesis (S), Gap 2 (G), and Mitosis (M). During G1 and G2 cells increase in size and pass through checkpoints ensuring they are ready to enter into the S and M phases. During the S phase, cells synthesize DNA, and in the M phase the equal division of genetic material between two daughter cells and cell division occurs. Quiescent, non-dividing cells exist in the Gap 0 (G0) phase.

Transition through the phases of the cell cycle is tightly regulated. At different stages, cyclin dependent kinases (CDKs) must be activated by their regulatory partner cyclins (CYC). CDKs are serine/threonine protein kinases, and are present throughout the cell cycle, unlike the CYCs, whose levels fluctuate. In addition to CYCs, there are also CDK inhibitors that inhibit CDK/CYC complexes, thereby preventing cell cycle progression (Satyanarayana & Kaldis, 2009; Shankland & Wolf, 2000).

Entry into the G1 phase is regulated by D type CYCs (D1-3). The D type CYCs respond to mitogens such as growth factors and interact with CDKs 4 and 6. This interaction results in phosphorylation of the retinoblastoma protein (pRb), resulting in release of the E2F transcription factor. E2F is then able to bind to target genes to initiate G1/S phase cell cycle progression (Satyanarayana & Kaldis, 2009; Shankland & Wolf, 2000).

CYCB binds to CDK1 and is required for M phase. When CYCB binds to CDK1, CDK1 undergoes a conformational change which allows access to phosphorylation sites that are important in regulating its activity. The Wee1 and Myt1 kinases are responsible

for the inhibitory phosphorylation of threonine 14 (Thr14) and tyrosine 15 (Tyr15) (Shankland & Wolf, 2000). Phosphorylation of Thr161 is activating, but is overridden by the inhibitory phosphorylation. The cdc25 phosphatase is responsible for dephosphorylation of Thr14 and Tyr15. When CDK1 is active (dephosphorylated) and bound to cyclin B, the complex phosphorylates targets such as H1 histone and nucleolin which are required for chromosomes to condense, for the breakdown of the nuclear envelope, and for formation of the mitotic spindle. When M phase has finished, CYCB is broken down by the ubiquitin-proteasome pathway, and CDK1 is dephosphorylated by the kinase-associated phosphatase (Satyanarayana & Kaldis, 2009; Shankland & Wolf, 2000).

1.17 Rationale and Objectives

Mice are commonly used as animal models of cardiovascular diseases as well as in experiments involving transgenic and knockout models. Despite the widespread use of mice, the majority of studies conducted on CFs have made use of either human or rat CFs. Mouse CF behaviour in culture has not, to our knowledge, been investigated and subsequently the distribution of βARs in mouse CFs is not known.

As discussed above, chronic βAR stimulation can lead to cardiac fibrosis. Chronic stimulation with the non-selective βAR agonist ISO was found to increase expression of CDK1 protein and activity of the CDK1/CYCB complex in mouse salivary glands, and increase cell proliferation (Zeng et al., 1996). Chronic ISO treatment was also found to increase expression of CDK1 in a mouse model of cardiac fibrosis, where

CDK1 is not normally expressed in the adult mammalian heart. *In vitro* ISO treatment of primary embryonic ventricular cells increased expression of CDK1 mRNA. This was localized to non-cardiomyocytes, and the CDK1 promoter was found to contain an ISO responsive element (Gaspard et al., In Press). Given the inherently low cell cycle activity of the adult heart, CDK1 is not normally detectable and its expression in non-cardiomyocytes in response to ISO suggests that CDK1 may be involved in cardiac fibrosis. Specifically, increased CDK1 may play a role in increasing CF proliferation in response to fibrotic stimuli such as βAR stimulation. The mechanisms regulating CF proliferation and differentiation are varied and complex, therefore it may be advantageous to investigate a more direct target to control proliferation, such as a cell cycle protein. Current treatments for cardiac fibrosis involve modulation of the RAS, as well as treatment with statins, βAR blockers and thiazolidinediones, as reviewed previously. As of yet the possibility of targeting a cell cycle protein to modulate the outcome of cardiac fibrosis by controlling CF proliferation has not been explored. Inhibition of the cell cycle has been examined with respect to tumor suppression, but may also have potential for use in disease states other than cancer.

ISO is able to activate AC via stimulation of βARs. Increased cAMP levels due to AC activation have been shown to decrease phenoconversion to CMFs as well as decrease CMF collagen synthesis (Swaney et al., 2005). In light of this, it is possible that treatment with ISO may influence phenoconversion of CFs to CMFs.

Given the increased sympathetic activity in diseased hearts it follows that βAR stimulation is an important factor in cardiovascular disease. Studies relating to βAR stimulated CF proliferation have been conducted, however, these studies were not done

with mouse cells and the status of CDK1 in CFs has not been investigated. Furthermore, the effects of βAR stimulation on CF gene expression have not been investigated.

In addition to increased sympathetic activity, the activity of natriuretic peptides is also modulated during heart disease. ANP in particular was shown to decrease CF DNA synthesis and proliferation *in vitro* (Cao & Gardner, 1995). As well, mice lacking the *Npr1* receptor (a high affinity receptor for ANP) exhibit symptoms of cardiomyopathy and heart failure before 6 months of age (Oliver et al., 1997). Given this, it would be of interest to investigate the effect of loss of the ANP receptor on CF proliferation, and the effect this may have on βAR stimulation in CFs.

We hypothesized that stimulation of mouse CFs with the non-selective βAR agonist ISO increases CDK1 levels and modulates CF gene expression. As well, we reasoned that inhibition of CDK1 and loss of the *Npr1* receptor can modulate CF proliferation.

The objectives of this study were to establish and characterize a cell culture system for adult mouse CFs. We also aimed to investigate the effects of ISO on adult mouse cardiac fibroblasts in an attempt to: i) confirm an increase in proliferation in this cell type, ii) investigate whether ISO is able to induce CDK1 expression *in vitro*, iii) determine the effect of CDK1 on cardiac fibroblast proliferation, iv) examine the effect of ISO treatment on CF gene expression and v) observe the effect of loss of *Npr1* on CF proliferation.

Chapter 2: Materials and Methods

2.1 Cardiac Myofibroblast Cell Culture

Mice were kept on a 12 hour light/dark cycle with access to food and water in the Carleton Animal Care Facility at Dalhousie University. All experiments were conducted according to the guidelines set by the Canadian Council on Animal Care and were approved by the Dalhousie University Committee on Laboratory Animals.

CMFs were cultured from the ventricles of adult male CD1 mice (Charles River, Montreal, Quebec, Canada) or *Npr1-/-* mice (obtained from Dr. Nobuyo Maeda, University of North Carolina, NC, USA). *Npr1-/-* mice have a mutated natriuretic peptide receptor A (NPRA) gene, *Npr1,* the first exon and intron of which was substituted with a neomycin resistance cassette. Mice were sacrificed by isoflurane anesthetic overdose followed by cervical dislocation. Hearts were removed from the mice and placed in sterile phosphate buffered saline (PBS: 0.138 M NaCl, 0.0027 M KCl, pH 7.4) containing 1X antibiotic/antimycotic (AB/AM: 1000 units penicillin G sodium, 1000 µg streptomycin sulfate, and 2.5 µg amphotericin B as Fungizone® in 0.85% saline, Gibco, Burlington, ON, Canada) warmed to 37°C. The ventricles were then separated from the atria, finely minced, placed in a 0.1% collagenase (Worthington Biochemical Corp, Lakewood, NJ, USA) digestion solution warmed to 37°C and incubated with rocking for 15 minutes at 37°C. Ventricles were subjected to five such digestions, and supernatants from the first and second digestions were discarded while those from the third to fifth digestions were pooled, centrifuged for 2 minutes at 2,000 rpm, and plated in 100 mm

dishes (Corning, Corning, NY, USA) in Dulbecco's Modified Eagle's Medium (DMEM, Wisent, Saint-Bruno, QB, Canada) with 10% fetal bovine serum (FBS, Wisent) and 1% AB/AM (10% FBS-DMEM). After a one hour incubation period at 37°C with 6% CO_2, media was replaced to remove unattached or weakly adherent cells, including cardiomyocytes and endothelial cells (Kim et al., 2002; Li et al., 2008). Cells that had never been passaged (P0) took 3 to 4 days of growth with two media changes (on days 1 and 2) to reach confluence. Approximately 10% of the cell population initially plated was floating at the time of the media changes. In light of this, the cells used for experiments were between passages one and three (P1-3).

2.2 *Npr1* Genotyping

Ear punching was performed on *Npr1* mice and genomic DNA was extracted using Sigma REDExtract-N-AMP tissue PCR kit (Sigma Aldrich) according to the manufacturer's instructions. Tissue samples from ear punches were ground using a sterile pipette in 50 µL of DNA extraction solution and incubated for 10 minutes at room temperature. Next, samples were heated to 95°C and 10 µL of neutralization buffer was added. The samples were centrifuged and the supernatant was used as a polymerase chain reaction (PCR) template. PCR was conducted with 5 µL REDExtract-N-AMP PCR mix, 0.5 µL of each primer, 2 µL of tissue extract and water to a final volume of 10 µL. PCR was performed for a total of 34 cycles, 30s at 94°C, 60s at 55°C and 60s at 72°C. The expected size of the PCR product was 339 base pairs for wildtype and 500 base pairs for the transgenic allele. No template controls were also run to confirm positive results.

2.3 Primary Embryonic Ventricular Cell Cultures

Hearts were removed from embryonic day 15.5 mice (E15.5) and washed in warmed PBS with 1X AB/AM. Ventricles were dissected and placed in 0.2% collagenase and incubated with rocking at 37°C to digest tissue. After the incubation, ventricles were triturated to dissociate remaining cells. Cells were centrifuged at 4,000 rpm for 4 minutes and then washed twice with 10% DMEM. Cells were counted with a hemocytometer and plated on fibronectin coated 2 or 4 well chamber slides (Nunc, Rochester, NY, USA).

2.4 Adult Mouse Heart Sections

Adult male mouse hearts were removed and washed in warmed PBS with 1X AB/AM. Hearts were cryoprotected in 30% sucrose and rocked at 4°C overnight. Next, hearts were embedded in Optimal Cutting Temperature compound medium (Tissue-Tek, Sakura Finetek, Torrance, CA, USA) and frozen at -80°C. Thin tissues sections (10 μm) were cut using a Cryostat (Leica CM3050S). Sections were collected on Superfrost Plus slides (Thermo Fischer Scientific, Nepean, ON, Canada) and processed for immunofluorescence.

2.5 Immunofluorescence

Cardiac myofibroblasts (CMFs) used for immunolabelling were grown on 2 or 4 well chamber slides. CMFs used for characterization were grown for 48 hours. For drug treatments, cells were allowed to attach overnight and the following day 5μM ISO (Sigma Aldrich) was added in 10% DMEM for 24 or 48 hours, while control cells received 10% DMEM for a period of 24 or 48 hours. For cells treated with NE (Sigma Aldrich), 10 μM of the drug was dissolved in 0.5 M HCl and added to cells in 10% DMEM for 48 hours. Control cells received 0.5 M HCl in 10% DMEM for 48 hours.

At the appropriate time point, slides were fixed in ice cold methanol for 15 minutes followed by three 5 minute washes in PBS. CMFs were then permeabilized in 0.1% Triton-X100 (Sigma Aldrich) in PBS for 5 minutes at room temperature. To prevent non-specific binding of antibodies, slides were blocked for one hour at room temperature in blocking buffer (1% v/v bovine serum albumin, 10% v/v goat serum in PBS). Primary antibodies for CDK1 (CDC2 p34, Santa Cruz Biotechnology, Dallas, TX, USA), αSMA (Sigma Aldrich), vWF (Santa Cruz Biotechnology), CYCB1 (Santa Cruz Biotechnology), vimentin (Developmental Studies Hybridoma Bank, Iowa City, IA, USA), nestin (Developmental Studies Hybridoma Bank), smooth muscle α actinin (Developmental Studies Hybridoma Bank), anti-5-bromo-2-deoxyuridine (BrdU: Developmental Studies Hybridoma Bank) and sarcomeric myosin (Developmental Studies Hybridoma Bank) were incubated for one hour at room temperature with the exception of DDR2 (Santa Cruz Biotechnology) which was left overnight at 4°C (for primary antibody dilutions in blocking buffer see Table 2.1). Unbound primary antibodies were removed by washing with PBS three times for 5 minutes. Secondary

antibodies were incubated at 1:200 in blocking buffer at room temperature for 1 hour. The secondary antibodies used were polyclonal anti-rabbit IgG conjugated to Alexa Fluor 488 or Alexa Fluor 555, and monoclonal anti-mouse IgG conjugated to Alexa Fluor 555 or anti-mouse IgM μ chain conjugated to Alexa Fluor 555 (Invitrogen, Burlington, ON, Canada). Unbound secondary antibodies were removed by washing with PBS three times for 5 minutes each. Slides were then incubated for 5 minutes at room temperature with Hoechst 33342 nuclear stain (Sigma Aldrich) at a dilution of 1:1000 in PBS. Slides were air dried and cover slips were mounted with 1% propyl gallate. Immunolabelling was examined using a Leica microscope equipped with a DFC500 camera (Leica, Concord, ON, Canada).

Approximately 200-300 cells were counted per experiment. The number of positive cells is expressed as a percentage of total cells counted. Counting was done on a minimum of three slides from three independent experiments.

Table 2.1. Primary antibodies and dilutions used for immunofluorescence.

Primary Antibody	Dilution	Source and Catalogue Number
Sarcomeric myosin	1:50 (supernatant)	Developmental Studies Hybridoma Bank: MF-20
Vimentin	1:10 (concentrate)	Developmental Studies Hybridoma Bank: 40E-C
Smooth muscle α actinin	Undiluted (supernatant)	Developmental Studies Hybridoma Bank: 1E12-s
Anti-BrdU	Undiluted (supernatant)	Developmental Studies Hybridoma Bank: G3G4
Von Willebrand Factor	1:50	Santa Cruz Biotechnology: sc-14014
α smooth muscle actin	1:50	Sigma Aldrich: A5228
Discoidin domain receptor 2	1:50	Santa Cruz Biotechnology: sc-8989
CDC2 p34	1:50	Santa Cruz Biotechnology: sc-954
Nestin	1:50	Developmental Studies Hybridoma Bank: rat-401
Pro collagen type I	Undiluted (supernatant)	Developmental Studies Hybridoma Bank: SP1.D8
Cyclin B1	1:50	Santa Cruz Biotechnology: sc-245

2.6 Cell Size Measurements

Images of cells immunolabelled for αSMA were captured with a 20X objective and saved in TIFF format. Cell size was determined using Image Processing Tool Kit 5.0 (Reindeer Graphics, Asheville, NC, USA) and Adobe Photoshop 7.0. A scale bar created for the 20X objective was used to calibrate the magnification of the images being used for cell size measurements. Cells were outlined in Photoshop using the polygonal lasso tool which was then filled in, and the IP Measure Features – Measure Regions option was used to calculate the filled area in μm^2.

2.7 Fluorescence Activated Cell Sorting

CFs were trypsinized, centrifuged at 2,000 rpm for 2 minutes, and washed with PBS. To prevent non-specific binding of antibodies, cells were then incubated in blocking buffer for one hour at room temperature. This was followed by a one hour incubation with the primary antibody, against either the β1AR (131024, Bioss, Woburn, MA, USA), or the β2AR (ab36956, Abcam, Toronto, ON, Canada) at a dilution of 1:100 in blocking buffer for one hour at room temperature. Cells were then washed three times for 5 minutes in PBS followed by a final incubation in secondary antibody (anti-rabbit Alexa Fluor 555) at 1:200 in blocking buffer. Cells were re-suspended in sorting buffer (0.1% BSA in PBS) and transported to the fluorescence activated cell sorting (FACS) facility for analysis.

2.8 Second Messenger Heterogeneous Time Resolved Fluorescence cAMP Assay

In order to measure the response of the second messenger cAMP in CMFs following treatment with ISO, a cAMP dynamic 2 HTRF assay (Cisbio, Bedford, MA, USA) was used. The competitive immunoassay occurred in two steps, a stimulation step and a detection step.

Stimulation step: CMFs were trypsinized, counted with a hemocytometer (Hausser Scientific, Horsham, PA, USA) and seeded into a 384 well plate (Greiner Bio-One, Monroe, NC, USA). Each well received 5µL of 10% FBS-DMEM containing 4,000 cells along with 0.5mM of the phosphodiesterase inhibitor 3-isobutyl-1-methylxanthine (IBMX, Sigma Aldrich) and 5µL of the respective drug treatment for a final volume of 10µL per well. Drug treatments consisted a range of doses of ISO (0.1, 0.5, 1, 5, or 10 µM) to determine the optimal dose to use for future experiments. To determine the contribution of β1 and β2ARs to the ISO-mediated cAMP response, the β1AR blocker metoprolol, β2AR blocker ICI-118,551 (ICI), or the non-selective βAR blockers propranolol or carvedilol (Sigma Aldrich) were used at a ratio of 10µM β blocker to 5µM ISO. Control wells received ddH_2O (Ambion, USA) in place of drug. Cells were incubated for 30 minutes at room temperature.

Detection step: 5µL each of d2-labeled cAMP and a cAMP monoclonal antibody labeled with the fluorescent molecule cryptate diluted in conjugate/lysis buffer were added to each well. The cAMP produced by the cells in the stimulation step competed with d2-labeled cAMP for binding to the anti-cAMP cryptate. Energy transfer between

d2-labeled cAMP and the anti-cAMP cryptate resulted in a fluorescent signal. The negative control received conjugate/lysis buffer instead of d2-labeled cAMP to allow for determination of the non-specific signal. A standard curve was created using a supplied reagent with a previously determined level of cAMP. Plates were incubated in the dark for one hour at room temperature at which point fluorescence was measured using a plate reader (Polarstar Omega, BMG Labtech, Guelph ON). cAMP levels were interpolated from the standard curve by nonlinear regression using Graphpad Prism 4 software (Graphpad Software, San Diego, CA, USA).

2.9 BrdU Labelling

After 48 hours of drug treatment, cells were incubated with 3µg/mL of BrdU (Sigma Aldrich) for 24 hours. CFs were then fixed in 1% paraformaldehyde at room temperature for 15 minutes, followed by 30 minutes in 70% ethanol at room temperature and permeabilized in 0.1% Triton-X100 in PBS for 15 minutes at 4°C.

Following this cells were treated with 70mM sodium hydroxide for two minutes followed by a 5 minute wash in PBS. Cells were subsequently immunolabelled for both BrdU (Section 2.3). Approximately, 200-300 cells were then assessed for BrdU expression per group in each experiment. The percentage of BrdU positive cells is referred to as the percent BrdU labelling index.

2.10 RNA Extraction and cDNA Synthesis

CMFs were treated in 100 mm dishes (Corning) with 10% FBS-DMEM containing 5μM ISO for 30 minutes, or 4 or 24 hours. Control CMFs received 10% FBS-DMEM for the indicated durations.

RNA was extracted from cells using the RNEasy Plus Kit (Qiagen, Mississauga, Ontario). According to manufacturer's instructions, cells were lysed and subjected to a series of washes and filtrations to remove genomic DNA and purify the RNA. RNA was eluted in RNase/DNase free water (Ambion). Purity of the RNA samples was determined using a spectrophotometer (SmartSpec^{TM} Plus, Bio Rad, Mississauga) to measure the A260/280 absorbance ratios. Samples with ratios between 1.8 and 2.0 were classified as pure and subsequently used in reverse transcription to make complementary DNA (cDNA) for further experimentation.

cDNA synthesis took place in 20μL reaction volumes consisting of 1 μg RNA, 5 μL 5X first strand buffer (Invitrogen), 1 μL of 0.1M DTT (Invitrogen), 1μL of 0.5μg/μL random primers (Invitrogen), 1μL of 10mM dNTPs 100U of superscript II reverse transcriptase (Invitrogen) and RNase/DNase free ddH_2O (Ambion) to a final volume of 20 μL. This mixture was incubated at 25°C for 10 minutes, 42°C for 50 minutes, and 70°C for 15 minutes. The resulting cDNA was then used for QPCR analysis.

2.11 QPCR Analysis

cDNA was used to measure the expression levels of mRNAs of interest. QPCR primers were designed using the qPrimerDepot website: http://mouseprimerdepot.nci.nih.gov/. The QPCR mixture was composed of 2µL cDNA, 0.5 µL each of 0.25 µM forward and reverse primers specific for the gene of interest (for primer sequences see Table 2.2), 2µL EVOlution EvaGreen QPCR mix (Montreal Biotech Inc., Montreal QB), and RNase/DNase free ddH_2O to a final volume of 10µL. This mixture was then run on an Eco Real-Time PCR System (Illumina Inc., San Diego, California) at 50°C for 2 minutes, 95°C for 10 minutes, and cycled through 95°C for 15s, and 60°C for 1 minute for a total of 40 cycles, followed by further incubation at 95°C for 15s, 60°C for 15s, and 95°C for 15s. Relative mRNA expression levels were determined by normalization to the mouse TATA box binding protein (mTbp) housekeeping gene using the ΔΔCt method (Livak & Schmittgen, 2001).

Table 2.2. Mouse primer pair sequences used to amplify genes of interest for QPCR analysis.

Gene of interest	Primer name	Forward (5' to 3')	Reverse (3' to 5')
TATA box binding protein	mTbp	CTGGTGTGGCAGGAGTGATA	ACATCTCAGCAACCCACACA
CDK1	CDK1	TGGCCAGTGACTCTGTGTCT	TCCGTCGTAACCTGTTGAGT
Collagen type 1 α1	Col1a1	GGGGCAGACAGTCATCGAA	GGTGGAGGGAACCAGATTG
α smooth muscle actin	aSMA	GTTCAGTGGTGCCTCTGTCA	ACTGGGACGACATGAAAAG
Connective tissue growth factor	CTGF	GCTTGGCGATTTTAGGTGTC	CAGACTGGAGAAGCAGAGCC
Fibronectin type 1	Fn1	CGGCATGAAGCACTCAATGG	CTCAACCCTCCCCGAAACAC
Plasminogen activator inhibitor	PAI	GCGTCTCTTCCCACTGTCAA	TCCCCATTCTCAACTGGCAC
Collagen type 3, α1	Col3a1	GGGCTGGAAAGTGAGGGAAG	ATAAAACTCAGCCGCTCGCT

2.12 Protein Extraction

CMFs used for Western blotting were treated with 10% FBS-DMEM containing 5μM ISO for 15 or 30 minutes, and 1 or 48 hours. Control cells received 10% FBS-DMEM for the duration of the drug treatments. Protein was extracted from CMFs in tumor lysis buffer (1% NP40, 5mM EDTA, 50mM Tris-HCl pH 8.0 and 10mM phenylmethylsulphonyl fluoride (PMSF) and 1mM Aprotinin) and samples were then incubated on ice for 15 minutes. This was followed by three 10s sonications at a setting of 3.5 (Sonic Dismembrator, Thermo Fisher Scientific) and a further 15 minute incubation on ice. The samples were then centrifuged at 13,300 rpm for 15 minutes at 4°C and detergent soluble supernatants containing cytosolic fractions were collected for further use. Protein concentrations were determined using a Bradford Assay (Bio-Rad, Mississauga, ON, Canada).

2.13 Gel Electrophoresis and Western blotting

Protein samples were denatured in Laemmli buffer (62.5 mM Tris-HCl pH6.8, 0.5mL β-mercaptoethanol, 25% v/v glycerol, 2% w/v sodium dodecyl sulfate (SDS), 0.02% w/v bromophenol blue, and ddH2O) and heated for 3 minutes at 95°C. Following this, 10 μg of protein was resolved on a 10% SDS-polyacrylamide gel (3.5mL 30% acrylamide, 2.5mL of 1.5M Tris HCl (pH=8.8), 100μL 10% sodium dodecyl sulfate, 5μL N,N,N',N'-tetramethylethylenediamine (TEMED) 50μL of ammonium persulfate and 3.85mL ddH_2O) along with a BLUeye Prestained molecular weight marker (FroggaBio, Toronto, ON, Canada) at a current of 100 volts. Separated proteins were transferred onto

a nitrocellulose membrane (Pall Life Sciences Corporation, Mississauga, ON, Canada) at 100V and 300 mA for 1 hour. Gel electrophoresis and protein transfer were done using a in a Mini-PROTEAN 3 gel electrophoresis unit (Bio-Rad).

The nitrocellulose membrane was then incubated for one hour at room temperature in blocking buffer (5% skim milk powder, 3% bovine serum albumin, 0.1% Tween in PBS (PBS-t) to prevent non-specific binding of antibodies followed by a primary antibody incubation which either took place for one hour at room temperature for β1AR (Santa Cruz Biotechnology), GAPDH (Santa Cruz Biotechnology), ERK1/2 (Cell Signaling Technology, Danvers MA, USA), pERK1/2 (Cell Signaling Technology), and β2AR antibodies (Abcam) or overnight at 4°C with rocking for pCDC2, CDC2, and CYCB1 antibodies (Cell Signaling Technology). For primary antibody dilutions see Table 2.3. The membrane was then washed three times for 5 minutes each in PBS-t and incubated in secondary antibody (1:2,000, goat-anti-rabbit or goat-anti-mouse conjugated to horse radish peroxidase, Bio-Rad, Catalogue #172-1019, #170-6516) for one hour at room temperature followed by three 10 minute washes in PBS-t. The peroxidase signal was detected using an ECL Plus Western Blotting Detection chemiluminescence kit (GE Healthcare Life Sciences, NJ, USA) according to manufacturer's instructions and then exposing the blots to an X-ray film (UltraCruz Autoradiography Film, Santa Cruz Biotechnology) to visualize the signal.

Quantification of protein was done by scanning Western blot films into the Image J software program and using densitometric analysis. GAPDH was used as a control to normalize the density measurements of the proteins of interest.

Table 2.3. Primary antibodies and dilutions used for Western blotting.

Antibody	Dilution	Source
pCDC2 p34	1:500	Cell Signaling Technology: cs-9111
CDC2 p34	1:500	Cell Signaling Technology: cs-9112
CYCB1	1:1000	Cell Signaling Technology: cs-4138
GAPDH	1:5000	Santa Cruz Biotechnology: sc-25778
ERK1/2	1:1000	Cell Signaling Technology: cs-4695
pERK1/2	1:1000	Cell Signaling Technology: cs-9101
β1AR	1:500	Santa Cruz Biotechnology: sc-568
β2AR	1:500	Abcam: AB36956

2.14 Adenoviral Transductions

CMFs were transduced with an adenoviral construct overexpressing either CDK1 (adenoCDK1) or a constitutively active form of CDK1 (adenoCDK1AF, Vector Biolabs, Philadelphia PA). AdenoCDK1AF was created by mutating amino acids 14 and 15 from threonine and tyrosine to alanine and phenylalanine, respectively. Control CMFs were transduced with an adenoviral construct overexpressing green fluorescent protein (adenoGFP, provided by Dr. Chris Sinal, Dalhousie University, Halifax, NS, CA). Cells were seeded and allowed to attach overnight. Transductions took place in reduced serum media (DMEM with 0.1% FBS and 1% AB/AM) and 8μg hexadimethrine bromide (Sigma Aldrich) was added per mL of media to increase the transduction efficiency. Cells were transduced with 100 MOI of virus which had been determined to result in optimal infection of cells with no visible toxicity. Hexadimethrine bromide was added to the reduced serum media and this was incubated with the virus for 15 minutes and added drop wise to the cells. After 24 hours media was topped up (50% of existing volume) with 10% FBS-DMEM. After 48 hours media was replaced with fresh 10% FBS-DMEM, and at 120 hours the effects of overexpression were examined. An experimental timeline is presented in figure 2.1.

2.15 Cells Counts Using a Hemocytometer

CMFs were seeded at 50,000 per 35 mm dish in 10% FBS-DMEM. After 24 hours media was replaced with reduced serum media to arrest cell growth. After an

additional 24 hours period, 5μM ISO was added in 10% FBS-DMEM, control cells received 10% FBS-DMEM only. Cells were trypsinized, centrifuged at 2,000 rpm for two minutes, re-suspended and counted using a hemocytometer at 24, 48 and 72 hours post drug treatment. An experimental timeline is presented in figure 2.1.

2.16 CyQUANT Cell Proliferation Assay

A CyQUANT cell proliferation assay (Invitrogen) was used to measure CMF proliferation according to manufacturer's instructions. Cells were seeded in a 96 well plate (UV-Star microplate, Greiner Bio One, catalogue #655809) coated with fibronectin. A standard curve was created using known numbers of cells, and the resulting fluorescence was measured with a plate reader. For various experiments, cells were plated at a density of 1,000 cells per well in 10% FBS-DMEM and allowed to attach overnight.

To examine the effects of various compounds on CMF proliferation, reduced serum media (0.1% FBS-DMEM) was added for 24 hours to arrest cell growth. The following day, the compounds of interest were added in 10% FBS-DMEM media. The drugs used were as follows: 5μM ISO, 10μM ICI-118,551 or carvedilol in the presence and absence of 5μM ISO, and 4μM or 10μM of the CDK1 inhibitor RO3306 (Sigma Aldrich). Control cells received 10% FBS-DMEM or dimethyl sulfoxide (DMSO, Thermo Fisher Scientific) as vehicle control in RO-3306 experiments. After 24, 48 or 72 hours cells were washed with PBS and plates were frozen at -80°C to assist with cell lysis (Figure 2.1).

To examine the effect of deletion of the *Npr1* gene on CMF growth, CMFs harvested from the ventricles of wild type and *Npr1* knockout mice (heterozygous and homozygous) were plated and allowed to attach overnight. Media was replaced with reduced serum media for 24 hours as explained previously, and the following day cells were treated with 5μM ISO or 10% FBS-DMEM as control. Following 24 hours treatment, cells were washed with PBS and plates were frozen at -80°C (Figure 2.1).

To examine the effect of adenoviral mediated overexpression of CDK1, transductions took place as described above in section 2.9. For experiments where transduced CMFs were treated with ISO the drug was added after 72 hours. Plates were frozen at -80°C at the end of the transduction protocol (Figure 2.1).

On the day of the assay, plates were thawed at room temperature and 200μL of CyQUANT GR dye diluted in cell lysis buffer (Invitrogen) was added to each well. Plates were then incubated in the dark at room temperature for 2 minutes before fluorescence was measured. A plate reader was used to take fluorescence readings at an excitation of 485nm and an emission of 530nm using top optics. Cell numbers were determined from the standard curve by linear regression using Graphpad Prism 4 software.

	0 hrs	24 hrs	48 hrs	72 hrs	96 hrs	120 hrs
Drug treated CD1 CMFs	Seed cells	Add reduced serum media	Add drug	Freeze 24 hr plates	Freeze 48 hr plates	Freeze 72 hr plates
***Npr1-/-* CMFs**	Seed cells	Add reduced serum media	Add drug	Freeze plates	-	-
Transduced CMFs	Seed cells	Add reduced serum media, transduce cells	Top up media with 10% DMEM	Change media to 10% DMEM or add drug	-	Freeze plates

Figure 2.1: CyQUANT cell proliferation assay timeline for drug treated CD1 cardiac myofibroblasts (CMFs), *Npr1-/-* CMFs and transduced CMFs.

2.17 Statistical Analysis

Statistical analysis was conducted using Graphpad Prism version 4 (Graphpad Software, San Diego). Data are presented as mean ± standard error of the mean (SEM). One way ANOVA with Tukey's multiple comparisons test was used to compare multiple groups, and an unpaired Student's t-test was used to compare between two groups. Statistical significance was assigned at $p<0.05$.

Chapter 3: Results

3.1 Characterization of Primary Adult Mouse Cardiac Myofibroblast Cultures

Cells were isolated from cardiac ventricles of adult male mice, subjected to periods of digestion in collagenase and plated for one hour to allow for preferential attachment of fibroblasts (Kim et al, 2002, Li et al., 2008). We observed morphological differences between freshly isolated cells (P0) and cells that had been passaged between one to three times (P1-3), therefore these two cell groups were individually characterized to examine for any potential differences in cell type distribution. In order to confirm that the isolated cells were fibroblasts, cell cultures were characterized by immunofluorescence using antibodies specific for different types of cardiac cells. Given the heterogeneous nature of fibroblasts, antibodies against αSMA, vimentin, and DDR2 (Figure 3.1 and 3.2, A-I) were used. In addition to fibroblast markers, cell cultures were also immunolabelled with the endothelial cell marker vWF (Figure 3.1 and 3.2, J-L) and antibodies against sarcomeric myosin (mf20, a cardiomyocyte marker) and smooth muscle α actinin (SMαA, a smooth muscle cell marker).

Quantification of immunofluorescence results from P0 cultures revealed that the majority of cells were positive for vimentin (66.9% ± 0.8) or αSMA (42.6% ± 18.8), while a relatively smaller percentage of cells were positive for DDR2 (22.5% ± 5.2). Endothelial cells, cardiomyocytes and smooth muscle cells were absent or nearly undetectable in P0 cultures (Figure 3.3 A). The majority of P1-3 cells were stained

positive for αSMA (94.9% ± 0.8), followed by DDR2 (54.2% ± 11.0) and vimentin (38.8% ± 4.0; Figure 3.3 B). Again, endothelial cells, cardiomyocytes and smooth muscle cells were absent or nearly undetectable in P1-3 cultures (Figure 3.3 B).

The proportion of αSMA and DDR2 positive cells significantly increased from P0 to P1-3, while the proportion of vimentin positive cells significantly decreased (Figure 3.3 C). In addition, there was a difference in localization of DDR2 in P0 (Figure 3.1 G-I) compared with P1-3 (Figure 3.2 G-I) cells. While DDR2 was located in perinuclear puncta in P0 cells, in P1-3 cells it showed a more diffuse staining pattern, and although it was found outside nuclei in these cells as well, it was also observed throughout the cytoplasm.

To ensure the immunolabelling of cells was due to specific binding of primary antibodies, but not due to non-specific binding of secondary antibodies, negative control experiments were routinely conducted by omitting primary antibodies. No immunoreactivity was detected with monoclonal anti-mouse IgG conjugated to Alexa Fluor 555 (Figure 3.4 A, B) or Alexa Fluor 488 (Figure 3.4 C, D), anti-mouse IgM μ chain conjugated to Alexa Fluor 555 (Figure 3.4 E, F), or polyclonal anti-rabbit IgG conjugated to Alexa Fluor 488 (Figure 3.4 G, H).

Given that cell cultures did not express sarcomeric myosin (mf20) or smooth muscle α actinin (SMαA), positive controls were conducted to confirm specificity of the primary antibodies. Embryonic day (E) 15.5 ventricular cell cultures contain cardiomyocytes and therefore were immunolabelled for mf20 expression (Figure 3.5 A, B) as a positive control. Adult CD1 ventricular tissue sections were immunolabelled for

SMαA as a positive control for smooth muscle cell identification (Figure 3.5 C, D). In both cases specificity of the primary antibody was confirmed by the positive controls.

Nestin expression was found to be localized to a small population of ventricular CMFs following injury to the adult rat myocardium (Beguin et al., 2011). In light of this, we investigated the expression of nestin in our cultures. Interestingly, when P0 cells were immunolabelled with an antibody against nestin, 22.7%±10.9 cells were found to be positive for nestin expression, however, nestin expression was undetectable in P1-3 cultures (Figure 3.6 A-G).

In addition to expression of nestin, P0 cells differed from P1-3 cells with respect to cell size. Adobe Photoshop 7.0 software was used to calculate cell area (μm^2). The mean area of P0 cells was significantly smaller than that of P1-3 cells (Figure 3.7: 4,303 μm^2±1106 vs. 32,267 μm^2±1,972).

Collectively these results suggest that the majority of cultured cells were CMFs, with very little contamination of endothelial cells and no evidence of contamination with cardiomyocytes or smooth muscle cells. We opted to use P1-3 CMFs for experiments as P0 cells were very heterogeneous and smaller in size. As well expression of the marker protein αSMA was less variable in P1-3 cells compared with P0 cells and P1-3 cells were more similar to CFs *in vivo* in the infarct. In addition, CMFs became senescent after P4.

3.2 βAR Expression in Adult Mouse Cardiac Myofibroblasts

Given that we intended to treat our CMF cultures with the non-selective βAR agonist ISO, βAR subtype expression was examined. Immunolabelling of P1-3 CMFs for β1 and β2ARs confirmed the presence of both subtypes. The expression of the β1AR was predominantly nuclear with very little staining at the plasma membrane (Figure 3.8 A-D). In contrast, expression of the β2AR could be seen throughout the cytoplasm and it also appeared stronger in the perinuclear region (Figure 3.8 E-H). Western blotting of lysates prepared from P1-3 CMFs confirmed protein expression of both the β1 and β2AR (Figure 3.8 I).

Subsequently, cell surface expression of βAR subtypes was examined using FACS analysis. In these experiments, CMFs were neither fixed nor permeabilized to prevent intracellular antibody staining. In addition, β1AR and β2AR antibodies specific for the respective extracellular domains were used for cell labelling to allow for measurement of receptor expression at the cell surface. For both the β1AR and β2AR FACS experiments, a no primary antibody control was used to determine the background level of fluorescence. This control was used to set the threshold levels of fluorescence for gating cells into either negative or positive categories (Figures 3.9 and 3.10 A-D). CMF β1AR expression was found to be 38.6%±1.3 at the cell surface while β2AR expression was found to be 5.8% ± 0.3 at the cell surface as determined by FACS analysis (Figure 3.11). These results indicate that β1AR positive cell number is significantly higher than the β2AR positive cells in P1-3 CMF cultures (≈6 fold higher, Figure 3.11).

3.3 Second Messenger Response to ISO in Adult Cardiac Myofibroblast Cultures

In order to determine the optimal dose of ISO, a high throughput heterogeneous time resolved fluorescence (HTRF) assay was used to measure levels of the second messenger cAMP in response to βAR stimulation by ISO. cAMP concentrations were extrapolated from a standard curve generated using samples with known concentrations of cAMP (Figure 3.12 A and B). CMFs were treated with 0.1, 0.5, 1, 5 or 10μM ISO. Although all doses of ISO resulted in significantly greater cAMP generation compared with basal cAMP levels (0.0017±0.0004 nM cAMP/cell), 5μM ISO elicited the greatest response (0.0085±0.0010 nM cAMP/cell) representing a 5 fold increase in cAMP generation vs basal, and was therefore selected for future experiments (Figure 3.13 A).

The same HTRF assay was used to determine βAR subtype contribution to the ISO mediated increase in cAMP levels. In combination with 5μM ISO, 10μM of a selective (metoprolol or ICI) or non-selective (carvedilol or propranolol) βAR blocker was added. Once again, treatment with 5μM ISO alone resulted in significantly more cAMP production compared with basal levels (Figure 3.13 B). Co-treatment with 10μM of the β1AR blocker metoprolol in combination with ISO was unable to prevent the ISO stimulated increase in cAMP production. In contrast, treatment with 10μM of the β2AR blocker ICI in combination with ISO did not significantly increase cAMP levels compared with basal, indicating that it prevented the ISO mediated increase in cAMP levels. In addition, treatment with two non-selective βAR blockers, propranolol and carvedilol, in combination with ISO did not result in a significant increase in cAMP

levels compared with basal (Figure 3.13 B). These data suggest that the β2AR may play a more prominent role in ISO mediated cAMP production compared with the β1AR.

3.4 Cardiac Myofibroblast CDK1 Expression Increases *in vitro* in Response to ISO

Previous work in the lab revealed that CDK1 expression was induced in non-cardiomyocytes of the adult mouse myocardium in response to chronic infusion of ISO for a period of 7 days (Gaspard et al, In Press). To examine whether the *in vivo* results could be reproduced *in vitro,* CMF cultures were treated with 5μM ISO for 30 minutes, 4 hours or 24 hours and levels of CDK1 mRNA expression were measured by QPCR. CDK1 gene expression levels were normalized to mRNA levels of mouse TATA box binding protein (mTBP). The mTBP expression levels were consistent between control and ISO treated samples. No significant differences in relative CDK1 mRNA expression were observed after 30 minutes or 4 hours of ISO treatment compared with controls (Figure 3.14 A). Following 24 hours of ISO treatment, CDK1 mRNA levels were significantly increased in ISO treated samples (Figure 3.14 A). Compared with control (expression=1.0) there was an approximately 1.5 fold increase (1.48±0.23 vs control) in CDK1 expression. These results suggest that ISO is able to increase CDK1 mRNA expression *in vitro* in CMFs.

To investigate whether the increase in mRNA was translated to an increase in protein expression, CMFs were treated with ISO for 24 or 48 hours and subsequently immunolabelled with antibodies specific for CDK1 and αSMA (Figure 3.14 B-E). To

determine the number of CDK1 positive CMFs following ISO treatment, only cells positive for αSMA were assessed for expression of CDK1. The localization of CDK1 in ISO treated CMFs was not different from control treated CMFs, as it was predominantly nuclear in both groups (Figure 3.14 B-E). When compared with control, a significant increase in the number of CDK-expressing cells was observed in ISO treated CMFs after both 24 (control: 9.9% ± 1.9 vs. ISO: 15.3 ± 1.0) and 48 hours (control: 7.7% ± 1.6 vs. ISO: 15.8 ± 2.4) of treatment (Figure 3.14 F and G). Therefore ISO is able to increase the percentage of CDK1 positive CMFs *in vitro* suggesting that it promotes proliferation.

We also examined the effects of stimulation with the endogenous catecholamine NE on CMF CDK1 expression. CMFs were treated with 10 μM NE for 48 hours and assessed by immunolabelling for the number of CDK1-expressing cells (Figure 3.15). When compared with control, an increase in the number of CDK1 positive cells was observed 48 hours after treatment with 10 μM NE (control: 9.0% ± 2.6 vs. NE: 15.6% ± 1.6).

3.5 ISO Induced Increase in CDK1 is not Detectable by Western Blotting and CDK1 Activation is not Affected by β-Adrenergic Receptor Activation

Given that ISO was found to increase the percentage of CDK1 expressing CMFs as demonstrated by immunofluorescence, we investigated if an increase in CDK1 protein expression could be detected by Western blotting. To this end, CMFs were treated with ISO for 48 hours and protein lysates were collected and examined for total CDK1

expression levels which were then normalized to levels of GAPDH. In contrast to the immunofluorescence results, Western blot analysis did not reveal any significant difference in the levels of total CDK1 after 48 hours of ISO treatment compared with the control (Figure 3.16 A and B).

In order to examine the activation state of CDK1 following ISO treatment, Western blot analysis was conducted on protein lysates from CMFs treated with or without ISO for 15 minutes, 30 minutes, or 1 hour. In order to be activated and allow progression through the G2/M phase of the cell cycle, CDK1 must be dephosphorylated at Tyr 15 and Thr 14 (4). An antibody specific for phosphorylated CDK1 at Tyr 15 was used and results were normalized to levels of total CDK1 protein. No significant differences in pCDK1 were observed between control and ISO treated samples at any of the time points examined (Figure 3.16 C and D). However, pCDK1 showed a trend toward a decrease in the ISO treated samples at 30 minutes and 1 hour, indicating that there may be a decrease in CDK1 inhibitory phosphorylation, which could translate to an increase in levels of active CDK1 protein in response to ISO treatment.

3.6 ISO does not Influence Cyclin B1 Levels

In order to progress through the G2/M phase of the cell cycle, CDK1 must be bound to its regulatory CYCB1 subunit (4). In light of this, CMFs were treated with control or ISO for 48 hours and immunolabelled with antibodies specific for CYCB1 and CDK1 (Figure 3.17 A-D). CYCB1 expression was localized to the nuclei of CMFs (Figure 3.17 A-D). The percentage of total cells positive for CYCB1 as well as CYCB1

co-localized with CDK1 (CYCB1/CDK1) was quantified. No significant differences in CYCB1 or CYCB1/CDK1 co-expressing cells were observed in ISO treated CMFs compared to controls (Figure 3.17 E). These results indicate that although ISO is able to increase the percentage of CDK1 positive in CMFs, it does not influence the number of CYCB1 positive cells, nor does it affect the association of CDK1 with CYCB1.

3.7 Cardiac Myofibroblast DNA Synthesis and Proliferation Increases in Response to ISO

Previous studies have demonstrated that catecholaminergic stimulation of CFs results in increased DNA synthesis and can be pro-mitogenic *in vitro*, however, none of these studies were conducted in adult mouse CMFs. Our results show that ISO increased CDK1 expression in CMFs which may increase proliferation, therefore we sought to examine the effect of ISO stimulation on adult mouse CMF DNA synthesis.

CMFs were treated with ISO for a total of 72 hours and pulsed with BrdU for the last 24 hours. BrdU is a thymidine analog and is incorporated into DNA during replication. Anti-BrdU antibodies were used to detect the presence of BrdU as a measure of proliferation (Figure 3.18 A-C). The percent BrdU labelling index in control cells was 19.3% ± 2.5 compared with 32.9% ± 0.9 in ISO treated cells. We concluded that ISO stimulation results in significantly increased CMF DNA synthesis compared with control (Figure 3.18 D).

Increased DNA synthesis does not necessarily lead to increased proliferation; therefore proliferation was measured more directly by counting the number of cells in

cultures treated with or without ISO. Cells were seeded at 50,000 cells per dish and treated with 5μM ISO. At 24, 48 and 72 hours post treatment CMFs were trypsinized and counted. No differences in proliferation were seen at 24 hours, however although not significant, 48 hours of ISO treatment was able to increase the number of CMFs compared with no treatment control (ISO: 215,875 ± 40,566 vs control: 139,250 ± 55,005). After 72 hours of ISO treatment the mean difference in cell number was statistically significant between ISO treated (361,667 ± 28,038) and control CMFs (277,667 ± 9,597; Figure 3.20 A).

In order to further confirm the mitogenic effect of ISO, CMFs seeded at a density of 1,000 cells per well were treated for 24, 48 or 72 hours and subjected to a CyQUANT cell proliferation assay to assess changes in cell number. Cell numbers were determined based on recorded fluorescence readings using a standard curve (Figure 3.19 A and B). In accordance with what was observed with the hemocytometer assay, no significant differences in proliferation were found 24 or 48 hours following ISO treatment. 72 hours after ISO treatment statistical analysis showed that the mean number of ISO treated CMFs was significantly increased compared with control treated cells (8,519 ± 167.1 vs 6,328 ± 52.5; Figure 3.20 B).

3.8 Overexpression of CDK1 is not Sufficient to Increase Cardiac Myofibroblast Proliferation

Given that stimulation with ISO resulted in both increased CDK1 expression and proliferation in CMFs, we examined whether overexpression of CDK1 alone was

sufficient to increase proliferation. Cells were transduced with adenoviral vectors harboring either CDK1 (adenoCDK1) or a constitutively active form of CDK1 (adenoCDK1AF) and immunofluorescence staining was conducted to confirm overexpression of CDK1. Using a GFP adenovirus (adenoGFP) the transduction efficiency was determined to be approximately 60%. Expression of CDK1 was notably stronger in cells transduced with either adenoCDK1 or adenoCDK1AF when compared with endogenous expression levels in non-transduced cultures (Figure 3.21 A-I). Transduced cultures had 50.0 ±7.0% of CDK1 positive CMFs while non-transduced cultures had 7.7±1.6% of CDK1 positive CMFs. CMFs were then transduced with either adenoCDK1, adenoCDK1AF or adenoGFP as a control and subsequently assayed for cell proliferation by CyQUANT. No significant differences in cell proliferation were observed between the different treatments 96 hours post transduction (Figure 3.21 J).

Treating CMFs with ISO for 48 hours during transduction resulted in significant increases in proliferation of cells expressing adenoGFP, adenoCDK1 and adenoCDK1AF compared with control transduced CMFs (Figure 3.21 K). Cells expressing adenoCDK1AF had a more modest increase in proliferation compared with those expressing adenoGFP or adenoCDK1.

3.9 Inhibition of CDK1 Activity was Sufficient to Decrease Cardiac Myofibroblast Proliferation

We next investigated whether pharmacological inhibition of CDK1 was able to decrease CMF proliferation. The ATP-competitive CDK1 inhibitor RO-3306 has been

shown to inhibit CDK1/CYCB1 activity and is more selective for CDK1 vs. CDK2 or CDK4. At a dose of 4 μM it has been shown to exhibit nearly 90% inhibition of CDK1 and at 10 μM almost 100% inhibition of CDK1 is achieved (Vassilev et al., 2006), thus both of these doses were tested for their ability to inhibit CMF proliferation.

CMFs were treated with either 4 or 10 μM RO-3306 or vehicle alone for 24, 48 or 72 hours and cell proliferation rates were assessed using the CyQUANT assay. No significant differences in proliferation were seen after 24 or 48 hours with either dose. After 72 hours treatment with 10 μM RO-3306, CMF proliferation was significantly decreased compared with vehicle control (5,577 ± 938.3 vs. 12,959 ± 1,374) (Figure 3.22). These results suggest that pharmacological inhibition of CDK1 is sufficient to decrease adult CMF proliferation.

3.10 βAR Blockade Prevents ISO Induced Cardiac Myofibroblast Proliferation

Carvedilol (a non-selective βAR blocker) and ICI (a β2AR specific blocker) were both able to prevent the ISO induced increase in cAMP (Figure 3.13 B), therefore we investigated the effects of those β-blockers on CMF proliferation. CMFs were treated with a single dose of ISO and one dose of either ICI or carvedilol at a ratio of 1:2 for 24 or 48 hours and cell proliferation was assessed by the CyQUANT assay.

Carvedilol was able to prevent ISO induced CMF proliferation after 24 hours treatment (a ≈7 fold decrease compared to control). It did not significantly modulate proliferation after 48 hours (Figure 3.23 A).

CMFs treated with ISO in combination with ICI for 24 hours showed a reduction in proliferation compared with ISO treated control CMFs (a ≈5.6 fold decrease compared to control). Treatment with ICI was not able to decrease proliferation after 48 hours compared with ISO treated control (Figure 3.23 B).

These data demonstrate that βAR blockade is capable of preventing ISO induced increases in CMF proliferation. The ability of ICI to prevent the ISO mediated increase in CMF proliferation highlights the importance of β2AR signalling in the regulation of CMF proliferation.

3.11 Phosphorylated ERK1/2 Protein Levels Increase in Response to ISO

βAR stimulation by ISO leads to an increase in active, phosphorylated ERK (pERK) in adult rat CFs (Kim et al., 2002), and ERK1/2 is well known to be activated by mitogenic signals and involved in cell proliferation, therefore we investigated pERK1/2 levels in adult mouse CMFs in response to ISO.

Western blot analysis was conducted on protein lysates from ISO and control samples treated for 15 minutes, 30 minutes or 1 hour. An antibody specific for pERK1/2 was used and normalized to levels of total ERK1/2. No significant differences in pERK1/2 levels were found after 15 minutes of ISO treatment, however, after 30 minutes of ISO treatment levels of pERK1/2 were significantly increased compared with the control (Figure 3.24 A, B). One hour post treatment pERK1/2 expression levels were

once again similar to the control (Figure 3.24 B). These results suggest that in response to ISO stimulation, ERK1/2 activation is transiently increased in adult mouse CFs.

3.12 ISO Modulates Cardiac Myofibroblast Gene Expression

Signalling in the heart after injury leads to fibroblast activation, and when in a more active state fibroblasts increase ECM remodelling and therefore changes in gene expression occur. In light of this, QPCR analysis was conducted on samples from CMFs treated for 30 minutes, 4 hours, or 24 hours to examine mRNA expression levels in response to ISO as a measure of fibroblast activation.

No significant differences in the mRNA expression levels of collagen type 1 α1 in response to ISO treatment were observed at any of the time points investigated (Figure 3.25 A). However, collagen type 3 α1 expression was significantly increased 24 hours after ISO treatment (Figure 3.25 B). There was an approximately 2.5 fold increase in collagen type 3 α1 levels relative to control (control expression=1.0, ISO treated=2.76±0.84). CTGF mRNA expression levels were also found to be significantly increased compared with no treatment control (Figure 3.25 C). Compared with the no treatment control (expression=1.0) there was an approximately 2.5 fold increase (2.69±0.87 vs control) in CTGF mRNA expression. Expression of αSMA was also increased 24 hours after ISO stimulation (1.74±0.34 vs control; Figure 3.25 D). There were no significant changes in mRNA levels of fibronectin 1 following ISO treatment compared with control (Figure 3.25 E). There was an approximately 2 fold increase in

plasminogen activator inhibitor mRNA expression following ISO treatment compared with no treatment control mRNA expression levels (Figure 3.25 F: 2.33±0.66 vs control).

These data suggest that CMFs are more active 24 hours following ISO stimulation with respect to the transcription of several genes known to be involved in the fibrotic response.

3.13 Pro-collagen Type 1 α1 Protein Expression is not Modulated by ISO

While collagen type 1 α1 mRNA levels were not changed by ISO treatment, it was possible that an increase could occur at the level of protein translation. In order to determine the effect of ISO on collagen type 1 α1 protein levels, CFs were treated with ISO for 48 hours and subsequently immunolabelled with an antibody against pro-collagen type I (a precursor of collagen type 1 α1; Figure 3.26 A-C). Quantification revealed no significant differences in the number of pro-collagen type 1 α1 positive CMFs following 48 hours of ISO treatment, suggesting that collagen type 1 α1 protein expression is not modulated by ISO (Figure 3.26 D).

3.14 Characterization of Cardiac Myofibroblast Proliferation in a Mouse Model of Heart Failure

ANP is known to exhibit antifibrotic effects in the heart (Cao & Gardner, 1995; Fujisaki et al., 1995; Glenn et al., 2009b). *Npr1* (ANP's high affinity receptor) knockout

mice develop symptoms of cardiomyopathy and heart failure before the age of 6 months (Oliver et al., 1997). In light of this, CMFs were harvested from the hearts of *Npr1* wild type, heterozygous, and homozygous knockout mice and differences in proliferation were examined after 24 hours.

While CMFs from wild type and heterozygous *Npr1* mice had similar levels of growth, *Npr1* knockout cells had significantly increased proliferation compared with wild type. Knockout CMFs showed a two fold increase compared with wild type (Figure 3.27 A: 15,994 ± 1,041 vs 7,419 ± 431.5).

The effect of ISO treatment on *Npr1-/-* was also examined. *Npr1* CMFs were treated with ISO for 24 hours and assessed with a CyQUANT cell proliferation assay. Treatment with ISO significantly increased CMF proliferation of wild type CMFs compared with basal proliferation (Figure 3.27 B: 12561 ± 211.3 vs 7419 ± 431.5). ISO was not able to modulate proliferation of heterozygous or knockout *Npr1* CMFs.

Figure 3.1: P0 Adult cardiac myofibroblast culture characterization. Unpassaged (P0) adult cardiac myofibroblast (CMF) cultures from male CD1 mouse hearts were immunolabelled to characterize cell types present. The first column shows representative fields of cells labelled with the antibody of interest, the second column shows the same field stained with Hoechst 33258 nuclear stain, the third column shows a merged image. White arrows indicate cells positive for the antibody of interest. P0 cell cultures were labelled with antibodies specific for αSMA (**A-C**), vimentin (**D-F**) and DDR2 (**G-I**) to identify cardiac fibroblasts and myofibroblasts. Of note is the expression of DDR2 in P0 cells, which occurs in puncta located just outside the nucleus (**G-I**). An antibody specific for vWF was used to identify endothelial cells (**J-L**). Insets corresponding to the boxed regions show cells of interest magnified (**G** and **J**). Scale bar = 100μm (**A-L**).

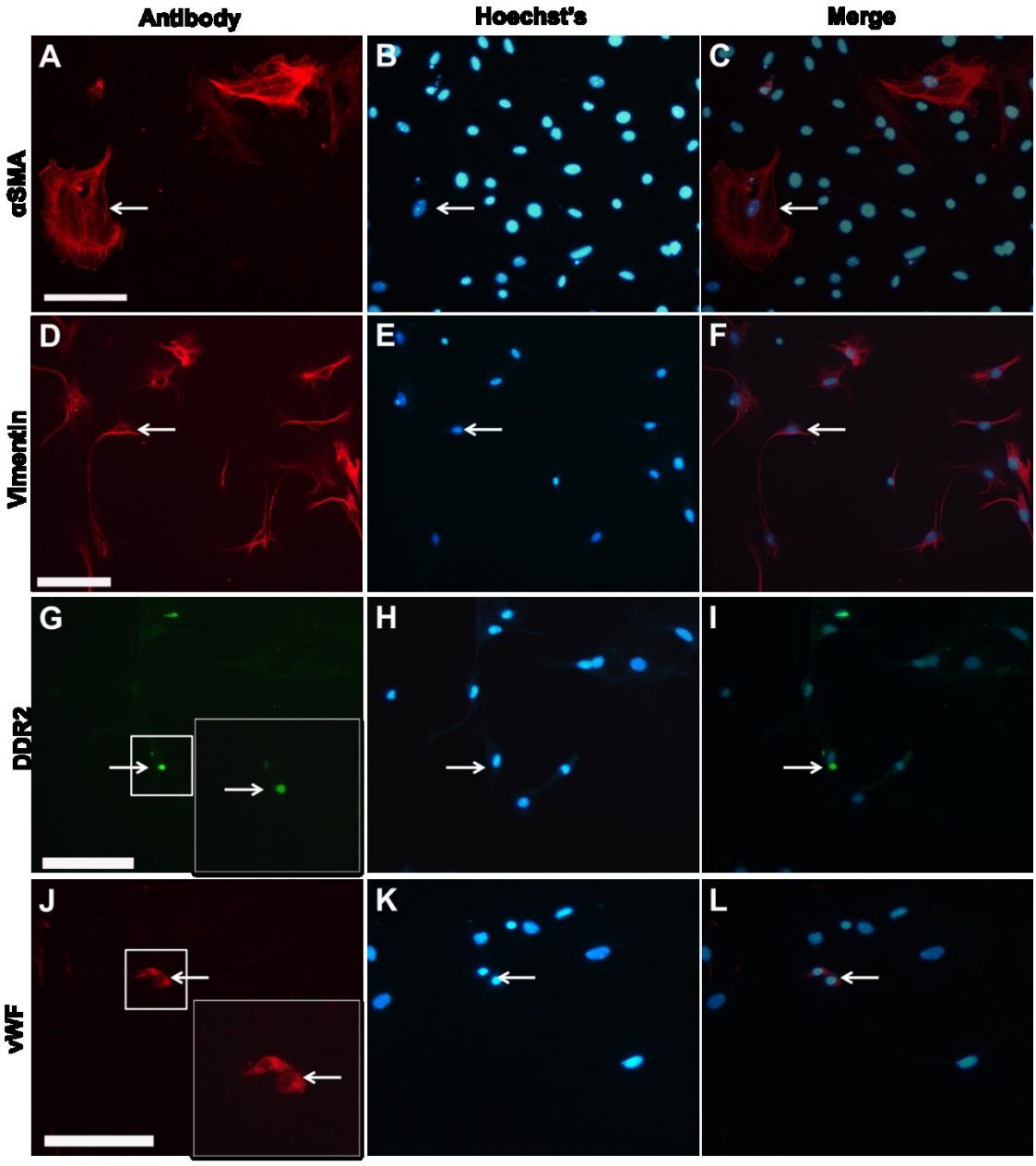
Antibody
Hoechst's
Merge
αSMA
Vimentin
DDR2
vWF
A
B
C
D
E
F
G
H
I
J
K
L

Figure 3.2: P1-3 Adult cardiac myofibroblast culture characterization. Passaged (P1-3) adult cardiac myofibroblast (CMF) cultures from male CD1 mouse hearts were immunolabelled to characterize cell types present. The first column shows representative fields of cells stained with the antibody of interest, the second column shows the same field stained with Hoechst 33258 nuclear stain, the third column shows a merged image. White arrows indicate cells positive for the antibody of interest. P1-3 cell cultures were labelled with antibodies specific for αSMA (**A-C**), vimentin (**D-F**) and DDR2 (**G-I**) to identify cardiac fibroblasts and myofibroblasts. An antibody against vWF was used to identify endothelial cells (**J-L**). Scale bar = 100μm (**A-L**).

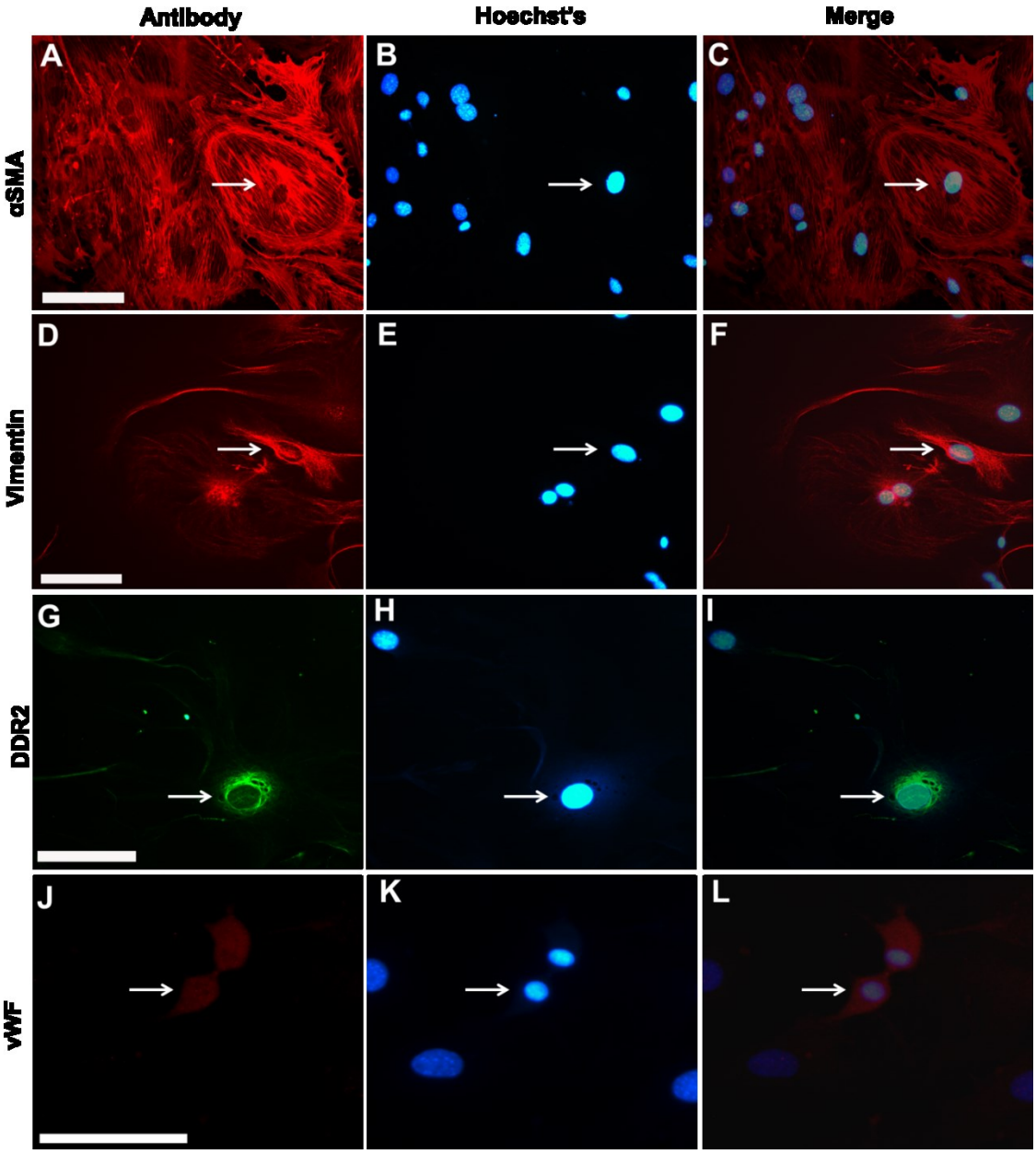
Antibody
Hoechst's
Merge
αSMA
Vimentin
DDR2
vWF
A
B
C
D
E
F
G
H
I
J
K
L

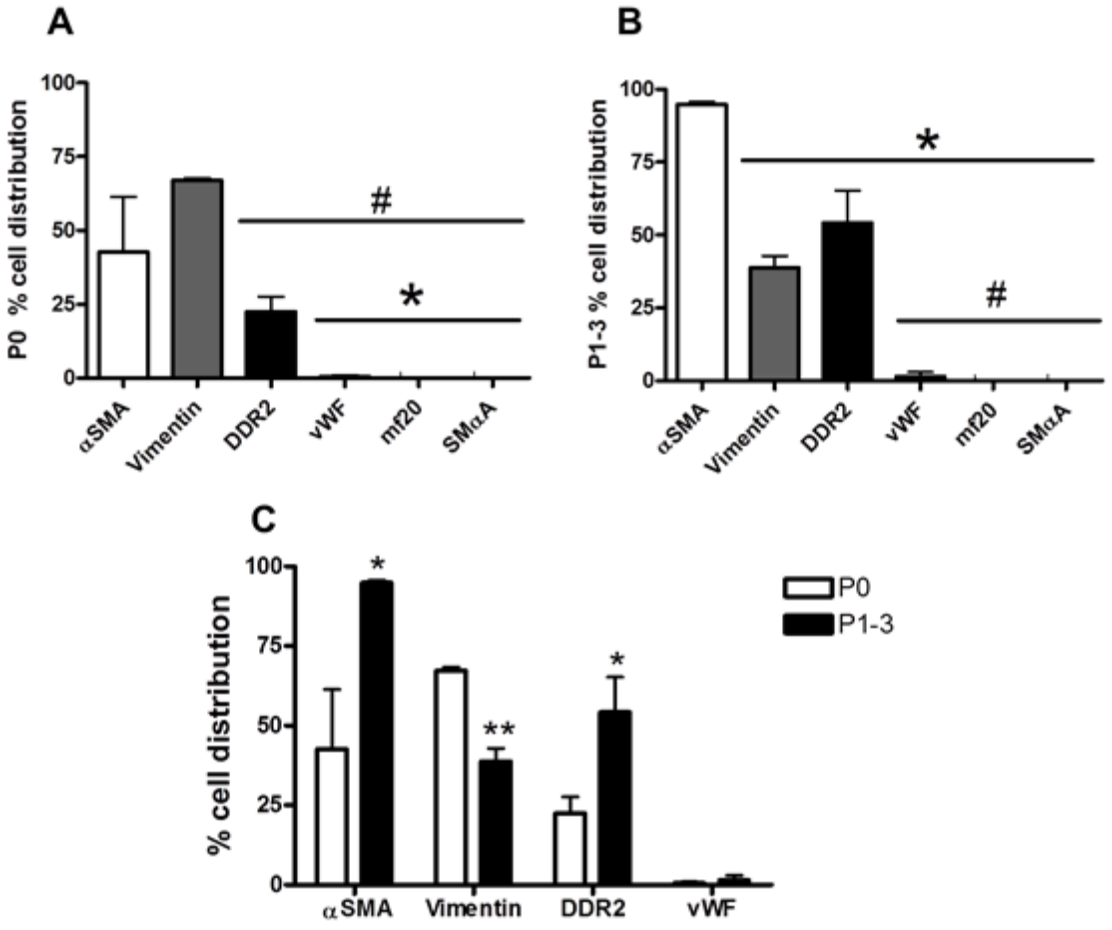

Figure 3.3: P0 and P1-3 adult cardiac myofibroblast culture characterization. Quantification of P0 CMF cultures immunolabelled with αSMA, vimentin, DDR2 and the endothelial cell marker vWF. No cells were found to express mf20 (sarcomeric myosin), a cardiomyocyte marker, or smooth muscle α actinin (SMαA), a smooth muscle cell marker. *P<0.05 vs αSMA, #P<0.05 vs vimentin, one way ANOVA with Tukey's Multiple Comparison Test (**A**). Quantification of P1-3 CMF cultures immunolabelled with αSMA, vimentin, DDR2 and vWF. No cells were found to express mf20, or SMαA, a smooth muscle cell marker. *P<0.05 vs αSMA, #P<0.05 vs vimentin and DDR2, one way ANOVA with Tukey's Multiple Comparison Test (**B**). Comparison of P0 and P1-3 CMF cultures indicated changes in CMF marker expression between the two groups. *P<0.05 vs P0, **P<0.005 vs P0, unpaired Student's t-test (**C**). Results are mean±SEM of N=3 experiments, approximately 200-300 cells counted per experiment.

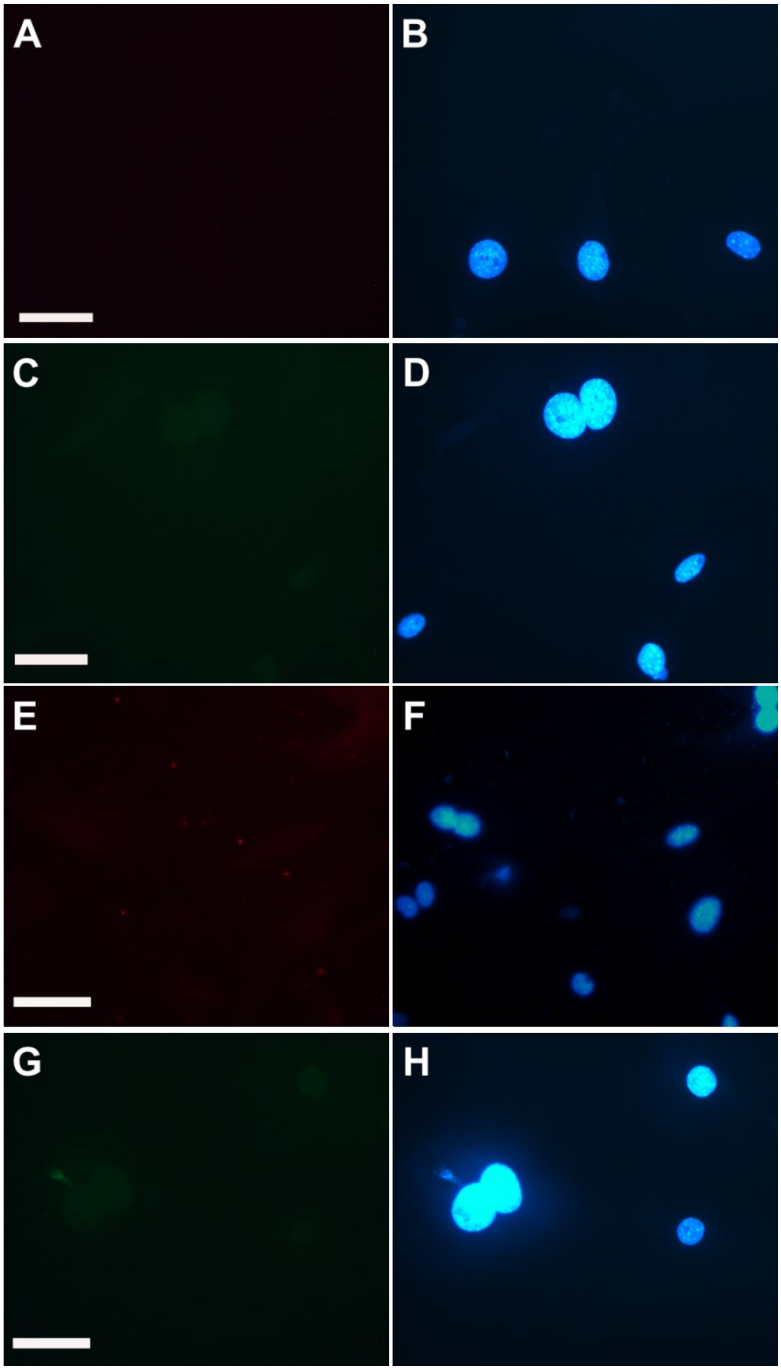

Figure 3.4: Negative antibody control experiments. In order to confirm the specificity of primary antibodies, adult P1-3 cardiac myofibroblasts (CMFs) were immunolabelled with the primary antibody omitted and Hoechst 33258 nuclear stain. No immunoreactivity was detected with monoclonal anti-mouse IgG conjugated to Alexa Fluor 555 (**A, B**) or Alexa Fluor 488 (**C, D**), anti-mouse IgM μ chain conjugated to Alexa Fluor 555 (**E, F**), or polyclonal anti-rabbit IgG conjugated to Alexa Fluor 488 (**G, H**). Scale bar = 100μm.

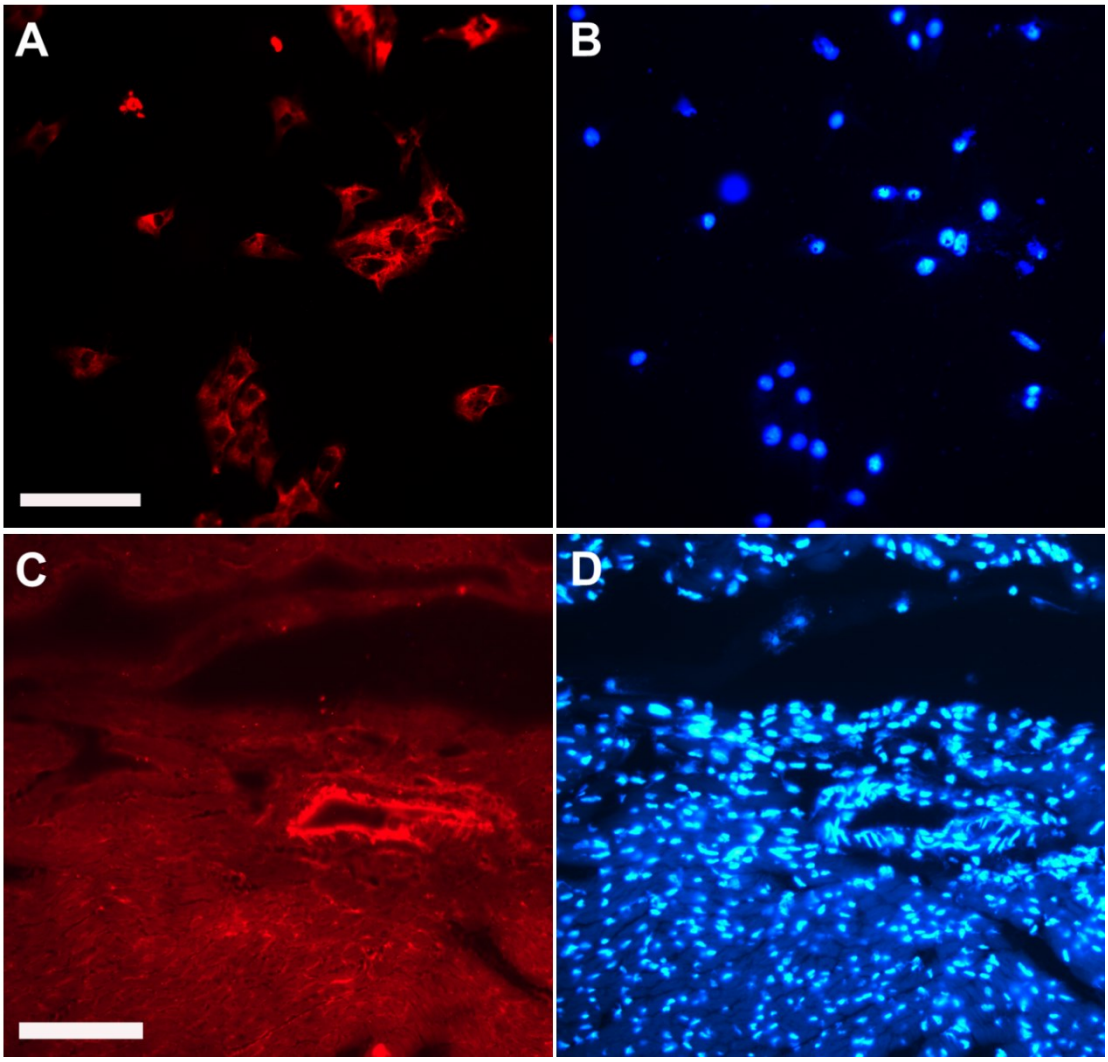

Figure 3.5: Positive antibody control experiments. E15.5 ventricular cell cultures were immunolabelled with a primary antibody specific for sarcomeric myosin (**A**) and Hoechst 33258 nuclear stain (**B**). Adult CD1 ventricular sections were immunolabelled with smooth muscle α actinin (**C**) and Hoechst 33258 nuclear stain (**D**). Scale bar = 100μm.

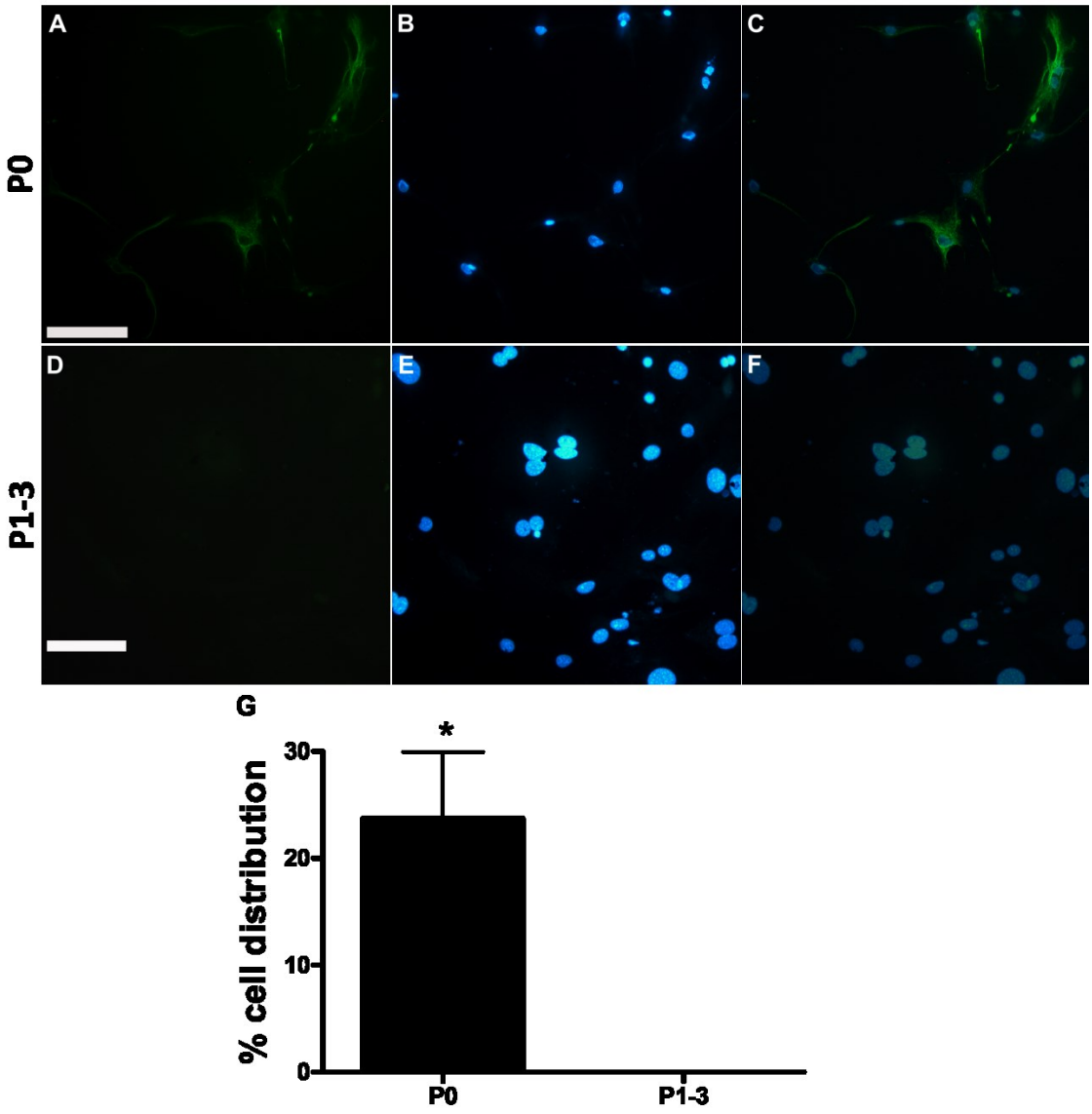

Figure 3.6: Expression of nestin in P0 and P1-3 cardiac myofibroblast cultures. CMFs from either P0 (**A-C**) or P1-3 (**D-F**) cultures were immunolabelled with an antibody against nestin. The first column shows representative fields of cells labelled with nestin, the second column shows the same field labelled with Hoechst 33258 nuclear stain, and the third shows a merged image. Quantification of nestin immunolabelling revealed that ≈23% of P0 CMFs were positive for nestin expression, no nestin positive cells were found in P1-3 CMF cultures. *P<0.05 vs. P0, unpaired Student's t-test (**G**). Results are mean±SEM, N=3 experiments, approximately 200-300 cells counted per group in each experiment. Scale bar = 100µm.

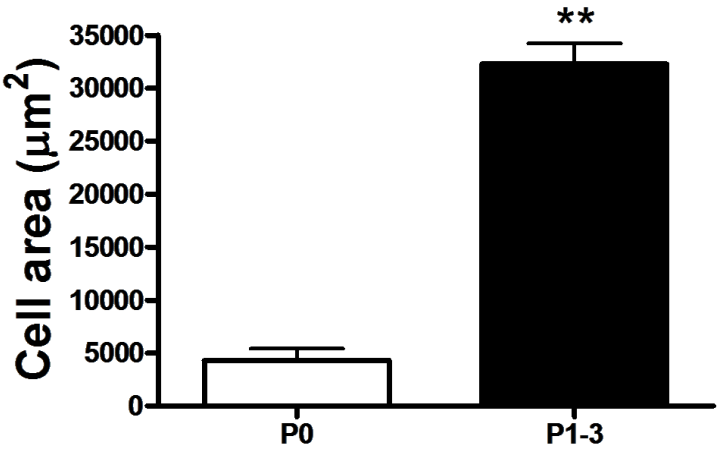

Figure 3.7: Cell area comparisons in P0 and P1-3 cardiac myofibroblast cultures. The area of CMFs from either P0 or P1-3 cultures was measured to determine cell size using cells immunolabelled with αSMA to indicate cell boundaries. The mean area of P0 cells (≈4,300 μm^2) was significantly smaller than P1-3 cells (32,000 μm^2). **P<0.005, unpaired Student's t-test. Results are mean±SEM, N=3 experiments, approximately 200-300 cells counted per experiment.

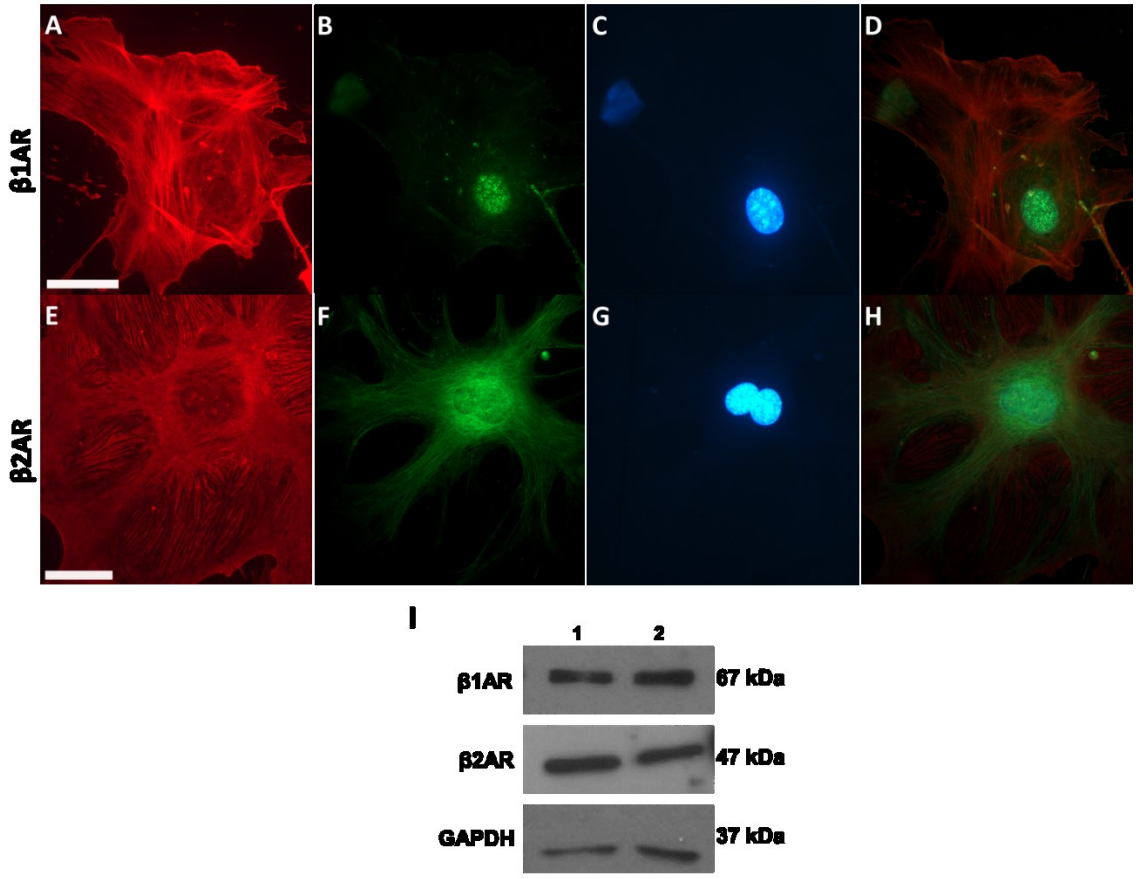

Figure 3.8. β1 and β2 adrenergic receptors are present in P1-3 cardiac myofibroblast cultures. Immunolabelling revealed expression of both the β1 and β2AR subtype in P1-3 CMFs. Representative images of CMFs immunolabelled with antibodies against αSMA (**A** and **E**), the β1AR (**B**) or β2AR (**F**), and Hoechst 33258 nuclear stain (**C** and **G**). Merged images are shown in **D** and **H**. Scale bar = 50μm. Presence of both β1 and β2ARs were also detected in cardiac fibroblast protein lysates by Western blotting, lanes 1,2 represent protein lysates prepared from two independent CMF cultures (**I**).

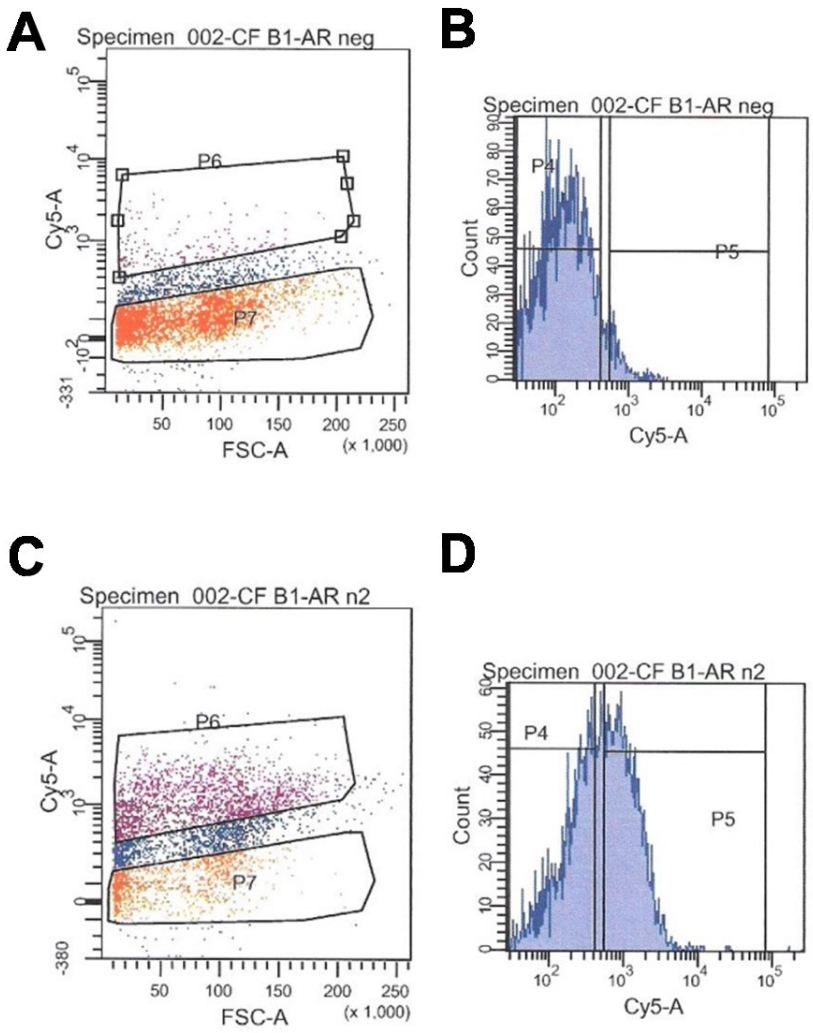

Figure 3.9: Representative FACS experiment for cell surface expression of the β1AR in unfixed cardiac myofibroblasts. The upper panel shows a representative negative control of CMFs labelled with secondary antibody only and subjected to FACS (**A**, **B**). The lower panel shows CMFs labelled with an antibody against the extracellular domain of the β1AR which then underwent FACS (**C, D**). Dot plots (**A, C**) show the measured fluoresence of each individual cell represented as a dot. Viable cells are outlined in the region labeled P6. Histograms (**B, D**) represent the percent of positive cells based on their fluoresence intensity. Results from the negative control FACS experiment were used to set a threshold level of fluoresence (**B**, double black vertical lines), above which any cell would be considered positive for β1AR expression. When labelled with the β1AR antibody, a shift to the right occurred representing the proportion of cells that were considered positive for β1AR expression at the cell surface (**D**).

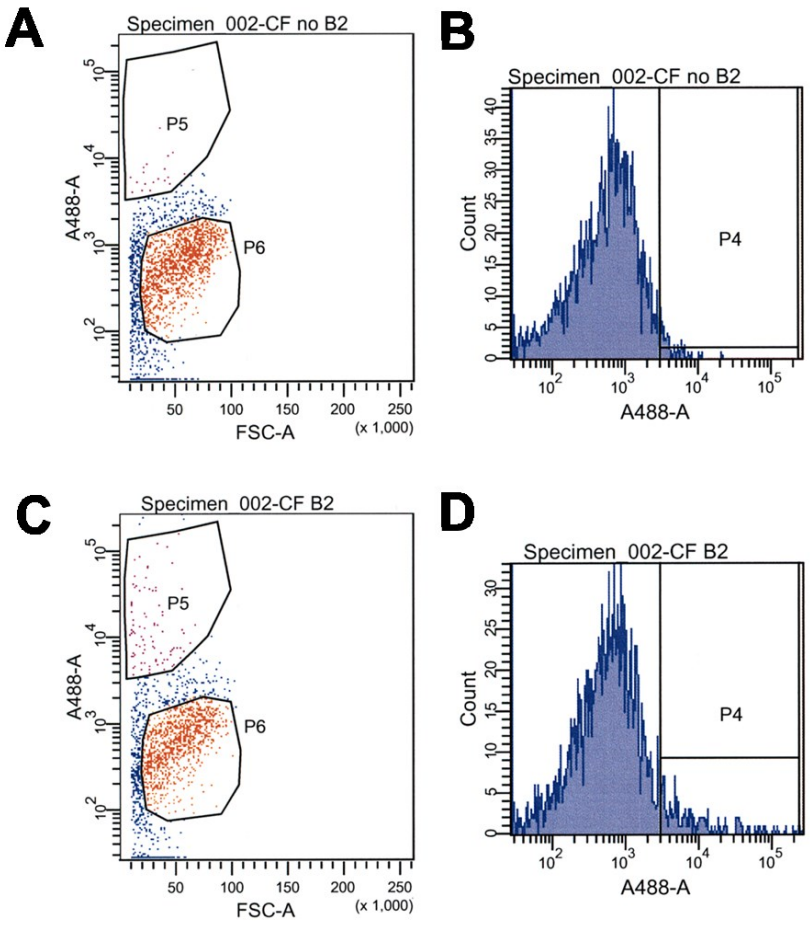

Figure 3.10: Representative FACS experiment for cell surface expression of the β2AR in unfixed cardiac myofibroblasts. The upper panel shows a representative negative control of CMFs labelled with secondary antibody only and subjected to FACS (**A**, **B**), while the lower panel shows cells labelled with an antibody against the extracellular domain of the β2AR which then underwent FACS (**C, D**). Dot plots (**A, C**) show the measured fluoresence of each individual cell represented as a dot. Viable cells are outlined in the region labelled P6. Histograms (**B, D**) represent the percent of positive cells based on their fluoresence intensity. Results from the negative control FACS experiment were used to set a threshold level of fluoresence (**B**, double black vertical lines), above which any cell would be considered positive for β2AR expression. When labelled with the β2AR antibody, a shift to the right occurred representing the proportion of CMFs that were considered positive for β2AR expression at the cell surface (**D**).

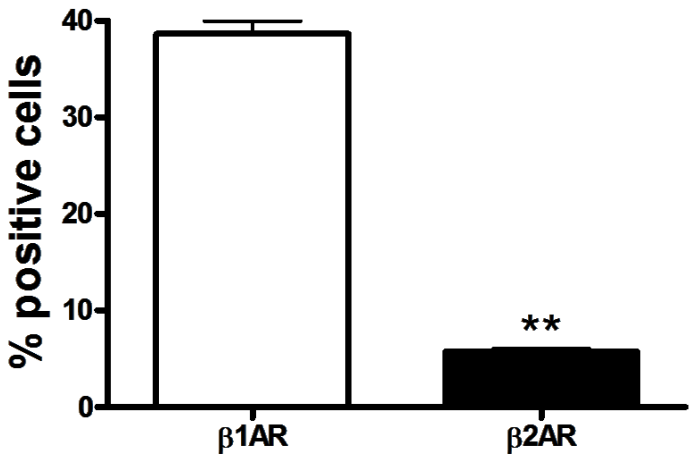

Figure 3.11. β1 and β2 adrenergic receptor expression at the cell surface of cardiac myofibroblasts. Data from FACS analysis indicated that β1ARs are present at the cell surface in 38.6%±1.3 of CMFs, while β2ARs are present at the surface of 5.8%±0.3 of CMFs. **P<0.005 vs β1AR, unpaired Student's t-test. Results are mean±SEM of 3 experiments/group.

A

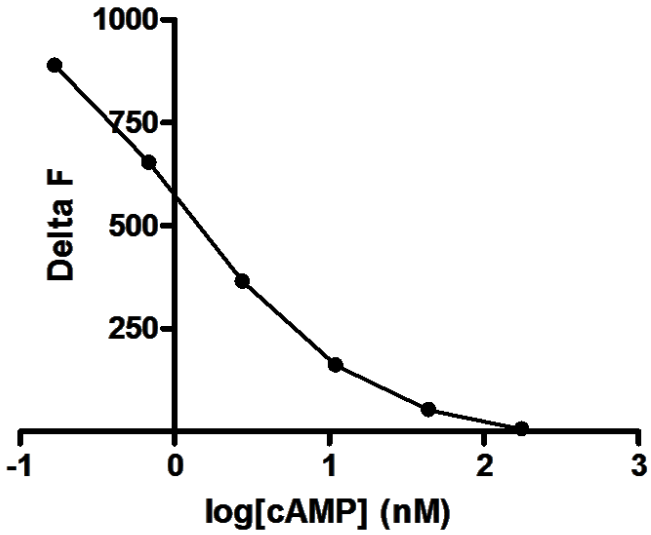

B

[cAMP] (nM)	Delta F
712	-9.3
178	5.3
44.5	51.8
11.1	160.8
2.78	363.9
0.69	652.3
0.17	888.0

Figure 3.12 cAMP standard curve. A cAMP standard curve was created by graphing Delta F values from standards with previously determined concentrations of cAMP ranging from 0.17 to 712 nM (**A**). The table shows the concentration of the standard and the corresponding Delta F value. Delta F values presented are the average of 5 experiments performed in duplicates (**B**).

Figure 3.13: Second messenger responses to ISO stimulation in cardiac myofibroblasts occur mainly through the β2 adrenergic receptor. All concentrations of ISO tested were able to significantly increase CMF cAMP levels. CMFs exhibited a maximal response to ISO at 5μM (**A**). *P<0.05 vs basal, **P<0.005 vs basal, one-way ANOVA with Tukey's Multiple Comparison Test. Results are mean±SEM of 10-15 experiments/group. The β1AR blocker metoprolol was unable to decrease cAMP levels in the presence of ISO, however, the β2AR blocker ICI-118,551 as well at the non-selective βAR blockers propranolol and carvedilol were able to prevent the ISO mediated increase in cAMP levels (**B**). *P<0.05 vs basal, one-way ANOVA with Tukey's Multiple Comparison Test. Results are mean±SEM of 5 experiments/group performed in duplicates.

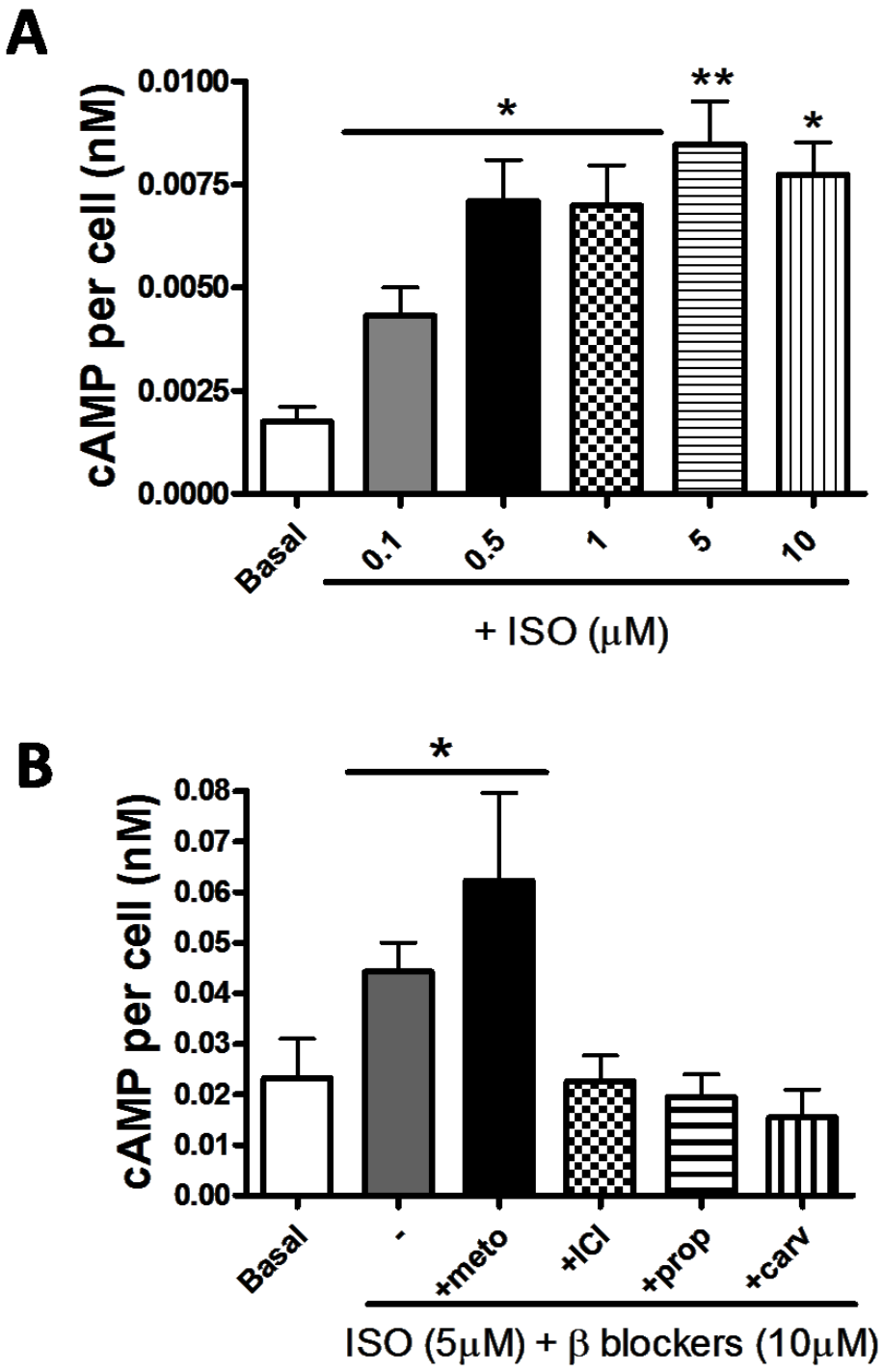
A
cAMP per cell (nM)
0.0100
0.0075
0.0050
0.0025
0.0000
*
**
*
Basal
0.1
0.5
1
5
10
+ ISO (μM)
B
cAMP per cell (nM)
0.08
0.07
0.06
0.05
0.04
0.03
0.02
0.01
0.00
*
Basal
-
+meto
+ICI
+prop
+carv
ISO (5μM) + β blockers (10μM)

Figure 3.14: ISO treatment increases CDK1 expression *in vitro*. QPCR analysis revealed that CDK1 mRNA levels were significantly increased after 24 hours of ISO treatment. *P<0.05 vs. control, unpaired student's t test. Results are mean±SEM of 5-6 experiments/treatment group (**A**). Representative images of CMFs immunolabelled with an antibody specific for CDK1 (**B**), αSMA (**C**), Hoechst 33258 nuclear stain (**D**) and a merged image (**E**). The arrow indicates a cell positive for αSMA and CDK1, the arrowhead indicates a cell positive for αSMA and negative for CDK1. Quantification of immunolabelling for CDK1 revealed that following both 24 (**F**) and 48 hours (**G**) of ISO treatment CDK1-expressing cells were significantly increased compared with control. *P<0.05 vs. control, unpaired Student's t-test. Results are mean±SEM of N=3 experiments/treatment group, approximately 200-300 cells counted per experiment. Scale bar = 100 μm.

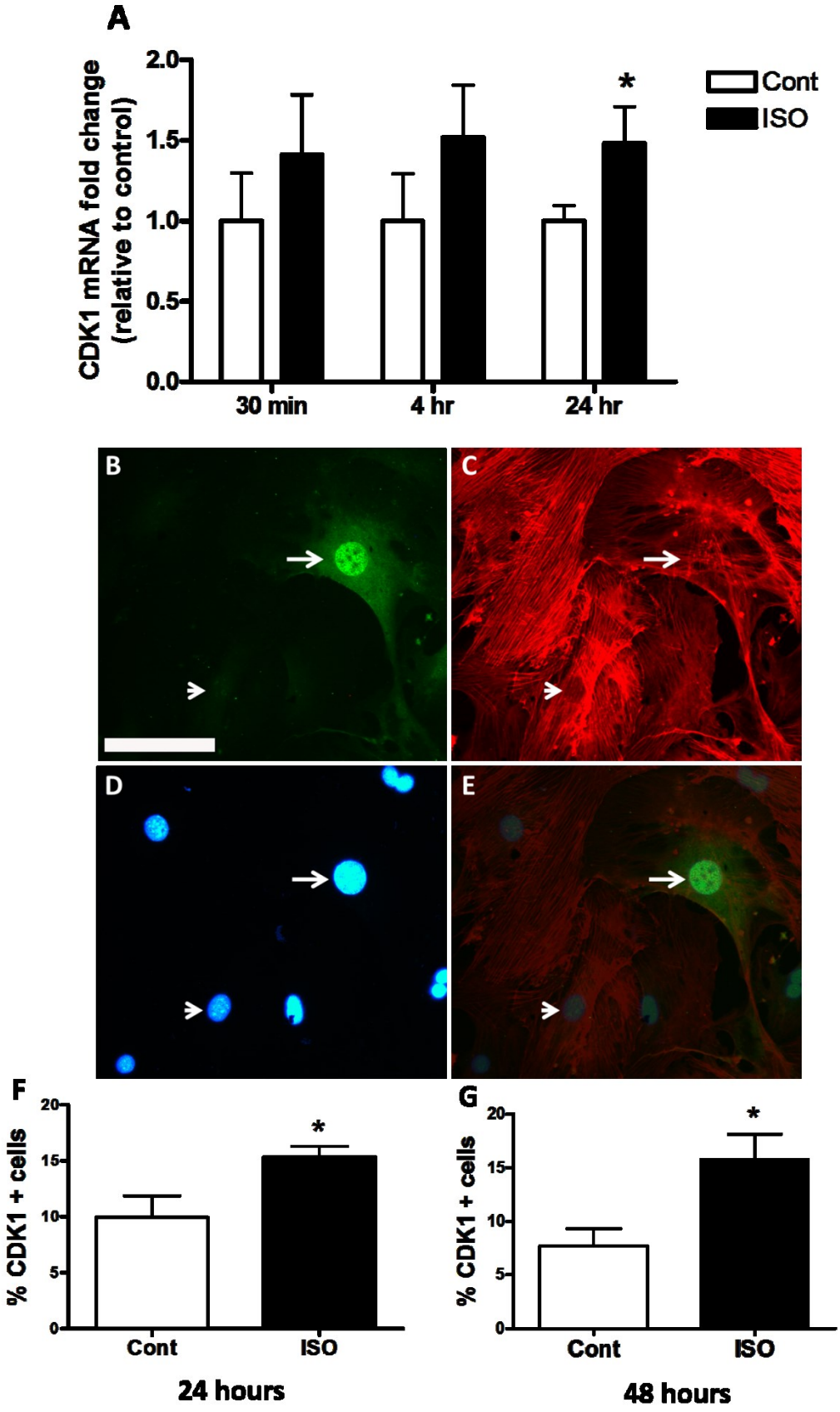
A
CDK1 mRNA fold change (relative to control)
2.0
1.5
1.0
0.5
0.0
30 min
4 hr
24 hr
*
Cont
ISO
B
C
D
E
F
% CDK1 + cells
20
15
10
5
0
Cont
ISO
24 hours
*
G
% CDK1 + cells
20
15
10
5
0
Cont
ISO
48 hours
*

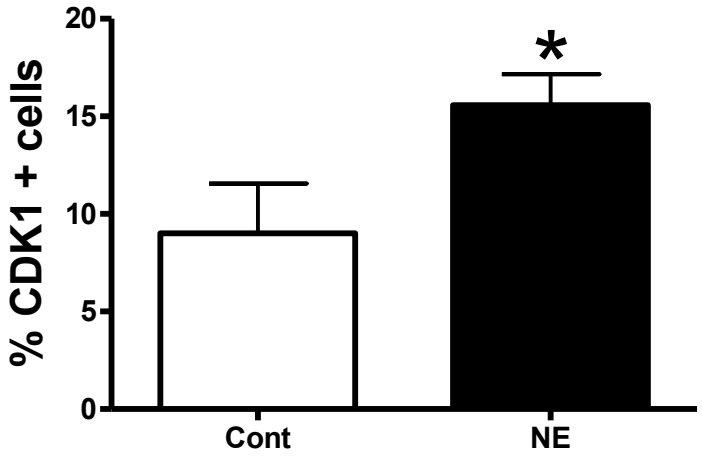

Figure 3.15: NE treatment increases CDK1 expression *in vitro*. Quantification of immunolabelling for CDK1 revealed that 48 hours following treatment with 10 μM NE CDK1-expressing CMFs were significantly increased compared with control. *P<0.05 vs. control, unpaired student's t-test. Results are mean±SEM of N=4 experiments/treatment group, 200-300 cells counted per experiment.

Figure 3.16: ISO induced changes in CDK1 are not detectable by Western blotting. Relative quantification of total CDK1 protein normalized to GAPDH protein expressed relative to control (control = 1) following 48 hours of ISO treatment showed no significant difference compared with control samples, unpaired student's t test (**A**). Representative Western blots for total CDK1 and GAPDH protein expression from CMFs treated with ISO for 48 hours (**B**). An antibody specific for phosphorylated CDK1 (pCDK1) at Tyr15 was used to investigate the activation state of CDK1 in response to ISO treatment. Relative quantification of pCDK1 protein expression normalized to total CDK1 protein expressed relative to control (control = 1) following 15 minutes, 30 minutes and 1 hour of ISO treatment showed no significant difference in the activation state of CDK1 compared with control, unpaired student's t-test (**C**). Representative Western blots for total CDK1 and pCDK1expression from CMFs treated with or without ISO for 15 minutes, 30 minutes and 1 hour (**D**). Results are mean±SEM of 3-4 experiments/treatment group.

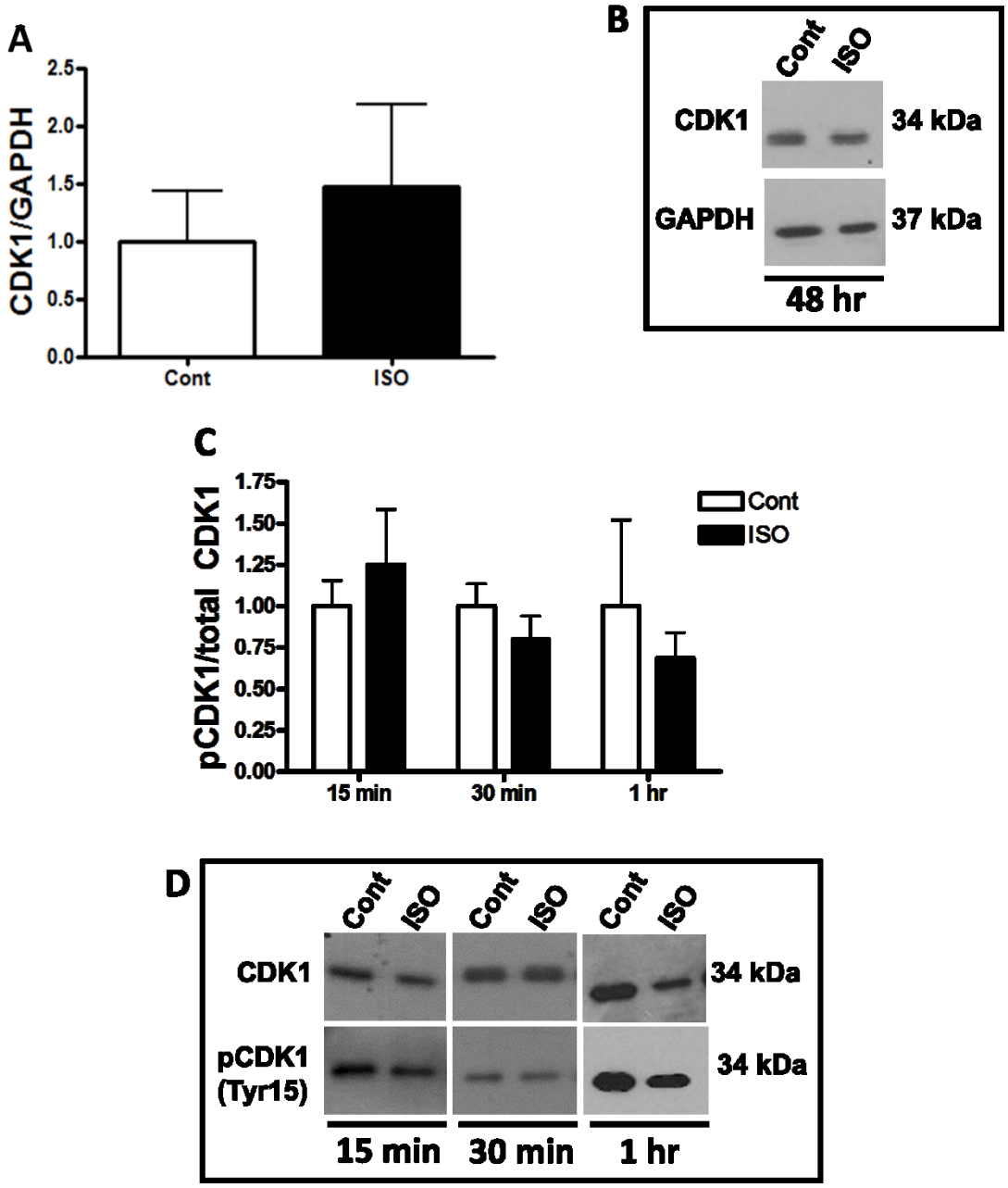
A
CDK1/GAPDH
2.5
2.0
1.5
1.0
0.5
0.0
Cont
ISO
B
Cont
ISO
CDK1
34 kDa
GAPDH
37 kDa
48 hr
C
pCDK1/total CDK1
1.75
1.50
1.25
1.00
0.75
0.50
0.25
0.00
Cont
ISO
15 min
30 min
1 hr
D
Cont
ISO
Cont
ISO
Cont
ISO
CDK1
34 kDa
pCDK1
(Tyr15)
34 kDa
15 min
30 min
1 hr

Figure 3.17: ISO treatment does not modulate Cyclin B1 expression in cardiac myofibroblasts. Representative images of CMF cultures immunolabelled for CYCB1 (**A**), CDK1 (**B**) and Hoechst 33258 nuclear stain (**C**). A merged image is shown in **D**. The arrow indicates a cell positive for CYCB1 and CDK1, the arrowhead indicates a cell negative for CYCB1 and positive for CDK1. Quantification of immunostaining revealed that following 48 hours of ISO treatment neither the number of cells positive for CYCB1 or CYCB1+CDK1 were significantly different compared with control, unpaired student's t-test (**E**). Results are mean±SEM of 3 experiments/treatment group. 200-300 cells were counted per experiment. Scale bar = 100 μm.

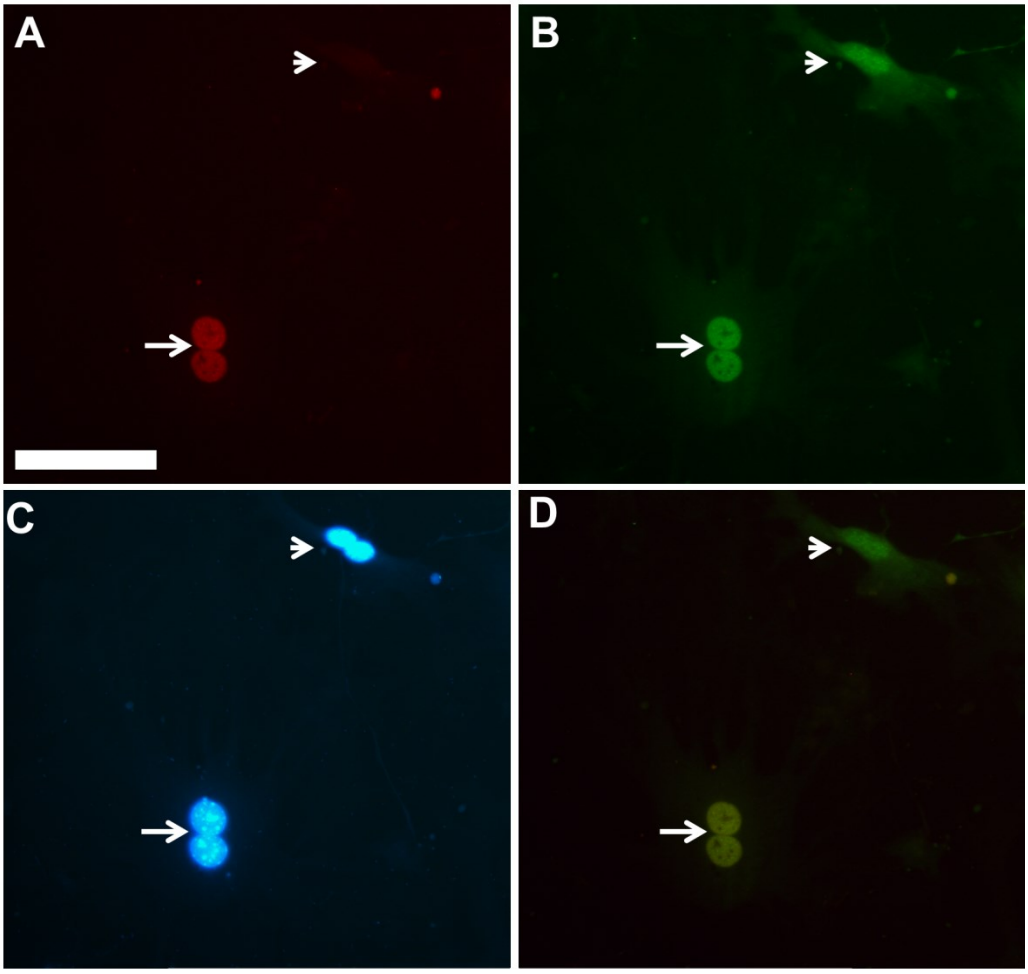
A
B
C
D

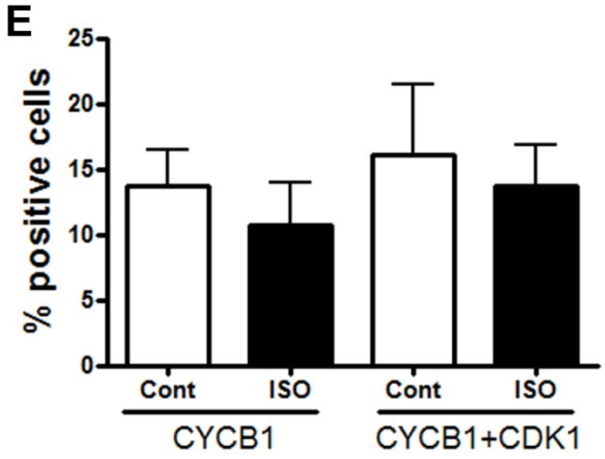
E
% positive cells
25
20
15
10
5
0
Cont
ISO
Cont
ISO
CYCB1
CYCB1+CDK1

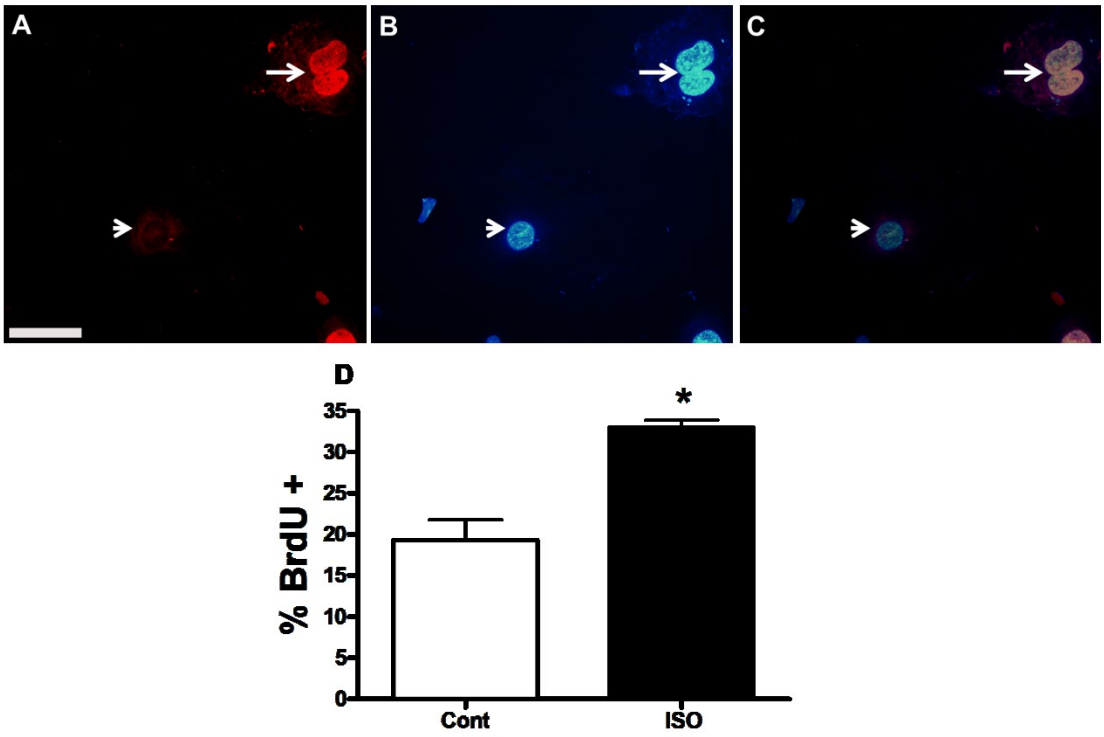

Figure 3.18: Cardiac myofibroblast DNA synthesis increases after 72 hours of ISO treatment. Representative images of CMF cultures immunolabelled with a primary antibody against BrdU (**A**) and Hoechst 33258 nuclear stain (**B**). A merged image is shown in **C**. The arrow indicates a cell positive for BrdU, the arrowhead indicates a cell negative for BrdU. Quantification of BrdU immunostaining revealed a significant increase in the number of BrdU positive cells in samples treated with ISO for 72 hours compared with control (**D**). Results are mean±SEM of 3 experiments/treatment group, *P<0.05 vs. control, unpaired Student's t-test. 200-300 cells were counted per experiment. Scale bar = 100 µm.

A

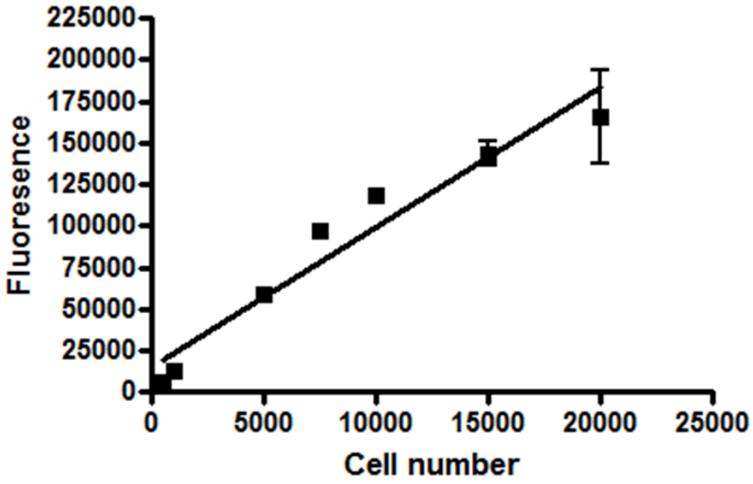

B

Cell number	Fluorescence
500	6290.7
1000	12134.7
5000	58184
7500	97480
10000	118424
15000	143597.3
20000	165122.7

Figure 3.19 CyQUANT standard curve. A CyQUANT standard curve was created by graphing fluorescence values measured from samples with known CMF cell numbers ranging from 500-20,000 cells (**A**). The table shows the cell number and the corresponding fluorescence value. Fluorescence values presented are the average of 3 experiments performed in duplicates (**B**).

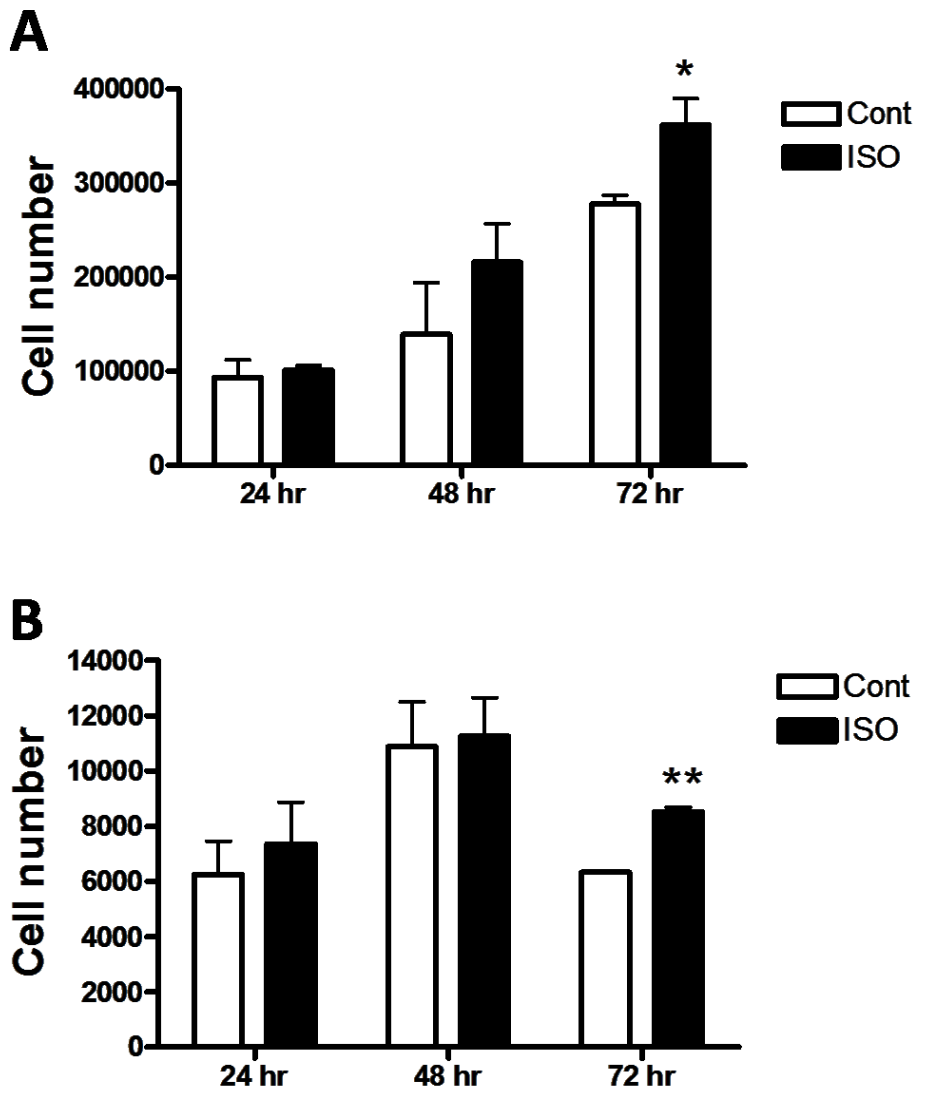

Figure 3.20: Cardiac myofibroblast proliferation increases after 72 hours of ISO treatment. CMFs were treated with or without ISO for 24, 48 or 72 hours and cell proliferation was assessed. No significant differences in proliferation were observed 24 or 48 hours after ISO treatment. Cell counts done using a hemocytometer (**A**) and a CyQUANT cell proliferation assay (**B**) revealed a significant increase in CMF proliferation compared with control 72 hours after ISO treatment. Results are mean±SEM of 3-8 experiments/treatment group, *P<0.05 vs. control in hemocytometer cell counts (**A**), *P<0.005 vs. control in CyQUANT assay (**B**), unpaired Student's t-test.

Figure 3.21: CDK1 overexpression is not sufficient to increase cardiac myofibroblast proliferation. Successful delivery of CDK1-expressing adenoviral vectors was confirmed by immunolabelling cells with an antibody specific for CDK1. Representative images of cells overexpressing CDK1 (**A-C**, adenoCDK1), a constitutively active form of CDK1 (**D-F**, adenoCDK1AF) and endogenous CDK1 (**G-I**, no adeno control). The first column represents CMFs immunolabelled for CDK1, the second column show the same field of cells stained with Hoechst 33258 nuclear stain, and the third column shows a merged image (**A-I**). In subsequent experiments, CMFs were transduced with the CDK1 expressing adenoviruses or a GFP expressing adenovirus (adenoGFP) as control, and proliferation was assessed using a CyQUANT cell proliferation assay after 72 hours. There were no significant differences in CMF proliferation among CMFs transduced with either CDK1 vector compared with the adenoGFP control. Results are mean±SEM of 3-6 experiments/treatment group, one-way ANOVA with Tukey's multiple comparison test (**J**). Transduction decreased CMF proliferation compared with non-transduced CMFs (no adeno; **K**). Following stimulation with a single dose of ISO, CMF proliferation was significantly increased compared with untreated transduced cells after 48 hours of ISO treatment (**K**). Results are mean±SEM of 3-6 experiments/treatment group. **=$P<0.005$ vs. control, *=$P<0.05$ vs. control, unpaired students t test.

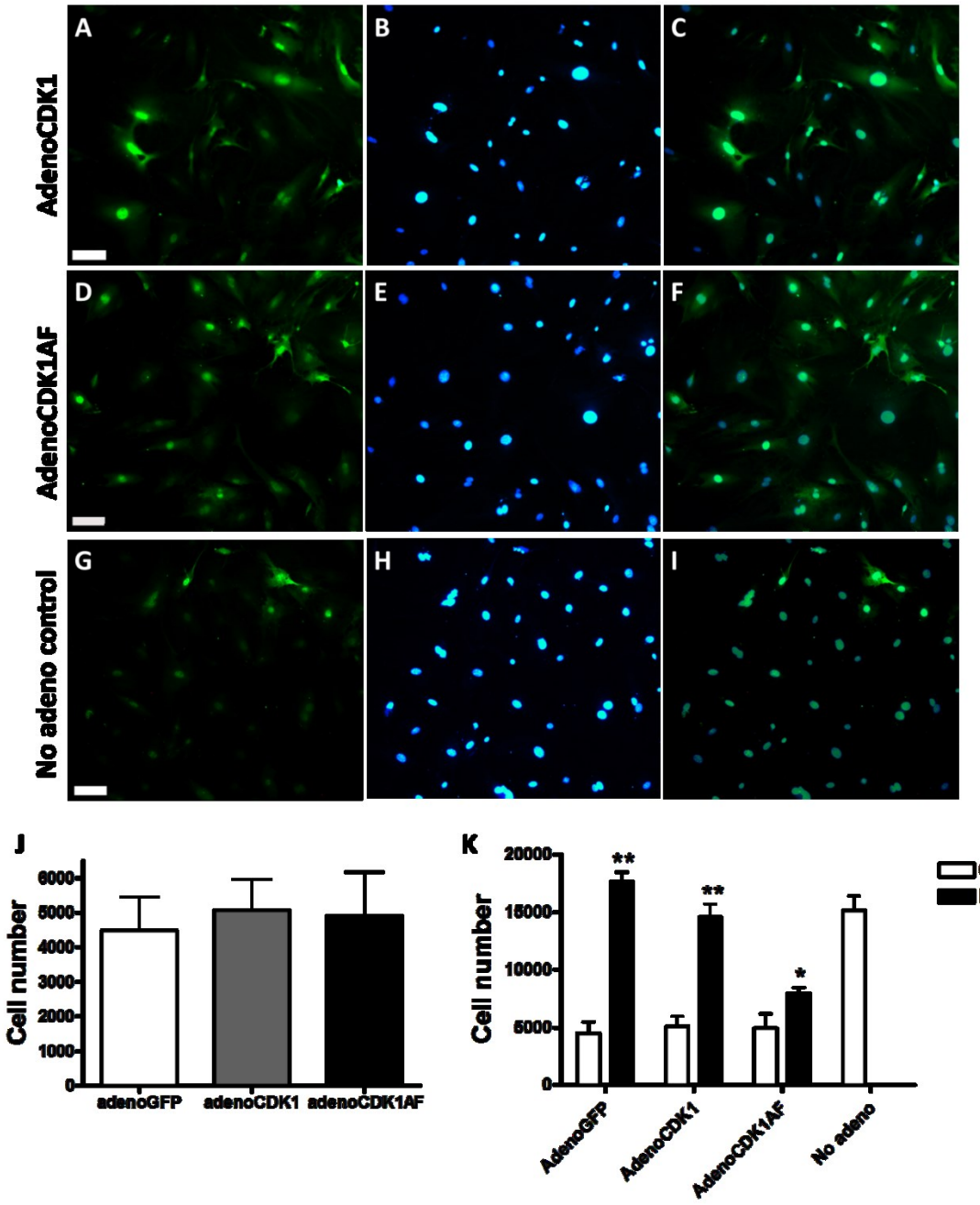
A
B
C
AdenoCDK1
D
E
F
AdenoCDK1AF
G
H
I
No adeno control
J
Cell number
6000
5000
4000
3000
2000
1000
0
adenoGFP
adenoCDK1
adenoCDK1AF
K
Cell number
20000
15000
10000
5000
0
**
**
*
Cont
ISO
AdenoGFP
AdenoCDK1
AdenoCDK1AF
No adeno

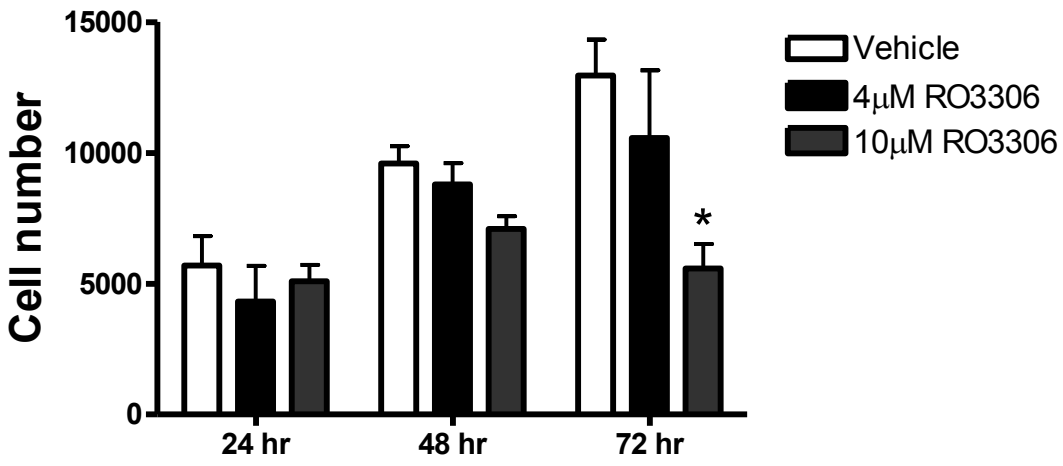

Figure 3.22: Inhibition of CDK1 is sufficient to decrease cardiac myofibroblast proliferation. CMFs were treated with either 4 or 10 μM of the CDK1 inhibitor RO3306 or vehicle alone for 24, 48 or 72 hours at which point proliferation was assessed with a CyQUANT cell proliferation assay. Pharmacological inhibition of CDK1 proved sufficient to decrease CMF proliferation at 72 hours treatment with 10μM RO-3306. Results are mean±SEM of 3-6 experiments/treatment group, *=P<0.05 vs. vehicle control, one way ANOVA with Tukey's Multiple Comparison Test.

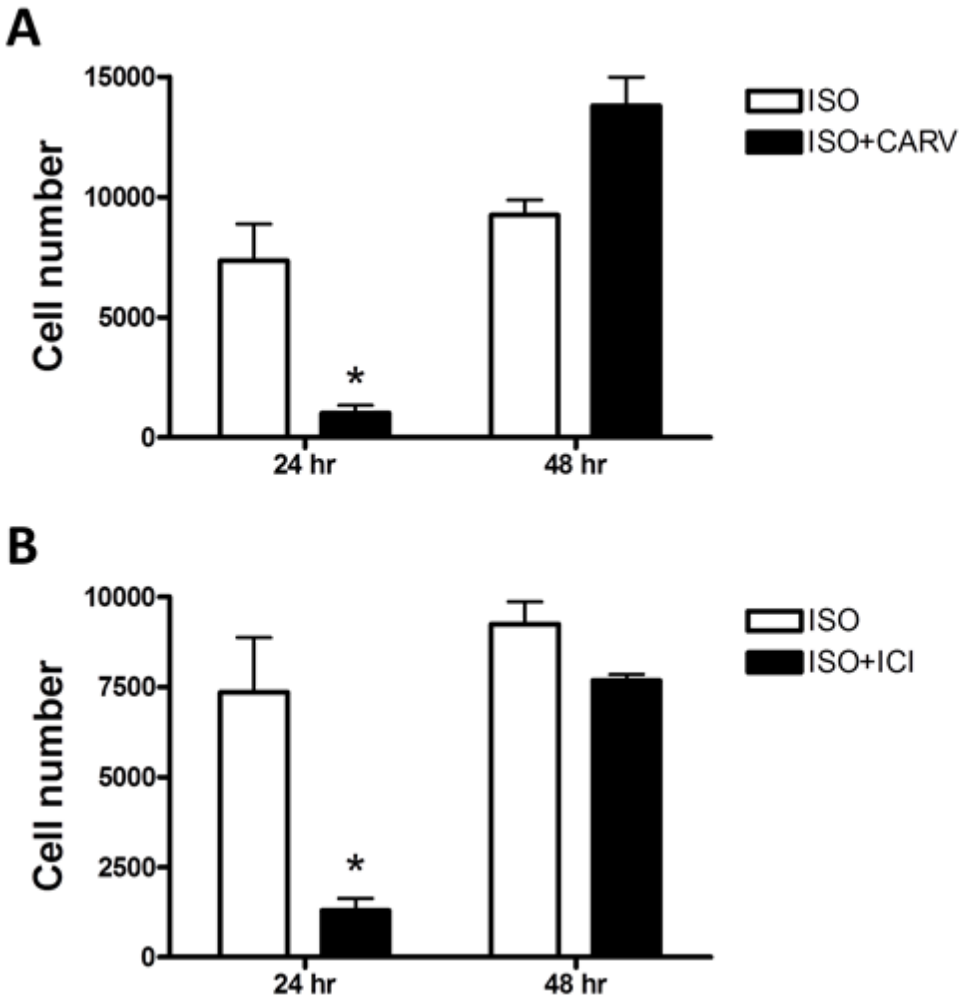

Figure 3.23: βAR blockade decreases cardiac myofibroblast proliferation. CMFs were treated with a single dose of 5μM ISO in the presence or absence of 10μM of either the non-selective βAR-blocker carvedilol (carv) or the β2AR-blocker ICI for 24 or 48 hours. Treatment with carvedilol was able to significantly decrease CMF proliferation after 24 hours treatment (**A**). ICI was also able to significantly decrease CMF proliferation after 24 hours treatment (**B**). Results are mean±SEM of 3-6 experiments/treatment group, *=P<0.05 vs. ISO, unpaired Student's t-test.

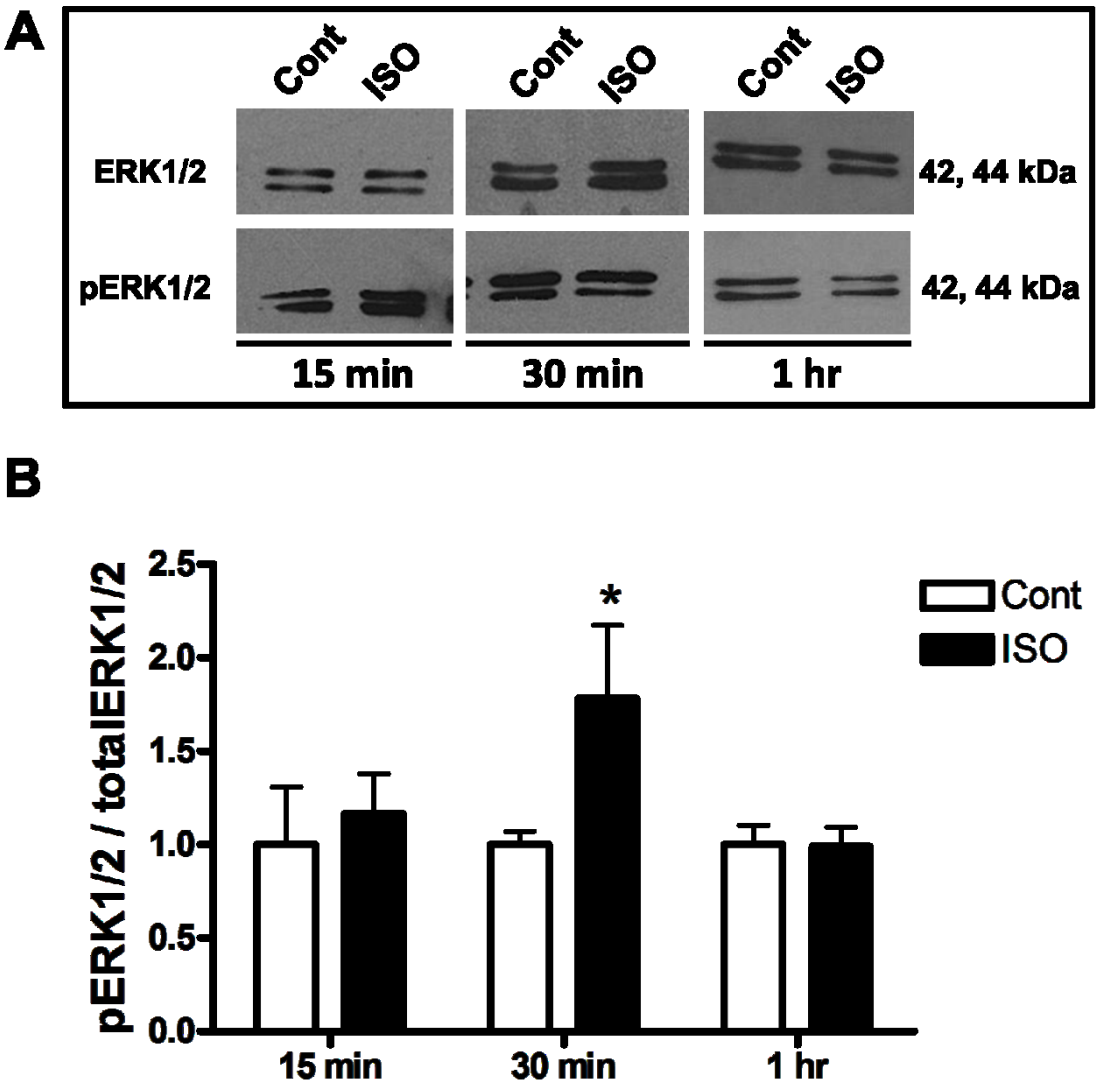

Figure 3.24: Levels of phosphorylated ERK1/2 protein increase in response to ISO treatment. ERK1/2 activity was examined by Western blotting for pERK1/2 following ISO treatment. Representative Western blot showing a time course of ERK1/2 phosphorylation in CMFs treated with or without ISO for 15 minutes, 30 minutes, and 1 hour (**A**). Relative quantification of pERK1/2 normalized to total ERK1/2 protein expressed relative to control (control=1) following 15 minutes, 30 minutes and 1 hour after ISO treatment. Phosphorylation of ERK1/2 was significantly increased 30 minutes after treatment with ISO compared with control (**B**). Results are mean±SEM of 3-4 experiments/treatment group *P<0.05 vs. control, unpaired Student's t-test.

Figure 3.25: Changes in cardiac myofibroblast gene expression in response to ISO. Quantitative polymerase chain reaction (QPCR) analysis was conducted on samples from CMFs treated for 30 minutes, 4 hours, or 24 hours to examine mRNA expression levels in response to ISO as a measure of fibroblast activation. Genes of interest include collagen type 1 α1 (col1a; panel **A**), collagen type 3 α1 (col3a1; **B**), connective tissue growth factor (CTGF; **C**), the myofibroblast marker protein α smooth muscle actin (αSMA; **D**), fibronectin 1 (Fn1; **E**), and plasminogen activator inhibitor (PAI; **F**). Expression of all mRNAs was normalized to levels of mouse TATA box binding protein (mTBP). No significant changes in mRNA expression levels were observed after 30 minutes or 4 hours of ISO treatment. After 24 hours of ISO treatment levels of col3α1 (**B**), CTGF (**C**), αSMA (**D**), and PAI (**F**) mRNA were all significantly increased compared with control (cont). Results are mean±SEM of N=5-7 experiments/treatment group, 2 replicates. *$P<0.05$ vs. control, unpaired Student's t-test.

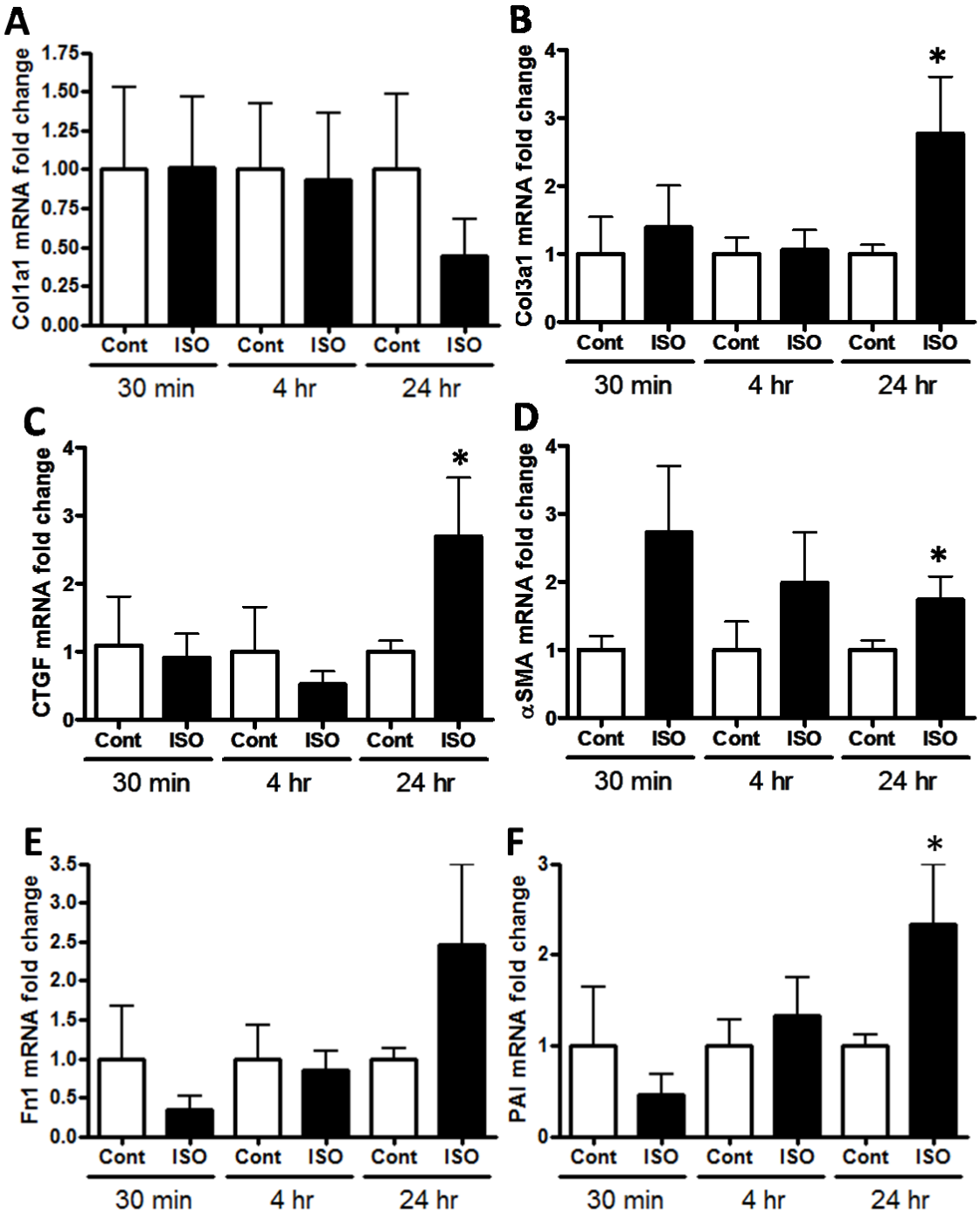
A
Col1a1 mRNA fold change
1.75
1.50
1.25
1.00
0.75
0.50
0.25
0.00
Cont ISO Cont ISO Cont ISO
30 min 4 hr 24 hr
B
Col3a1 mRNA fold change
4
3
2
1
0
*
Cont ISO Cont ISO Cont ISO
30 min 4 hr 24 hr
C
CTGF mRNA fold change
4
3
2
1
0
*
Cont ISO Cont ISO Cont ISO
30 min 4 hr 24 hr
D
αSMA mRNA fold change
4
3
2
1
0
*
Cont ISO Cont ISO Cont ISO
30 min 4 hr 24 hr
E
Fn1 mRNA fold change
3.5
3.0
2.5
2.0
1.5
1.0
0.5
0.0
Cont ISO Cont ISO Cont ISO
30 min 4 hr 24 hr
F
PAI mRNA fold change
3
2
1
0
*
Cont ISO Cont ISO Cont ISO
30 min 4 hr 24 hr

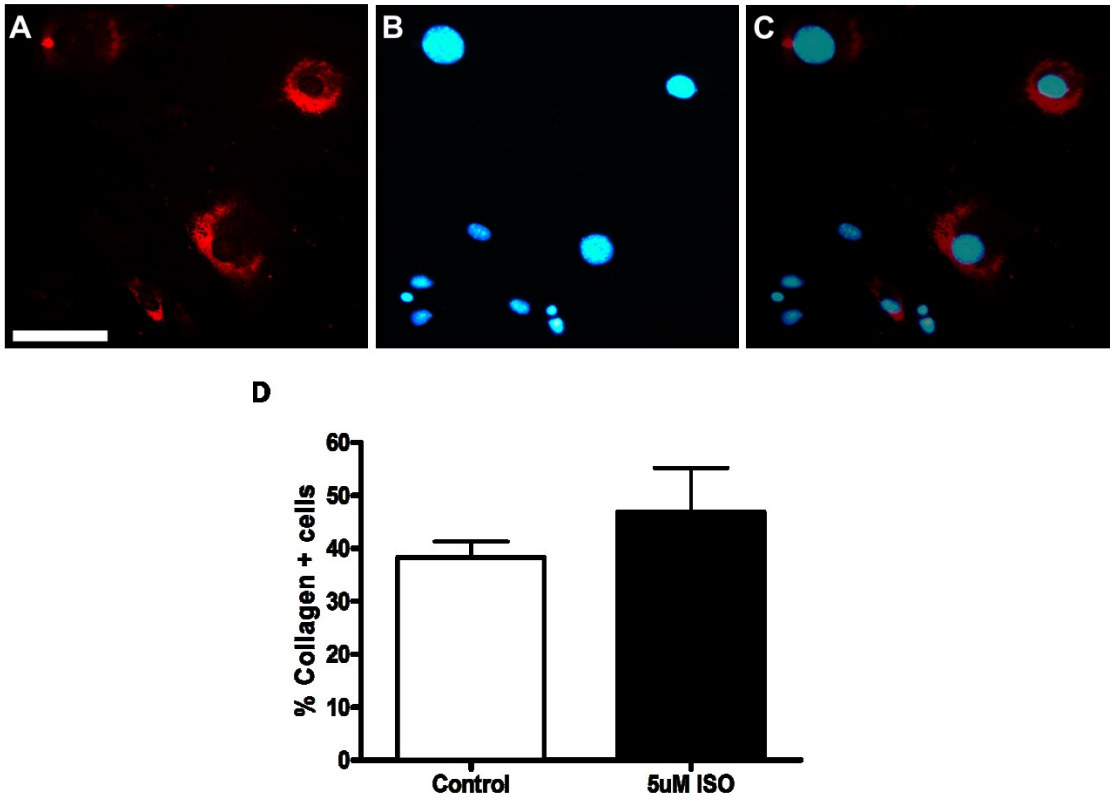

Figure 3.26: ISO treatment does not increase pro-collagen type 1 α1 protein expression. CMFs were treated with ISO for 48 hours and immunolabelled with an antibody against pro-collagen type 1 α1. Representative image of CMFs immunolabelled for pro-collagen type 1 α1 (**A**), the same field of cells stained with Hoechst 33258 nuclear stain (**B**), a merged image (**C**). Scale bar = 100μm. Quantification of immunostaining revealed no significant difference in the number of cells positive for pro-collagen type 1 α1 in control compared with ISO treated CMFs (**D**). Results are mean±SEM of 3 experiments/treatment group. Results were not statistically significant, unpaired Student's t-test.

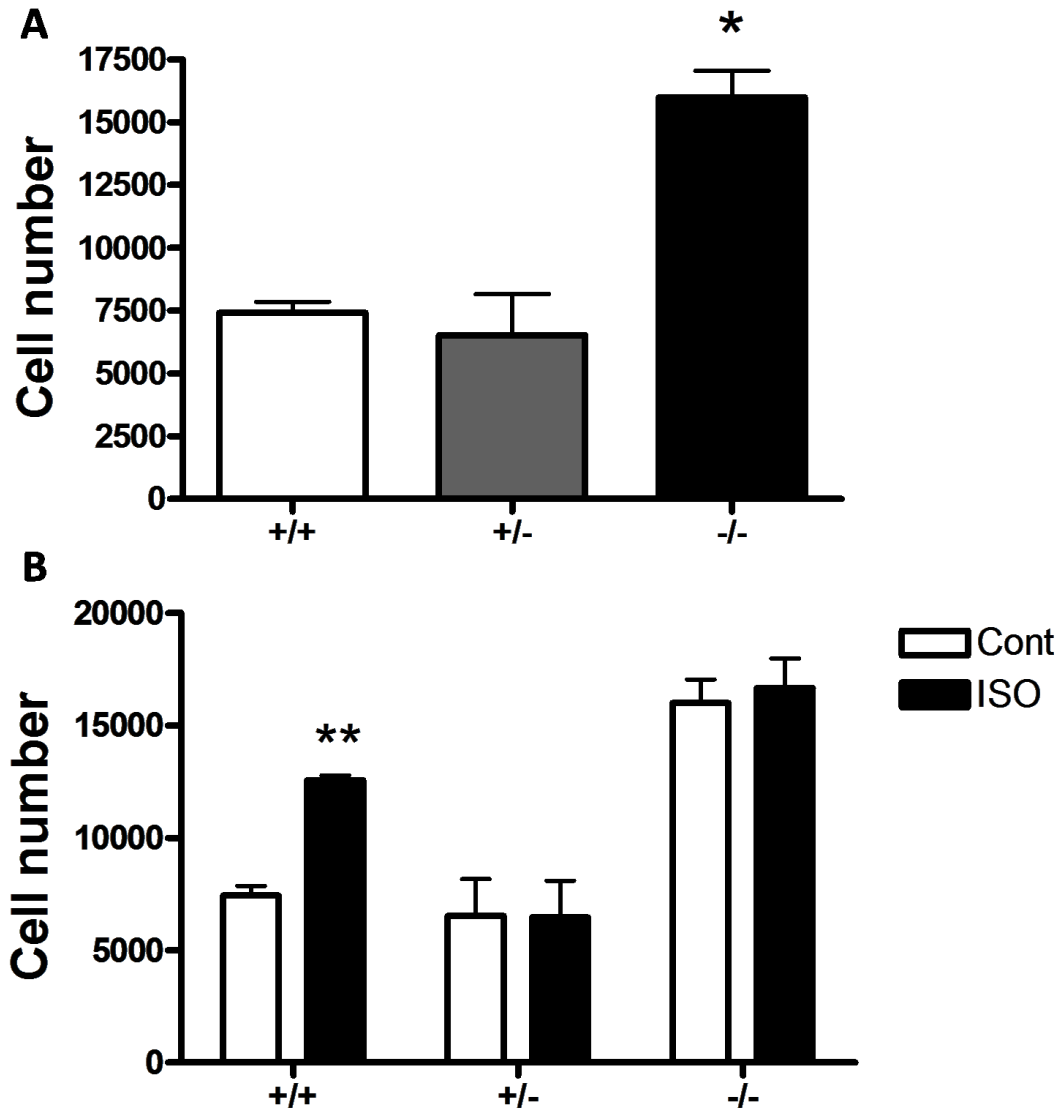

Figure 3.27: *Npr1 -/-* mice have increased cardiac myofibroblast proliferation. Cell numbers were assessed using a CyQUANT cell proliferation assay. After 24 hours, basal proliferation of CMFs was significantly increased in *Npr1* knockout (-/-) mice compared with both *Npr1* wild type (+/+) and *Npr1* heterozygous (+/-) mice. *=P<0.05 vs. wild type, unpaired Student's t-test (**A**). 24 hours after ISO treatment CMF proliferation was significantly increased compared with control only in the wild type (+/+) CMFs. **=P<0.005 vs. control, unpaired Student's t-test (**B**). Results are mean±SEM of 3-6 experiments/group.

Chapter 4: Discussion

4.1 Summary

The overall aims of this project were to establish and characterize a mouse CF cell culture system, investigate the status of CDK1 expression after ISO stimulation in adult mouse CMFs, and determine the response of these cells to catecholamine treatment and loss of the *Npr1* receptor. Cardiac fibrosis is an underlying pathology in many forms of cardiovascular disease, and the dysregulation of CMF proliferation is a major factor in causing cardiac fibrosis. Catecholamines have been shown to stimulate CMF proliferation and possible signalling pathways regarding this have been proposed. However, the possibility of a role for CDK1 in this process has not been examined, nor have changes in CMF gene expression in response to catecholamines. In addition, ANP is able to decrease CF proliferation, thus we sought to study the effect of loss of the ANP receptor on CMF proliferation.

The major results of this study are: i) when grown in culture, mouse CFs differentiate into CMFs, ii) CMF CDK1 expression increases *in vitro* in response to ISO, iiI) CMF DNA synthesis and proliferation increase in response to ISO in adult mouse CMFs, iv) pharmacological inhibition of CDK1 decreases cell proliferation, v) ISO modulates CMF gene expression, and vi) loss of *Npr1* increases CMF proliferation.

4.2 Cardiac Myofibroblast Characterization

When cultured on plastic plates, rat CFs undergo phenoconversion to CMFs. Compared with quiescent P0 cells, expression of vimentin, αSMA, and SMemb proteins was found to be increased in P1-3 cells. In addition, expression of both intracellular procollagen and secreted collagen type I increased with passage number, suggesting cells acquire a more active myofibroblast phenotype (Santiago et al., 2010). However, there are no reports on the phenoconversion of human or mouse CFs in culture. In this study, fibroblasts isolated from the ventricles of adult male CD1 mice were characterized by immunostaining. These studies revealed that the majority of cells expressed CMF markers (Figure 3.3 A and B). Cells that had not been passaged (P0) were different from those passaged 1-3 times (Figure 3.3 C), and expression of αSMA and DDR2 increased with passaging. In addition to differences in marker protein expression, we observed a significant increase in cell size between P0 and P1-3 cells (Figure 3.7). This is, to our knowledge, the first report of CMF cell size differences based on passage number. These results suggest that phenoconversion also occurred in mouse CMF cultures in response to our culture conditions.

Recent reports indicated that conversion of CFs to CMFs can be prevented and partially reversed by experimental manipulations. Overexpression of c-Ski (a proto-oncoprotein) in P1 cultures was able to prevent secretion of collagen type I, decrease αSMA expression and inhibit the contractile ability of CMFs in response to TGF-β stimulation (Cunnington et al., 2011). As well, addition of the compound resveratrol (a plant phenol with antioxidant properties) before treatment with Ang II or TGF-β (both

stimulate phenoconversion) was able to decrease the number of αSMA-expressing cells, suggesting that it may be useful in preventing phenoconversion (Olson et al. 2005).

Santiago et al. (2010) conducted a comparison between CMFs *in vitro* and those located *in vivo* in infarcted regions of the heart. CMFs do not express desmin, and cells lacking desmin in the infarct scar were found to express αSMA, DDR2, SMemb and ED-A fibronectin. This indicates that myofibroblasts grown in culture are phenotypically similar to those *in vivo*, supporting their use for experiments *in vitro*.

Based on this report as well as our marker protein expression analysis, we used mouse CMFs between P1-3 as marker protein expression was found to be consistent compared to P0 cells (Santiago et al., 2010). In addition, our CMFs became senescent after P4.

One limitation of this study is the heterogeneous nature of the CMF cultures. Expression of the marker proteins we used revealed that the cells had different levels of expression of DDR2, αSMA and vimentin, suggesting that they could be different cell types. However, as the majority of our antibodies were monoclonal we were unable to co-stain, so it is possible that these cells could have overlapping expression and be positive for multiple markers, as opposed to being different cell types expressing different markers. There is also likely a spectrum of myofibroblast differentiation and therefore the CMFs may have had different expression based on their stage of differentiation.

The neural stem cell marker nestin (an intermediate filament protein) was initially investigated in relation to the innervation of myocardial scars post-injury due to

recruitment of neural stem cells (Drapeau et al., 2005). Nestin expression was also found to be increased in patients in the later stages of heart failure (Scobioala et al., 2008). Expression of nestin was localized to a population of ventricular CMFs after injury in the rat myocardium (Beguin et al., 2011). Interestingly, we observed nestin expression in P0 cells, however it was not detectable in P1-3 cells (Figure 3.6). This could be due to the fact that P0 cells are freshly isolated and may have been injured during this process thereby inducing expression of nestin. It is also possible that the nestin expressing cells we observed may be a population of cardiac stem cells that do not survive beyond P0 in our culture conditions, or they may have differentiated into CMFs.

4.3 Second Messenger Response to ISO and βAR Distribution

Stimulation of βARs with ISO results in production of the second messenger cAMP. A cAMP assay using various doses of ISO indicated that 5μM ISO was the optimal dose to treat CMFs (Figure 3.13 A). Doses reported for ISO from other studies using CFs varied from 0.1 nM to 10 μM (Colombo et al. 2003; Kim et al. 2002; Leicht et al. 2000; Turner et al., 2003), however, none of these studies performed dose-response experiments to determine the optimal dose for *in vitro* experiments. The 10 μM dose of NE was selected based on a previous study which demonstrated that NE is less potent than ISO at blocking binding of [^{125}I]-iodohydroxybenzylpindolol (a very potent βAR antagonist) in rat CFs. In addition, this concentration falls within the peak range of NE concentrations in sympathetic nerve synapses, 0.3-10 μM (Bevan, 1978).

Given that cells were treated with 5 μM ISO for up to 48 hours, it is likely that the βARs would have been desensitized. A study conducted in adult rat cardiomyocytes revealed that a 1 μM ISO treatment over 24 hours significantly increased levels of β-adrenergic receptor kinase 1 (βARK1), an enzyme responsible for βAR desensitization (Iaccarino et al., 1999). However, despite possible receptor desensitization, a significant increase in CDK1 levels was observed after 48 hours, suggesting these cells still respond to ISO despite receptor desensitization (Figure 3.14 G).

Immunoblotting and immunolabelling studies revealed that mouse CMF cultures express both β1 and β2ARs (Figure 3.8). However, FACS analysis for percentage of cells positive for cell surface β1AR expression was significantly higher compared to that of cells positive for β2AR expression (Figure 3.11; ≈6 fold). Results from a cAMP assay using ISO in the presence of various βAR blockers indicated that the β2AR was likely the subtype involved in mediating the increase in cAMP (Figure 3.13 B). Thus, while there may be more β1ARs at the cell surface, the β2 subtype may be more important in terms of mediating the downstream actions of ISO in mouse CMF cultures. This is in line with other studies which indicate that β2ARs are predominant in adult rat CFs (Leicht et al., 2000; Meszaros et al., 2000). Interestingly, the β2AR subtype was found to be the only βAR expressed in human atrial CFs. No evidence of β1AR mRNA expression was found, indicating a difference in receptor subtype expression between species that may have important implications for the translation of experimental results to therapeutic approaches (Turner et al., 2003).

We chose to use 10 μM of the various βAR blockers in a cAMP assay based on findings indicating that a 10 μM dose of carvedilol was able to decrease CF proliferation

significantly (Leicht et al., 2000). As this was an exploratory experiment we chose the same dose for all βAR blockers. Although we used 10 μM for all the blockers, testing different doses should be done in future experiments to ensure that the differences in cAMP production that we saw were due to differences in the distribution of the specific βAR subtypes.

To our knowledge, this is the first report indicating that β1ARs are more readily detectable on the cell surface of adult mouse CMFs compared with β2ARs. In contrast, experimental results measuring the cAMP response of these cells to ISO in the presence of receptor specific blockers indicates that, despite decreased number, the β2AR is the predominant receptor subtype involved in this response.

4.4 Catecholamine Treatment Increases CDK1 Expression in Adult Mouse Cardiac Myofibroblasts

ISO treatment was able to induce CDK1 expression in both acinar cells of rodent salivary glands (Zeng et al., 1996) and non-myocytes in adult mouse hearts (Gaspard et al., In Press). ISO is able to directly activate the CDK1 promoter by interacting with an NF-Y binding site in mouse embryonic ventricular cells (Gaspard et al., In Press). Treatment of adult mouse CMFs with ISO increased CDK1 mRNA expression and the number of CDK1-expressing CMFs as assessed by immunofluorescence (Figure 3.14). In addition, treatment with NE was able to increase the number of CDK1-expressing CMFs, indicating that this is not an effect specific to ISO and endogenous catecholamines are able to induce CDK1 expression *in vitro* (Figure 3.15). The increase in CDK1 was

not detectable by Western blot. This could be due to the fact that a small number of cells have increased CDK1 expression and although they are detectable by immunofluorescence (≈1.5-2 fold increase vs control; Figure 3.14 F and G) it may be too modest an increase to be detected in whole cell protein lysates used for Western blotting (Figure 3.16).

Patients with heart failure had increased levels of βARK and decreased β1AR levels compared with non-failing hearts, whereas β2AR levels were not affected (Ungerer et al., 1993). This suggests that β1ARs may be more susceptible to desensitization and down-regulation. Previous work in our lab reported that induction of CDK1 promoter activity occurred via the β1AR in embryonic ventricular cells (Pasumarthi Lab, unpublished data) it is also possible that the modest increase in CDK1 protein that we observed could be due to the fact that β1ARs were down-regulated in response to ISO stimulation over this time period, thus leading to less induction of CDK1 in adult CMFs. In addition, FACS analysis revealed that only 40% of CMFs express the β1AR at the cell surface (Figure 3.11), thus only 40% of CMFs are able to respond to ISO to induce CDK1 and this too may be insufficient to show an increase in protein by Western blotting. Given that we saw an increase in the percentage of CDK1 positive CMFs following ISO and NE treatment it is likely that the β1AR may be involved in induction of CDK1 expression. ISO binds both β1 and β2ARs, while NE has more affinity for β1 compared with β2. In addition, treatment with Epi (data not shown) did not impact CDK1 expression, and Epi has a higher affinity for β2 compared to β1ARs. Nevertheless, receptor specific blockers should be used in future experiments to identify the involvement of βAR subtypes responsible for CDK1 induction in adult CMFs.

4.5 ISO does not Modulate CDK1 Activation or its Association with Cyclin B1

In order to be activated, CDK1 must be dephosphorylated at the Thr 14 and Tyr 15 residues (Shankland and Wolf, 2000). Western blots conducted with an antibody specific for phosphorylated CDK1 at Tyr 15 did not detect any changes in phosphorylation at this site, suggesting that ISO does not influence CDK1 activation. However, it is possible that ISO treatment may decrease phosphorylation at Thr 14 in CMFs, and this should be examined in future experiments. In addition, Zeng et al. (1996) found that CDK1 kinase activity increased in parotid acinar cells in response to intraperitoneal injections of ISO, reaching a maximum at 72 hours post-injection. Zeng et al. (1996) examined phosphorylation of a downstream target (histone H1) as a measure of CDK1 activity. It would be of interest to examine this in relation to our studies to confirm the status of CDK1 activation in CMFs following ISO treatment.

Treatment with ISO was also able to increase protein expression of cyclins D and A, and CDKs 4 and 2 in acinar cells from the parotid gland, however no increases in cyclins A or B occurred (Zeng et al., 1996). In line with these results, we also did not observe any increases in cyclin B1 levels as indicated by immunofluorescence. From 3-6 days after treatment with ISO, CDK1/cyclin B complex levels were decreased compared with control in parotid acinar cells (Zeng et al., 1996), however we did not observe any difference in levels of cyclin B1 co-localized with CDK1. It possible that, because cyclin B1 is degraded in a cyclical fashion (Ekholm & Reed, 2000), the time points examined in our study did not coincide with increased cyclin B1 levels.

4.6 Cardiac Myofibroblast DNA Synthesis and Proliferation Increase in Response to ISO

We observed a significant increase in mouse CMF DNA synthesis as measured by BrdU (Figure 3.17) 72 hours after ISO treatment. In neonatal and adult rat CFs, treatment with 1 μM ISO for 24 or 48 hours was able to increase DNA synthesis as measured by ^{3}H thymidine incorporation. In adult rat CFs this increase in DNA synthesis was attributed to stimulation of ERK by the EGFR and Src (which is involved in EGFR transactivation), and also involved the PI3K pathway (Kim et al., 2002). In neonatal rat CFs stimulation of DNA synthesis occurred via the β2AR, and was suggested to occur independently of ERK, as direct activation of ERK alone was not sufficient to increase DNA synthesis. It was, however, found to be dependent on PI3K and involved activation of mTOR/p70S6K (Colombo et al., 2003).

Conflicting results related to the involvement of ERK in DNA synthesis could be due to the developmental stage of the cells used (neonatal vs adult CFs). In our studies, we observed a significant increase in ERK1/2 activation in response to ISO treatment in adult mouse CMFs (Figure 3.23). It would be interesting in future studies to use both an ERK and a PI3K inhibitor to examine their roles in mouse CMF proliferation.

The increase in DNA synthesis in our study translated to increased cell number 72 hours following ISO treatment (Figure 3.19), indicating that ISO stimulates adult mouse CMF proliferation. The doubling time of these cells appears to be more than 24 hours (Figure 3.19 A). Results from the CyQUANT proliferation assay (Figure 3.19 B) are not consistent with cell numbers seen by hemocytometer counting (Figure 3.19 A). This

could be due to the fact that cells used for the CyQUANT assay were grown in 96 well plates. These cells may have reached a maximal number in the wells by 48 hours, and therefore at 72 hours there are fewer cells due to cell death. It is important to note, however, that with both assays ISO treatment was able to significantly increase CMF proliferation after 72 hours compared with basal levels of CMF growth. It would be of interest to run a cell death assay in the future to determine the status of CMFs in 96 well plates after 48 hours.

Studies conducted in adult rat CFs treated with 1 μM ISO for 48 hours and human CFs treated for up to 6 days also revealed an increase in cell number (Leicht et al., 2000; Turner et al., 2003). In adult rat CFs, Leicht et al (2003) concluded that catecholamine induced CF proliferation occurs via the β2AR and activation of ERK1/2, while in human CFs they proposed an autocrine mechanism stimulates proliferation via secretion of a heat sensitive growth factor (Turner et al., 2003).

Despite previous studies conducted on the effect of ISO on CF DNA synthesis and proliferation, our study is unique as it is the first to report that ISO is able to elicit these effects in adult mouse CMFs.

4.7 Adenoviral Mediated Overexpression of CDK1 is not Sufficient to Increase Proliferation

Treatment with ISO increases CDK1 levels and proliferation in CMFs. CMFs were transduced with adenoviral constructs overexpressing either CDK1 or a constitutively active form of CDK1. Overexpression of CDK1 alone was not able to

increase CMF proliferation compared with control. Addition of ISO alone was sufficient to increase CMF proliferation in these experiments. In contrast to the expected results, CMFs overexpressing CDK1 in the presence of ISO showed reduced proliferation compared with the adenoGFP ISO-treated control. This decrease in proliferation is even more pronounced between CMFs overexpressing the constitutively active form of CDK1 (adenoCDK1AF) and control CMFs when treated with ISO. These results suggest that overexpression of CDK1 is cell cycle inhibitory, while a modest increase in CDK1 levels induced by ISO may be sufficient for CMF proliferation.

4.8 Pharmacological Inhibition of CDK1 Decreases Cardiac Myofibroblast Proliferation

The CDK1 inhibitor RO-3306 was able to significantly decrease CMF proliferation at a dose of 10 μM after 72 hours (Figure 3.21). At a concentration of 10 μM, inhibition of CDK1 is almost 100% effective, inhibition of CDK2 is ≈85% and that of CDK4 is ≈15%. However, investigation of pRb phosphorylation (a target of CDKs 4 and 2) revealed that at a dose of 9 μM RO-3306 did not affect phosphorylation of pRb *in vitro* in HeLa cells. Thus, while it almost completely inhibits CDK1 at this dose, CDKs 2 and 4 are still functional (Vassilev et al., 2006). Therefore in our cell culture, CDKs 2 and 4 should not be affected, and the reduction of proliferation in response to 10 μM RO-3306 should be mainly due to CDK1 inhibition. Vassilev et al. (2006) also measured the ability of RO-3306 to block other kinases (including PKA, Akt and ERK) and it was found to be 15 fold more selective for CDK1 than any of the related kinases tested.

Future experiments should be conducted to confirm that RO-3306 is indeed inhibiting CDK1 by examining the activation state of known CDK1 downstream targets such as phosphorylated histone H3. In addition, it is also important to determine that the results observed after 72 hours of treatment with RO-3306 are due to the effects of the inhibitor and not cell death. We could look at expression of the apoptotic mediator caspase 3 or conduct TUNEL staining. As well, it would be of interest to confirm these results by transfecting CMFs with an shRNA for CDK1 and assessing CMF proliferation.

The CDK inhibitor flavopiridol (an inhibitor of CDKs 1, 2, 4 and 7) was the first CDK inhibitor used in clinical trials. It has been investigated for use in several different cancers including non-Hodgkin's lymphoma, renal and colon cancers (Senderowicz, 1999; Senderowicz, 2002). CY-202, another CDK inhibitor, is undergoing clinical trials for use in cancer therapy as well. Malumbres et al. (2008) highlight the fact that these inhibitors have modest inhibitory activity, and point out that second generation CDK inhibitors may have more luck in clinical trials (Malumbres et al., 2008).

In addition to cancer treatment, CDK inhibition is being explored for treatment of proliferative glomerulonephritis with respect to controlling proliferation of mesangial cells in this disease state. Roscovitine is a CDK2 inhibitor that showed promise in a rat model of this disease. Roscovitine decreased proliferation of mesangial cells and production of matrix, which increased kidney function in diseased rats (Kurogi, 2003).

In light of the promise of CDK inhibitors in treating other diseases, our results suggest that CDK1 inhibition may be of use in controlling the excessive CMF proliferation in catecholamine induced cardiac fibrosis.

4.9 βAR Blockade Prevents the ISO-Induced Increase in Proliferation

Previous studies in human and adult rat CFs revealed that treatment with the β2-selective blocker ICI or the non-selective β blockers carvedilol and propranolol inhibited catecholamine-induced increases in proliferation. β1AR blockade was unable to prevent this increase (Leicht et al., 2000; Turner et al., 2003). Our results with mouse CMFs are also consistent with studies performed on human and rat CFs. Our results revealed that both ICI and carvedilol are able to decrease mouse CMF proliferation 24 hours after treatment (Figure 3.22 A and B). These effects were not apparent 48 hours post-treatment. As treatment with the β1-selective blocker metoprolol was not able to attenuate the ISO induced increase in cAMP levels, we did not test the effects of β1AR blockade on CMF proliferation.

Drugs such as ACE inhibitors are often used in the treatment of heart failure and are known to influence remodelling in the left ventricle. βAR blockers are recommended for use alongside ACE inhibitors in the treatment of heart failure, and have been shown in clinical trials to improve survival in patients with heart failure (McMurray et al., 2012). In light of the results of our study and others, it is possible that treatment with βAR blockers, if started soon enough after myocardial injury, may be able to prevent excessive CF proliferation and pathological remodelling.

4.10 ISO Treatment Activates ERK1/2

The ERK class of MAPKs is well known to be involved in cell proliferation. In order to investigate the mechanisms through which ISO acts to induce CMF proliferation, we chose to examine activation of ERK1/2. In our study, treatment with ISO increased pERK1/2 protein expression after 30 minutes (Figure 3.23 B), indicating an increase in ERK1/2 activity. This observation is consistent with previous studies which demonstrated that treatment of rat and human CFs with NE (10 μM) and ISO (10 μM) led to ERK1/2 phosphorylation shortly after treatment (Kim et al., 2002; Leicht et al., 2000; Turner et al., 2003).

In adult rat CFs inhibition of the EGFR or Src tyrosine kinase was able to attenuate ISO induced ERK activation and PI3K was implicated in activation of ERK as well (Colombo et al., 2003). A study conducted in rat lung alveolar epithelial cells demonstrated that inhibition of pertussis toxin sensitive G proteins and the EGFR was able to inhibit ERK1/2 activation (Correa-Meyer et al., 2002), indicating that this is not a cardiac specific phenomenon. Activation of GPCRs was also reported to result in EGFR transactivation and subsequent ERK activation in the rat-1 fibroblast cell line (New & Wong, 2007). In this case the GPCRs activated were the lysophosphatidic acid, ET-1, and thrombin receptors. Transactivation of the EGFR was reported to occur by MMPs cleaving EGF allowing activation of the EGFR and downstream signalling events including activation of PI3K and ERK (New & Wong, 2007).

Additional experiments are required to address the involvement of the EGFR in ISO-mediated increases in ERK1/2 phosphorylation in adult mouse CMFs.

4.11 ISO Modulates Cardiac Myofibroblast Gene Expression

Treatment with ISO for 24 hours was able to increase expression of collagen type III α1, CTGF, αSMA and PAI mRNAs (Figure 3.24). Increased expression of αSMA and collagen type III mRNAs, suggests that ISO activates CMFs causing increased expression of myofibroblast markers.

Collagen type I constitutes approximately 80% of the ECM (Porter & Turner, 2009) and therefore plays an important role in cardiac fibrosis. Given that mRNA levels of collagen type 1α1 were not different after ISO treatment, we examined its expression by immunofluorescence to confirm this result. There was no change in collagen type Iα1 levels in response to ISO treatment after 24 hours (Figure 3.25). Collagens are produced as pro-collagens and cleaved into mature collagens by proteinases and subsequently secreted (Diez et al., 2001). Our antibody is specific for pro-collagen type Iα1, therefore it is possible that no changes were detected because mature collagen was secreted from the cells into the media.

Expression of CTGF is associated with conditions that favour fibrosis (Leask, 2010). Therefore an increase in CTGF expression after ISO treatment is suggestive of CMF activation. In addition an increase in PAI also demonstrates activation of CMFs by ISO as the majority of studies conducted on the role of PAI in cardiac fibrosis support a pro-fibrotic role (Ghosh & Vaughan, 2012; Moriwaki et al., 2004; Weisberg et al., 2005).

Increased cAMP due to stimulation of adenylyl cyclase (AC) by forskolin or AC overexpression resulted in reduced phenoconversion of adult rat CFs to CMFs following stimulation with TGF-β or Ang II. This was measured as decreased collagen synthesis

and decreased expression of αSMA (Swaney et al., 2005). Increased levels of cAMP (by forskolin) reduced col1α1 mRNA expression and forskolin was also able to reverse contractile ability and decrease expression of αSMA and PAI in adult rat CFs (Lu et al., 2013).

The above studies related to cAMP activators are in stark contrast to our results, where we showed that stimulation of βARs and cAMP levels by ISO was able to increase expression of fibrotic and CMF marker mRNAs. However, our study used ISO which interacts with βARs whereas the studies mentioned above either overexpressed AC, or directly activated AC or PKA. This would stimulate signalling pathways downstream of βARs. It is possible that the cells may respond differently based on where in the signalling pathway activation occurs. In support of the importance of βAR activation in activating CMFs, an *in vitro* study using rats subjected to MI revealed that treatment with carvedilol decreased myocardial collagen content (Wei et al., 2000).

It is also possible that ISO-mediated CMF activation may be independent of cAMP levels. For instance ISO treatment in embryonic ventricular cells was shown to increase CDK1 expression via the nuclear factor-YA (NF-YA) transcription factor. Interestingly, the CDK1 promoter region lacks a cAMP response element but contains an NF-YA binding site (Gaspard et al., In Press). As well, treating adult ventricular CMFs with 5 μM ISO resulted in translocation of NF-YA and NF-YB from the cytoplasm to the nucleus (Pasumarthi lab, unpublished data). Recent studies in human rhabdomyosarcoma, and rat and mouse chondrocytes showed that NF-YA regulates collagen gene transcription (Brilla et al., 1994; Hida et al., 2013), and therefore could play a role in activating the transcription of other genes involved in fibrosis.

In the future it would be interesting to block NF-YA expression and examine levels of the mRNAs tested in this study to determine if NF-YA is able to modulate their expression.

4.12 *Npr1-/-* Cardiac Myofibroblasts show Increased Proliferation, ISO Only Increases Wild Type *Npr1* Cardiac Myofibroblast Proliferation

ANP is able to decrease DNA synthesis and proliferation in CFs (Cao & Gardner, 1995). In light of its antifibrotic effects, we opted to examine the growth of CMFs isolated from mice lacking the receptor for ANP, natriuretic peptide receptor A (*Npr1*). *Npr1-/-* mouse CMFs had increased proliferation compared with heterozygous or wild type CMFs (Figure 3.26). This supports the finding that ANP is anti-fibrotic, as a lack of the ANP receptor is associated with increased CMF proliferation.

Aside from a lack of ANP signalling leading to CMF proliferation, there are other pathways through which loss of NPR-A signalling may lead to increased proliferation. Mice lacking the NPR-A have increased levels of MMPs 2 and 9 (Potter et al., 2006). MMPs have been implicated in βAR stimulated DNA synthesis in CFs, and in particular MMP-13 was shown to activate PAR-1 leading to EGFR transactivation in neonatal rat CFs (Kim et al., 2002; Sabri et al., 2002). It is possible that increased levels of MMPs in *NPR1-/-* mice are resulting in increased transactivation of the EGFR, which could also contribute to their increased proliferation. Future studies on EGFR activation levels between *Npr1 -/-* and wild type CMFs will provide more mechanistic insight.

Treatment with ISO did not lead to a further increase in proliferation of CMFs derived from *Npr1 -/-* or +/- hearts. However, consistent with previous findings, ISO treatment significantly increased proliferation of CMFs from wild type hearts. βAR stimulated proliferation involves activation of the same MMP-PAR-1-EGFR pathway mentioned above (Kim et al., 2002; Sabri et al., 2002). If this pathway is already active in *Npr1-/-* CMFs due to increased expression of MMPs (Potter et al., 2006), it may explain the inability of ISO to increase proliferation of *Npr1 -/-* CMFs. The inability of ISO to increase proliferation in *Npr1* +/- CMFs could be due to receptor heterodimerization. GPCRs are well known to form heterodimers and this has been demonstrated in the heart where the β2AR complexes with the AT1 receptor (Barki-Harrington et al., 2003). It is possible that due to having only one copy of the *Npr1* gene the NPR-A receptor (which functions as a homodimer) heterodimerizes with the β2AR. This could interfere with normal β2AR signalling and prevent an ISO-induced increase in CMF proliferation.

4.13 Significance

This study has examined several aspects relating to CMF proliferation. The factors controlling CMF proliferation and activation are both complex and diverse, ranging from catecholamines to growth factors and hormones such as ANP. In order to properly treat cardiac fibrosis, it will be important to obtain a better understanding of these factors and how they interact with one another.

We have shown that catecholamine treatment increases CDK1 expression, DNA synthesis and proliferation in adult mouse CMFs *in vitro* and that inhibition of CDK1 is able to decrease CMF proliferation. Treatment with ISO is also able to modulate CMF gene expression. Finally, we demonstrated that *Npr1-/-* CMFs have increased proliferation compared with wild type and heterozygous cells.

One major limitation of this study is the fact that it was conducted in cultured CMFs. CMFs *in vivo* may respond differently to stimuli as they are growing in a 3D environment with a complete ECM and interactions with other types of cardiac cells. It would be interesting to conduct these experiments with a 3D matrix substrate for the cells to grow on and examine any differences in results. Despite this drawback, we still observed expression of the myofibroblast marker αSMA, indicating that our CMF cultures are similar to those observed in the heart.

The fact that the catecholamines ISO and NE increase CDK1 expression in CMFs suggests that this may be occurring *in vivo* in response to the increased sympathetic activation during heart failure. Inhibition of CDK1 may be a possible drug target for the treatment of cardiac fibrosis. It would be ideal to prevent excessive CMF proliferation thereby decreasing the size of the fibrotic scar. However, targeting CDK1 to fibroblasts in the infarct area may impair the healing process post injury, and proper healing of the wound is required to ensure the structural integrity of the heart. Another possibility would be targeting CDK1 levels during reactive fibrosis, which occurs in uninjured areas of the heart. Reactive fibrosis results in an increase in collagen deposition and perimysial strands condense in the interstitial space and is seen in cardiovascular diseases such as hypertension and cardiac hypertrophy (Doering et al., 1988; Jalil et al., 1988; Weber et

al., 1989). It is not associated with cardiomyocyte death, and therefore impairing CF proliferation in this case should not affect wound healing (Brown et al., 2005; Takeda & Manabe, 2011).

We recently reported that ISO increases CDK1 transcription through binding of the NF-Y transcription factor (Gaspard et al., In Press). Modulation of this process could also serve as a target for controlling CMF proliferation. The NF-Y transcription factor consists of three subunits, NF-YA, YB and YC. The NF-YA subunit is responsible for DNA binding (Liu et al., 1998) and given that we observed translocation of this subunit to the nucleus after ISO treatment (Pasumarthi lab, unpublished data), it is possible that blocking the NF-YA subunit may decrease transcription of the CDK1 gene in response to catecholamine stimulation and prevent the induced increase in CMF proliferation. As mentioned above, if NF-YA was targeted during reactive fibrosis, it should not impair wound healing as it is not related to cardiomyocyte necrosis.

Future studies should include blockade of NF-YA and subsequent assessment of CMF proliferation to determine the involvement of NF-Y in this process and confirm that it activates CDK1 transcription in adult CMFs. In addition, it would be important to elucidate the signalling pathway by which ISO stimulation leads to NF-Y activity. Activation of β1 and β2ARs increases levels of cAMP and subsequently PKA. It is possible that NF-Y may be activated in response to phosphorylation by PKA similar to the PKA activation of the transcription factors cAMP response element binding protein (CREB) and activating transcription factor-1 (ATF-1) (Liu et al., 1993; Meyer & Habener, 1993; Sheng et al., 1991). As well, it is possible that CDK1 regulation could be

independent of the cAMP-PKA pathway. Possible pathways for NF-Y mediated activation of CDK1 are highlighted in figure 4.1

Results from our work and other studies (Colombo et al., 2003; Kim et al., 2002; Leicht et al., 2000; Turner et al., 2003) indicate that ISO-mediated CF and CMF proliferation occurs due to activation of the β2AR. However, we have not shown if activation of CMF gene expression and CDK1 expression are β1 or β2AR dependent. It would be of interest to conduct future experiments investigating the status of the expression of these genes in the presence of β1 and β2-selective blockers.

Thus far studies conducted on CF proliferation suggest that the use of β2AR blockers or non-selective βAR blockers would be most useful for controlling cardiac fibrosis. Although inhibition of the β2AR was able to prevent an ISO-induced increase in CMF proliferation, the effects of blocking the β1AR also need further investigation. Many patients with asthma are at an increased risk for cardiovascular disease (Iribarren et al., 2012). Since use of βAR blockers in asthmatic patients leads to bronchoconstriction and exacerbation of their existing respiratory conditions, finding an effective β1AR blocker to control cardiac fibrosis and the underlying cardiovascular condition is highly desirable.

We have shown that lack of the *Npr1* receptor results in greatly increases CMF proliferation compared with wild type and heterozygous cells. This underscores the importance of ANP signalling in CMFs. Given that lack of this receptor increases CMF proliferation (Figure 3.27 A) and that treatment of CMFs with ANP decreases Ang II or ET-1 induced DNA synthesis (Fujisaki et al., 1995), ANP treatment may be useful in

modulating CMF proliferation. In addition, studying the mechanism of CMF proliferation in *Npr1*-/- cells could be useful in elucidating pathways that may be dysregulated in cardiac fibrosis.

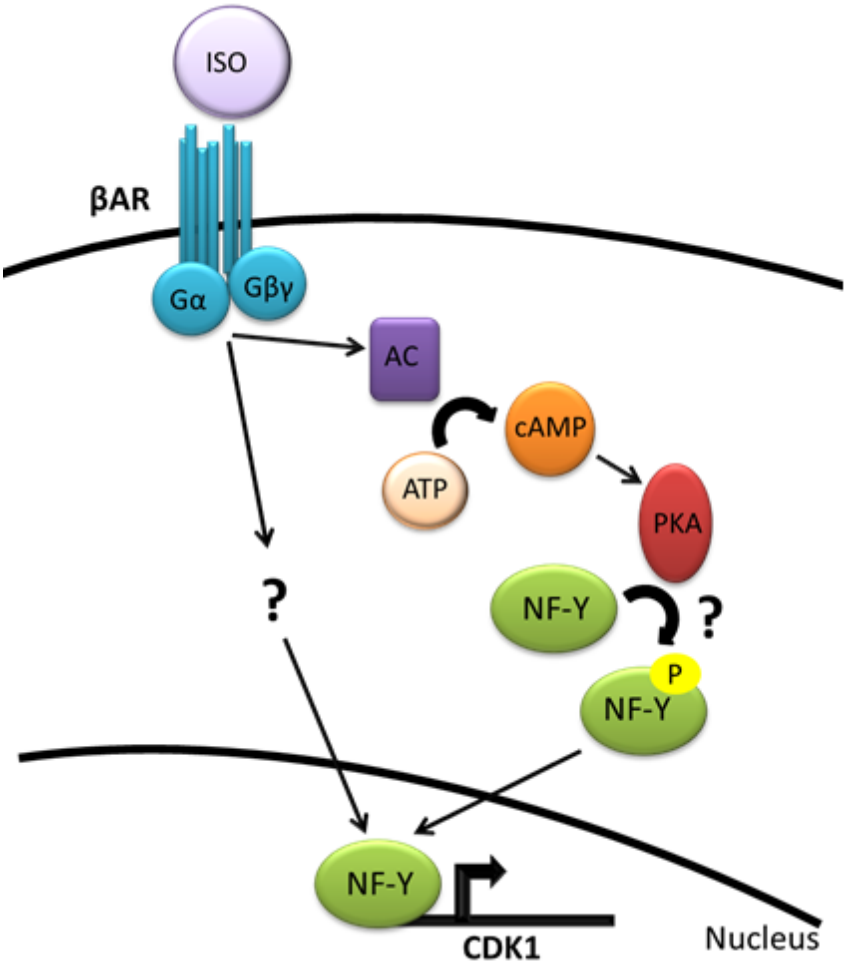

Figure 4.1: NF-Y mediated activation of CDK1. ISO activates a βAR (likely the β2AR) which we propose acts via adenylyl cyclase (AC) to increase intracellular levels of cAMP. This activates protein kinase A (PKA) which may in turn phosphorylate the nuclear factor-Y (NF-Y) transcription factor. NF-Y binds to the CDK1 promoter resulting in expression of CDK1 in CFs. It is also possible that activation of a βAR leads to activation of NF-Y independent of PKA.

References

Ahmed, M. S., Øie, E., Vinge, L. E., Yndestad, A., Øystein Andersen, G., Andersson, Y., … Attramadal, H. (2004). Connective tissue growth factor--a novel mediator of angiotensin II-stimulated cardiac fibroblast activation in heart failure in rats. *Journal of Molecular and Cellular Cardiology*, *36*(3), 393–404. doi:10.1016/j.yjmcc.2003.12.004

Banerjee, I., Fuseler, J. W., Price, R. L., Borg, T. K., & Baudino, T. A. (2007). Determination of cell types and numbers during cardiac development in the neonatal and adult rat and mouse. *Am J Physiol Heart Circ Physiol*, *293*(3), H1883–91.

Barki-Harrington, L., Luttrell, L., & Rockman, H. (2003). Dual inhibition of beta-adrenergic and angiotensin II receptors by a single antagonist: a functional role for receptor-receptor interaction in vivo. *Circulation*, *108*(13), 1611–1618.

Baudino, T. A., Carver, W., Giles, W., & Borg, T. K. (2006). Cardiac fibroblasts: friend or foe? *Am J Physiol Heart Circ Physiol*, *291*(3), H1015–26.

Beguin, P. C., Gosselin, H., Mamarbachi, M., & Calderone, A. (2011). Nestin expression is lost in ventricular fibroblasts during postnatal development of the rat heart and re-expressed in scar myofibroblasts. *J Cell Physiol*, *227*(2), 813–820.

Benjamin, I. J., Jalil, J. E., Tan, L. B., Cho, K., Weber, K. T., & Clark, W. a. (1989). Isoproterenol-induced myocardial fibrosis in relation to myocyte necrosis. *Circulation Research*, *65*(3), 657–670. doi:10.1161/01.RES.65.3.657

Benjamin, I. J., Jalil, J. E., Tan, L. B., Cho, K., Weber, K. T., Clark, W. A., & Anonymous. (1989). Isoproterenol-induced myocardial fibrosis in relation to myocyte necrosis. *Circulation Research*, *65*(3), 657–670.

Benson, S., Iguchi, R., Ho, C., Yamamoto, K., & Kurtz, T. (2008). Inhibition of cardiovascular cell proliferation by angiotensin receptor blockers: are all molecules the same? *Journal of Hypertension*, *26*(5), 973–980.

Berk, B. C., Fujiwara, K., Lehoux, S., & Anonymous. (2007). ECM remodeling in hypertensive heart disease. *The Journal of Clinical Investigation*, *117*(3), 568–575.

Bevan, J. (1978). Norepinephrine and the presynaptic control of adrenergic transmitter release. *Federation Proceedings*, *37*, 187–190.

Boluyt, M. O., Long, X., Eschenhagen, T., Mende, U., Schmitz, W., Crow, M. T., … Anonymous. (1995). Isoproterenol infusion induces alterations in expression of hypertrophy-associated genes in rat heart. *The American Journal of Physiology*, *269*(2 Pt 2), H638–47.

Bos, R., Mougenot, N., Me, O., Vanhoutte, P. M., & Lechat, P. (2004). Potassium Canrenoate , an Aldosterone Receptor Antagonist , Reduces Isoprenaline-Induced Cardiac Fibrosis in the Rat, *309*(3), 1160–1166. doi:10.1124/jpet.103.063388.The

Brilla, C. G., Funck, R. C., & Rupp, H. (2000). Lisinopril-Mediated Regression of Myocardial Fibrosis in Patients With Hypertensive Heart Disease. *Circulation*, *102*(12), 1388–1393. doi:10.1161/01.CIR.102.12.1388

Brilla, C. G. Zhou, Guoping, Matsubara, Luiz, W. K. . (1994). Collagen Metabolism in Cultured Adult Rat Cardiac Fibroblasts: Response to Angiotensin II and Aldosterone. *Journal of Molecular and Cellular Cardiology*, (26), 809–820.

Brouri, F., Hanoun, N., Mediani, O., Saurini, F., Hamon, M., Vanhoutte, P. M., … Anonymous. (2004). Blockade of beta 1- and desensitization of beta 2-adrenoceptors reduce isoprenaline-induced cardiac fibrosis. *European Journal of Pharmacology*, *485*(1-3), 227–234.

Brown, R. D., Ambler, S. K., Mitchell, M. D., & Long, C. S. (2005a). The cardiac fibroblast: therapeutic target in myocardial remodeling and failure. *Annu Rev Pharmacol Toxicol*, *45*, 657–687.

Brown, R. D., Ambler, S. K., Mitchell, M. D., & Long, C. S. (2005b). The cardiac fibroblast: therapeutic target in myocardial remodeling and failure. *Annu Rev Pharmacol Toxicol*, *45*, 657–687.

Brown, R. D., Ambler, S. K., Mitchell, M. D., & Long, C. S. (2005). The cardiac fibroblast: therapeutic target in myocardial remodeling and failure. *Annual Review of Pharmacology and Toxicology*, *45*(1), 657–87. doi:10.1146/annurev.pharmtox.45.120403.095802

Bujak, M., Dobaczewski, M., Chatila, K., Mendoza, L. H., Li, N., Reddy, A., & Frangogiannis, N. G. (2008). Interleukin-1 receptor type I signaling critically regulates infarct healing and cardiac remodeling. *Am J Pathol*, *173*(1), 57–67.

Calderone, A., Thaik, C. M., Takahashi, N., Chang, D. L., & Colucci, W. S. (1998). Nitric oxide, atrial natriuretic peptide, and cyclic GMP inhibit the growth-promoting effects of norepinephrine in cardiac myocytes and fibroblasts. *J Clin Invest*, *101*(4), 812–818.

Campbell, S. E., & Katwa, L. C. (1997). Angiotensin II stimulated expression of transforming growth factor-beta1 in cardiac fibroblasts and myofibroblasts. *Journal of Molecular and Cellular Cardiology*, *29*(7), 1947–58. doi:10.1006/jmcc.1997.0435

Cao, L., & Gardner, D. G. (1995). Natriuretic peptides inhibit DNA synthesis in cardiac fibroblasts. *Hypertension*, *25*(2), 227–234.

Carthy, J. M., Garmaroudi, F. S., Luo, Z., & McManus, B. M. (2011). Wnt3a induces myofibroblast differentiation by upregulating TGF-β signaling through SMAD2 in a β-catenin-dependent manner. *PloS One*, *6*(5), e19809. doi:10.1371/journal.pone.0019809

Chen, K., Li, D., Zhang, X., Hermonat, P., & Mehta, J. L. (2004). Anoxia-Reoxygenation Stimulates Collagen Type-I Modulation by the PPAR- g Ligand Pioglitazone. *Journal of Cardiovascular Pharmacology*, *44*(6), 682–687.

Chen, M. M., Lam, A., Abraham, J. A., Schreiner, G. F., & Joly, A. H. (2000). CTGF Expression is Induced by TGF- in Cardiac Fibroblasts and Cardiac Myocytes : a Potential Role in Heart Fibrosis, *1819*, 1805–1819. doi:10.1006/2000.1215

Chen, W., & Frangogiannis, N. G. (2013). Fibroblasts in post-infarction inflammation and cardiac repair. *Biochimica et Biophysica Acta*, *1833*(4), 945–53. doi:10.1016/j.bbamcr.2012.08.023

Chen, Y., & Mehta, J. (2006). Angiotensin II-mediated oxidative stress and procollagen-I expression in cardiac fibroblasts: blockade by pravastatin and pioglitazone. *American Journal of Physiology Heart and Circulatory Physiology*, (291), 1738–1745.

Chintalgattu, V., Harris, G. S., Akula, S. M., & Katwa, L. C. (2007). PPAR-gamma agonists induce the expression of VEGF and its receptors in cultured cardiac myofibroblasts. *Cardiovascular Research*, *74*(1), 140–50. doi:10.1016/j.cardiores.2007.01.010

Cohn, J., Levine, T., Olivari, M., Garberg, V., Lura, D., Francis, G., … Rector, T. (1984). Plasma norepinephrine as a guide to prognosis in patients with chronic congestive heart failure. *The New England Journal of Medicine*, *311*, 819–823.

Colombo, F., Gosselin, H., El-Helou, V., & Calderone, A. (2003). Beta-adrenergic receptor-mediated DNA synthesis in neonatal rat cardiac fibroblasts proceeds via a phosphatidylinositol 3-kinase dependent pathway refractory to the antiproliferative action of cyclic AMP. *J Cell Physiol*, *195*(2), 322–330.

Colombo, F., Noel, J., Mayers, P., Mercier, I., & Calderone, A. (2001). beta-Adrenergic stimulation of rat cardiac fibroblasts promotes protein synthesis via the activation of phosphatidylinositol 3-kinase. *J Mol Cell Cardiol*, *33*(6), 1091–1106.

Correa-meyer, E., Pesce, L., Guerrero, C., & Sznajder, J. I. (2002). Mechanotransduction in the Lung: Cyclic stretch activates ERK1/2 via G proteins and EGFR in alveolar epithelial cells. *American Journal of Physiology Lung Cellular and Molecular Physiology*, *282*, 883–891.

Cossu, G., & Bianco, P. (2003). Mesoangioblasts — vascular progenitors for extravascular mesodermal tissues. *Current Opinion in Genetics & Development*, *13*(5), 537–542. doi:10.1016/j.gde.2003.08.001

Crawford, D. C., Chobanian, a V, & Brecher, P. (1994). Angiotensin II induces fibronectin expression associated with cardiac fibrosis in the rat. *Circulation Research*, *74*(4), 727–39.

Cucoranu, I., Clempus, R., Dikalova, A., Phelan, P. J., Ariyan, S., Dikalov, S., & Sorescu, D. (2005). NAD(P)H oxidase 4 mediates transforming growth factor-beta1-induced differentiation of cardiac fibroblasts into myofibroblasts. *Circulation Research*, *97*(9), 900–7. doi:10.1161/01.RES.0000187457.24338.3D

Cunnington, R. H., Wang, B., Ghavami, S., Bathe, K. L., Rattan, S. G., & Dixon, I. M. C. (2011). Antifibrotic properties of c-Ski and its regulation of cardiac myofibroblast phenotype and contractility. *American Journal of physiology.Cell Physiology*, *300*(46), 176–186. doi:10.1152/ajpcell.00050.2010.

De Mello, W. C. De, & Specht, P. (2006). Chronic blockade of angiotensin II AT1 receptors increased cell-to-cell communication, reduced fibrosis and improved impulse propagation in the failing heart. *Journal of the Renin-Angiotensin-Aldosterone System : JRAAS*, *7*(4), 201–205.

Dean, R. G., Balding, L. C., Candido, R., Burns, W. C., Cao, Z., Twigg, S. M., … Anonymous. (2005). Connective tissue growth factor and cardiac fibrosis after myocardial infarction. *The Journal of Histochemistry and Cytochemistry : Official Journal of the Histochemistry Society*, *53*(10), 1245–1256.

Díez, J., López, B., González, a, & Querejeta, R. (2001). Clinical aspects of hypertensive myocardial fibrosis. *Current Opinion in Cardiology*, *16*(6), 328–35.

Diez, J., Lopez, B., Gonzalez, A., Querejeta, R., & Anonymous. (2001). Clinical aspects of hypertensive myocardial fibrosis. *Current Opinion in Cardiology*, *16*(6), 328–335.

Diez, J., Querejeta, R., Lopez, B., Gonzalez, A., Larman, M., Ubago, M. (2002). Losartan-Dependent Regression of Myocardial Fibrosis Is Associated With Reduction of Left Ventricular Chamber Stiffness in Hypertensive Patients. *Circulation*, *105*(21), 2512–2517. doi:10.1161/01.CIR.0000017264.66561.3D

Doering, C. W., Jalil, J. E., Janicki, J. S., Pick, R., Aghili, S., Abrahams, C., … Anonymous. (1988). Collagen network remodelling and diastolic stiffness of the rat left ventricle with pressure overload hypertrophy. *Cardiovascular Research*, *22*(10), 686–695.

Drapeau, J., El-Helou, V., Clement, R., Bel-Hadj, S., Gosselin, H., Trudeau, L. E., … Calderone, A. (2005). Nestin-expressing neural stem cells identified in the scar following myocardial infarction. *J Cell Physiol*, *204*(1), 51–62.

Ekholm, S. V, & Reed, S. I. (2000). Regulation of G(1) cyclin-dependent kinases in the mammalian cell cycle. *Current Opinion in Cell Biology*, *12*(6), 676–84.

Frangogiannis, N. G., Michael, L. H., & Entman, M. L. (2000). Myofibroblasts in reperfused myocardial infarcts express the embryonic form of smooth muscle myosin heavy chain (SMemb). *Cardiovascular Research*, *48*(1), 89–100.

Freed, D. H., Borowiec, A. M., Angelovska, T., & Dixon, I. M. (2003). Induction of protein synthesis in cardiac fibroblasts by cardiotrophin-1: integration of multiple signaling pathways. *Cardiovasc Res*, *60*(2), 365–375.

Freed, D. H., Cunnington, R. H., Dangerfield, A. L., Sutton, J. S., & Dixon, I. M. (2005). Emerging evidence for the role of cardiotrophin-1 in cardiac repair in the infarcted heart. *Cardiovasc Res*, *65*(4), 782–792.

Freed, D. H., Moon, M. C., Borowiec, A. M., Jones, S. C., Zahradka, P., & Dixon, I. M. (2003). Cardiotrophin-1: expression in experimental myocardial infarction and potential role in post-MI wound healing. *Mol Cell Biochem*, *254*(1-2), 247–256.

Fujisaki, H., Ito, H., Hirata, Y., Tanaka, M., Hata, M., Lin, M., … Hiroe, M. (1995). Natriuretic peptides inhibit angiotensin II-induced proliferation of rat cardiac fibroblasts by blocking endothelin-1 gene expression. *J Clin Invest*, *96*(2), 1059–1065.

Gaspard, G. J., Maclean, J., Rioux, D., & Pasumarthi, K. B. S. (2014). A Novel β-Adrenergic Response Element Regulates both Basal and Agonist Induced Expression of Cyclin Dependent Kinase 1 Gene in Cardiac Fibroblasts. *American Journal of Physiology. Cell Physiology*. doi:10.1152/ajpcell.00206.2013

Ghosh, A., & Vaughan, D. E. (2012). PAI-1 in Tissue Fibrosis. *Journal of Cellular Physiology*, *227*(2), 493–507. doi:10.1002/jcp.22783.PAI-1

Glenn, D. J., Rahmutula, D., Nishimoto, M., Liang, F., & Gardner, D. G. (2009a). Atrial natriuretic peptide suppresses endothelin gene expression and proliferation in cardiac fibroblasts through a GATA4-dependent mechanism. *Cardiovasc Res*, *84*(2), 209–217.

Glenn, D. J., Rahmutula, D., Nishimoto, M., Liang, F., & Gardner, D. G. (2009b). Atrial natriuretic peptide suppresses endothelin gene expression and proliferation in cardiac fibroblasts through a GATA4-dependent mechanism. *Cardiovasc Res*, *84*(2), 209–217.

Goldsmith, E. C., Hoffman, A., Morales, M. O., Potts, J. D., Price, R. L., McFadden, A., … Anonymous. (2004). Organization of fibroblasts in the heart. *Developmental Dynamics : An Official Publication of the American Association of Anatomists*, *230*(4), 787–794.

Goumans, M.-J., van Zonneveld, A. J., & ten Dijke, P. (2008). Transforming growth factor beta-induced endothelial-to-mesenchymal transition: a switch to cardiac fibrosis? *Trends in Cardiovascular Medicine*, *18*(8), 293–8. doi:10.1016/j.tcm.2009.01.001

Grimm, D., Huber, M., Jabusch, H. C., Shakibaei, M., Fredersdorf, S., Paul, M., … Kromer, E. P. (2001). Extracellular matrix proteins in cardiac fibroblasts derived from rat hearts with chronic pressure overload: effects of beta-receptor blockade. *J Mol Cell Cardiol*, *33*(3), 487–501.

Gustafsson, A. B., & Brunton, L. L. (2000). Beta-Adrenergic Stimulation of Rat Cardiac Fibroblasts Enhances Induction of Nitric-Oxide Synthase by Interleukin-1beta Via Message Stabilization. *Molecular Pharmacology*, *58*(6), 1470–1478.

Hafizi, S., Chester, A. H., & Yacoub, M. H. (1999). Inhibition of human cardiac fibroblast mitogenesis by blockade of mitogen-activated protein kinase and phosphatidylinositol 3-kinase. *Clin Exp Pharmacol Physiol*, *26*(7), 511–513.

Hafizi, S., Wharton, J., Chester, A. H., & Magdi, H. (2004). Profibrotic Effects of Endothelin-1 via the ET A Receptor in Cultured Human Cardiac Fibroblasts. *Cellular Physiology and Biochemistry*, *14*(4-6), 285–292.

Hao, G.-H., Niu, X.-L., Gao, D.-F., Wei, J., & Wang, N.-P. (2008). Agonists at PPAR-gamma suppress angiotensin II-induced production of plasminogen activator inhibitor-1 and extracellular matrix in rat cardiac fibroblasts. *British Journal of Pharmacology*, *153*(7), 1409–19. doi:10.1038/bjp.2008.21

Hattori, K., Kim, K. Y., Sporn, M. B., Karin, M., Roberts, A. B., Angel, P., & Lafyatis, R. (1990). Autoinduction of Transforming Growth Factor the AP-1 Complex Is Mediated by. *Molecular and Cellular Biology*, *10*(4), 1492–1497.

Haudek, S. B., Xia, Y., Huebener, P., Lee, J. M., Carlson, S., Crawford, J. R., … Entman, M. L. (2006). Bone marrow-derived fibroblast precursors mediate ischemic cardiomyopathy in mice. *Proceedings of the National Academy of Sciences of the United States of America*, *103*(48), 18284–9. doi:10.1073/pnas.0608799103

Hayashidani, S., Tsutsui, H., Shiomi, T., Suematsu, N., Kinugawa, S., Ide, T., Wen, J., & Takeshita, A. (2002). Fluvastatin, a 3-Hydroxy-3-Methylglutaryl Coenzyme A Reductase Inhibitor, Attenuates Left Ventricular Remodeling and Failure After Experimental Myocardial Infarction. *Circulation*, *105*(7), 868–873. doi:10.1161/hc0702.104164

Hida, M., Hamanaka, R., Okamoto, O., Yamashita, K., Sasaki, T., Yoshioka, H., & Matsuo, N. (2013). Nuclear factor Y (NF-Y) regulates the proximal promoter activity of the mouse collagen α1(XI) gene (Col11a1) in chondrocytes. *In Vitro Cellular & Developmental Biology. Animal*, *1*(Xi). doi:10.1007/s11626-013-9692-3

Hinz, B. (2010). The myofibroblast: paradigm for a mechanically active cell. *J Biomech*, *43*(1), 146–155.

Hinz, B., Mastrangelo, D., Iselin, C. E., Chaponnier, C., & Gabbiani, G. (2001). Mechanical tension controls granulation tissue contractile activity and myofibroblast differentiation. *The American Journal of Pathology*, *159*(3), 1009–20. doi:10.1016/S0002-9440(10)61776-2

Hinz, B., Phan, S. H., Thannickal, V. J., Galli, A., Bochaton-Piallat, M. L., & Gabbiani, G. (2007). The myofibroblast: one function, multiple origins. *Am J Pathol*, *170*(6), 1807–1816.

Hofman, C., Leitz, M., Oberdorf-Maass, S., Lohse, M., & Klotz, K. (2004). Comparative pharmacology of human Beta-adrenergic receptor subtypes. *Naunyn-Schmiedeberg's Archives of Pharmacology*, *369*(2), 151–159.

Hudon-David, F., Bouzeghrane, F., Couture, P., & Thibault, G. (2007). Thy-1 expression by cardiac fibroblasts: lack of association with myofibroblast contractile markers. *Journal of Molecular and Cellular Cardiology*, *42*(5), 991–1000. doi:10.1016/j.yjmcc.2007.02.009

Iaccarino, G., Dolber, P. C., Lefkowitz, R. J., & Koch, W. J. (1999). Bbeta-adrenergic receptor kinase-1 levels in catecholamine-induced myocardial hypertrophy: regulation by beta- but not alpha1-adrenergic stimulation. *Hypertension*, *33*(1 Pt 2), 396–401.

Ieda, M., Tsuchihashi, T., Ivey, K. N., Ross, R. S., Hong, T., Shaw, R. M., & Srivastava, D. (2010). Cardiac fibroblasts regulate myocardial proliferation through beta1 integrin signaling. *Developmental Cell*, *16*(2), 233–244. doi:10.1016/j.devcel.2008.12.007.Cardiac

Ihm, S.-H., Chang, K., Kim, H.-Y., Baek, S. H., Youn, H.-J., Seung, K.-B., & Kim, J.-H. (2010). Peroxisome proliferator-activated receptor-gamma activation attenuates cardiac fibrosis in type 2 diabetic rats: the effect of rosiglitazone on myocardial expression of receptor for advanced glycation end products and of connective tissue growth factor. *Basic Research in Cardiology*, *105*(3), 399–407. doi:10.1007/s00395-009-0071-x

Iribarren, C., Tolstykh, I. V, Miller, M. K., Sobel, E., & Eisner, M. D. (2012). Adult asthma and risk of coronary heart disease, cerebrovascular disease, and heart failure: a prospective study of 2 matched cohorts. *American Journal of Epidemiology*, *176*(11), 1014–24. doi:10.1093/aje/kws181

Jaffré, F., Friedman, A. E., Hu, Z., Mackman, N., & Blaxall, B. C. (2012). B-Adrenergic Receptor Stimulation Transactivates Protease-Activated Receptor 1 Via Matrix Metalloproteinase 13 in Cardiac Cells. *Circulation*, *125*(24), 2993–3003. doi:10.1161/CIRCULATIONAHA.111.066787

Jalil, J. E., Doering, C. W., Janicki, J. S., Pick, R., Clark, W. A., Abrahams, C., … Anonymous. (1988). Structural vs. contractile protein remodeling and myocardial stiffness in hypertrophied rat left ventricle. *Journal of Molecular and Cellular Cardiology*, *20*(12), 1179–1187.

Junker, J. P. E., Kratz, C., Tollbäck, A., & Kratz, G. (2008). Mechanical tension stimulates the transdifferentiation of fibroblasts into myofibroblasts in human burn scars. *Burns : Journal of the International Society for Burn Injuries*, *34*(7), 942–6. doi:10.1016/j.burns.2008.01.010

Kanekar, S., Hirozanne, T., Terracio, L., & Borg, T. K. (1998). Cardiac Fibroblasts : Form and Function. *Cardiovascular Pathology*, *8807*(10), 127–133.

Kania, G., Blyszczuk, P., Stein, S., Valaperti, A., Germano, D., Dirnhofer, S., … Eriksson, U. (2009). Heart-infiltrating prominin-1+/CD133+ progenitor cells represent the cellular source of transforming growth factor beta-mediated cardiac fibrosis in experimental autoimmune myocarditis. *Circulation Research*, *105*(5), 462–70. doi:10.1161/CIRCRESAHA.109.196287

Kawano, H., Do, Y. S., Kawano, Y., Starnes, V., Barr, M., Law, R. E., & Hsueh, W. A. (2000). Angiotensin II has multiple profibrotic effects in human cardiac fibroblasts. *Circulation*, *101*(10), 1130–1137.

Kelm, M., Schafer, S., Mingers, S., Heydthause, M., Vogt, M., Motz, W., & Strauer, B. (1996). Left ventricular mass is linked to cardiac noradrenaline in normotensive and hypertensive patients. *Journal of Hypertension*, *14*(11), 1357–1364.

Kim, J., Eckhart, A. D., Eguchi, S., & Koch, W. J. (2002). Beta-adrenergic receptor-mediated DNA synthesis in cardiac fibroblasts is dependent on transactivation of the epidermal growth factor receptor and subsequent activation of extracellular signal-regulated kinases. *J Biol Chem*, *277*(35), 32116–32123.

Krenning, G., Zeisberg, E. M., & Kalluri, R. (2010). The origin of fibroblasts and mechanism of cardiac fibrosis. *Journal of Cellular Physiology*, *225*(3), 631–7. doi:10.1002/jcp.22322

Kudej, R. K., Iwase, M., Uechi, M., Vatner, D. E., Oka, N., Ishikawa, Y., … Anonymous. (1997). Effects of chronic beta-adrenergic receptor stimulation in mice. *Journal of Molecular and Cellular Cardiology*, *29*(10), 2735–2746.

Kurogi, Y. (2003). Mesangial cell proliferation inhibitors for the treatment of proliferative glomerular disease. *Medicinal Research Reviews*, *23*(1), 15–31. doi:10.1002/med.10028

Kuruvilla L., Nair R R., Umashankar PR., Lal AV., K. C. (2007). Endocardial Endothelial Cells Stimulate Proliferation and Collagen Synthesis of Cardiac Fibroblasts. *Cell Biochemistry and Biophysics*, *47*(1), 65–72.

Laflamme, M. a, & Murry, C. E. (2011). Heart regeneration. *Nature*, *473*(7347), 326–35. doi:10.1038/nature10147

Lau, Y. H., Robinson, R. B., Rosen, M. R., & Bilezikian, J. P. (1980). Subclassification of beta-adrenergic receptors in cultured rat cardiac myoblasts and fibroblasts. *Circulation Research*, *47*(1), 41–48. doi:10.1161/01.RES.47.1.41

Leask, A. (2007). TGFbeta, cardiac fibroblasts, and the fibrotic response. *Cardiovascular Research*, *74*(2), 207–12. doi:10.1016/j.cardiores.2006.07.012

Leask, A. (2010). Potential therapeutic targets for cardiac fibrosis: TGFbeta, angiotensin, endothelin, CCN2, and PDGF, partners in fibroblast activation. *Circulation Research*, *106*(11), 1675–80. doi:10.1161/CIRCRESAHA.110.217737

Lee, a a, Dillmann, W. H., McCulloch, a D., & Villarreal, F. J. (1995). Angiotensin II stimulates the autocrine production of transforming growth factor-beta 1 in adult rat cardiac fibroblasts. *Journal of Molecular and Cellular Cardiology*, *27*(10), 2347–57.

Lefkowitz, R. J., Rockman, H. a., & Koch, W. J. (2000). Catecholamines, Cardiac -Adrenergic Receptors, and Heart Failure. *Circulation*, *101*(14), 1634–1637. doi:10.1161/01.CIR.101.14.1634

Leicht, M., Greipel, N., & Zimmer, H. (2000). Comitogenic effect of catecholamines on rat cardiac fibroblasts in culture. *Cardiovascular Research*, *48*(2), 274–284.

Li, J., Liu, N. F., & Wei, Q. (2008). Effect of rosiglitazone on cardiac fibroblast proliferation, nitric oxide production and connective tissue growth factor expression induced by advanced glycation end-products. *The Journal of International Medical Research*, *36*(2), 329–35.

Li, P., Wang, D., Lucas, J., Oparil, S., Xing, D., Cao, X., … Chen, Y.-F. (2008). Atrial natriuretic peptide inhibits transforming growth factor beta-induced Smad signaling and myofibroblast transformation in mouse cardiac fibroblasts. *Circulation Research*, *102*(2), 185–92. doi:10.1161/CIRCRESAHA.107.157677

Liu, F., Thompson, M., Wagner, S., Greenberg, M., & Green, M. (1993). Activating transcription factor-1 can mediate Ca(2+)- and cAMP-inducible transcriptional activation. *Journal of Biological Chemistry*, *268*, 6714–6720.

Liu, Q., Yan, H., Dawes, N. J., Lu, Y., Zhu, H., & Anonymous. (1998). Transcriptional activation of the p34cdc2 gene by cdc2 promoter binding factor/nuclear factor-Y in fetal rat ventricular myocytes. *Circulation Research*, *82*(2), 251–260.

Liu, S., Shi-wen, X., Kennedy, L., Pala, D., Chen, Y., Eastwood, M., … Leask, A. (2007). FAK Is Required for TGF beta-induced JNK Phosphorylation in Fibroblasts : Implications for Acquisition of a Matrix-remodeling Phenotype, *18*(June), 2169–2178. doi:10.1091/mbc.E06

Livak, K. J., & Schmittgen, T. D. (2001). Analysis of relative gene expression data using real-time quantitative PCR and the 2(-Delta Delta C(T)) Method. *Methods (San Diego, Calif.)*, *25*(4), 402–8. doi:10.1006/meth.2001.1262

Lohse, M. J., Engelhardt, S., & Eschenhagen, T. (2003). What is the role of beta-adrenergic signaling in heart failure? *Circulation Research*, *93*(10), 896–906. doi:10.1161/01.RES.0000102042.83024.CA

Lu, D., Aroonsakool, N., Yokoyama, U., Patel, H. H., & Insel, P. a. (2013). Increase in cellular cyclic AMP concentrations reverses the profibrogenic phenotype of cardiac myofibroblasts: a novel therapeutic approach for cardiac fibrosis. *Molecular Pharmacology*, *84*(6), 787–93. doi:10.1124/mol.113.087742

Makino, N., Sugano, M., Satoh, S., Oyama, J., & Maeda, T. (2006). Peroxisome proliferator-activated receptor-gamma ligands attenuate brain natriuretic peptide production and affect remodeling in cardiac fibroblasts in reoxygenation after hypoxia. *Cell Biochemistry and Biophysics*, *44*(1), 65–71. doi:10.1385/CBB:44:1:065

Malumbres, M., Pevarello, P., Barbacid, M., & Bischoff, J. R. (2008). CDK inhibitors in cancer therapy: what is next? *Trends in Pharmacological Sciences*, *29*(1), 16–21. doi:10.1016/j.tips.2007.10.012

McMurray, J. J. V, Adamopoulos, S., Anker, S. D., Auricchio, A., Böhm, M., Dickstein, K., … Zeiher, A. (2012). ESC Guidelines for the diagnosis and treatment of acute and chronic heart failure 2012: The Task Force for the Diagnosis and Treatment of Acute and Chronic Heart Failure 2012 of the European Society of Cardiology. Developed in collaboration with the Heart. *European Heart Journal*, *33*(14), 1787–847. doi:10.1093/eurheartj/ehs104

Means, C. K., & Brown, J. H. (2009). Sphingosine-1-phosphate receptor signalling in the heart. *Cardiovascular Research*, *82*(2), 193–200. doi:10.1093/cvr/cvp086

Meszaros, J. G., Gonzalez, A. M., Endo-mochizuki, Y., Villegas, S., Villarreal, F., Brunton, L. L., … Endo-, Y. (2000). Identification of G protein-coupled signaling pathways in cardiac fibroblasts : cross talk between G q and G s. *American Journal of physiology.Cell Physiology*, *278*(28), 154–162.

Mewton, N., Liu, C. Y., Croisille, P., Bluemke, D., & Lima, J. a C. (2011). Assessment of myocardial fibrosis with cardiovascular magnetic resonance. *Journal of the American College of Cardiology*, *57*(8), 891–903. doi:10.1016/j.jacc.2010.11.013

Meyer, T., & Habener, J. (1993). Cyclic adenosine 3’5'-monophosphate response element binding protein (CREB) and related transcription-activating deoxyribonucleic acid-binding proteins. *Endocrine Reviews*, *14*, 269–290.

Moorman, A. F. M., & Christoffels, V. M. (2003). Cardiac chamber formation: development, genes, and evolution. *Physiological Reviews*, *83*(4), 1223–67. doi:10.1152/physrev.00006.2003

Moreo, A., Ambrosio, G., De Chiara, B., Pu, M., Tran, T., Mauri, F., & Raman, S. V. (2009). Influence of myocardial fibrosis on left ventricular diastolic function: noninvasive assessment by cardiac magnetic resonance and echo. *Circ Cardiovasc Imaging*, *2*(6), 437–443.

Moriwaki, H., Stempien-Otero, A., Kremen, M., Cozen, A. E., & Dichek, D. a. (2004). Overexpression of urokinase by macrophages or deficiency of plasminogen activator inhibitor type 1 causes cardiac fibrosis in mice. *Circulation Research*, *95*(6), 637–44. doi:10.1161/01.RES.0000141427.61023.f4

Motte, S., McEntee, K., & Naeije, R. (2006). Endothelin receptor antagonists. *Pharmacology & Therapeutics*, *110*(3), 386–414. doi:10.1016/j.pharmthera.2005.08.012

New, D. C., & Wong, Y. H. (2007). Molecular mechanisms mediating the G protein-coupled receptor regulation of cell cycle progression. *Journal of Molecular Signaling*, *2*, 2. doi:10.1186/1750-2187-2-2

Norris, R. a, Borg, T. K., Butcher, J. T., Baudino, T. a, Banerjee, I., & Markwald, R. R. (2008). Neonatal and adult cardiovascular pathophysiological remodeling and repair: developmental role of periostin. *Annals of the New York Academy of Sciences*, *1123*, 30–40. doi:10.1196/annals.1420.005

Ogata, T., Miyauchi, T., Irukayama-Tomobe, Y., Takanashi, M., Goto, K., & Yamaguchi, I. (2004). The peroxisome proliferator-activated receptor alpha activator fenofibrate inhibits endothelin-1-induced cardiac fibroblast proliferation. *Journal of Cardiovascular Pharmacology*, *44 Suppl 1*(November), S279–82.

Ogata, T., Miyauchi, T., Sakai, S., Irukayama-Tomobe, Y., Goto, K., & Yamaguchi, I. (2002). Stimulation of peroxisome-proliferator-activated receptor alpha (PPAR alpha) attenuates cardiac fibrosis and endothelin-1 production in pressure-overloaded rat hearts. *Clin Sci (Lond)*, *103 Suppl* , 284S–288S.

Oliver, P. M., Fox, J. E., Kim, R., Rockman, H. a, Kim, H. S., Reddick, R. L., … Maeda, N. (1997). Hypertension, cardiac hypertrophy, and sudden death in mice lacking natriuretic peptide receptor A. *Proceedings of the National Academy of Sciences of the United States of America*, *94*(26), 14730–5.

Olson, E. R., Naugle, J. E., Zhang, X., Bomser, J. a, & Meszaros, J. G. (2005). Inhibition of cardiac fibroblast proliferation and myofibroblast differentiation by resveratrol. *American Journal of Physiology. Heart and Circulatory Physiology*, *288*(3), H1131–8. doi:10.1152/ajpheart.00763.2004

Palmer, J. N., Hartogensis, W. E., Patten, M., Fortuin, F. D., & Long, C. S. (1995). Interleukin-1 beta induces cardiac myocyte growth but inhibits cardiac fibroblast proliferation in culture. *J Clin Invest*, *95*(6), 2555–2564.

Piacentini, L., Gray, M., Honbo, N. Y., Chentoufi, J., Bergman, M., & Karliner, J. S. (2000). Endothelin-1 stimulates cardiac fibroblast proliferation through activation of protein kinase C. *Journal of Molecular and Cellular Cardiology*, *32*(4), 565–76. doi:10.1006/jmcc.2000.1109

Pick, R., Jalil, J. E., Janicki, J. S., & Weber, K. T. (1989). The fibrillar nature and structure of isoproterenol-induced myocardial fibrosis in the rat. *The American Journal of Pathology*, *134*(2), 365–371.

Porter, K. E., & Turner, N. a. (2009). Cardiac fibroblasts: at the heart of myocardial remodeling. *Pharmacology & Therapeutics*, *123*(2), 255–78. doi:10.1016/j.pharmthera.2009.05.002

Potter, L. R., Abbey-Hosch, S., & Dickey, D. M. (2006). Natriuretic peptides, their receptors, and cyclic guanosine monophosphate-dependent signaling functions. *Endocrine Reviews*, *27*(1), 47–72. doi:10.1210/er.2005-0014

Querejeta, R., Varo, N., Lopez, B., Larman, M., Artinano, E., Etayo, J. C., … Diez, J. (2000). Serum Carboxy-Terminal Propeptide of Procollagen Type I Is a Marker of Myocardial Fibrosis in Hypertensive Heart Disease. *Circulation*, *101*(14), 1729–1735. doi:10.1161/01.CIR.101.14.1729

Rosin, N. L., Falkenham, A., Sopel, M. J., Lee, T. D. G., & Légaré, J.-F. (2013). Regulation and role of connective tissue growth factor in AngII-induced myocardial fibrosis. *The American Journal of Pathology*, *182*(3), 714–26. doi:10.1016/j.ajpath.2012.11.014

Sabri, A., Short, J., J, G., & Steinberg, S. (2002). Protease-Activated Receptor-1-Mediated DNA Synthesis in Cardiac Fibroblast Is via Epidermal Growth Factor Receptor Transactivation: Distinct PAR-1 Signaling Pathways in Cardiac Fibroblasts and Cardiomyocytes. *Circulation Research*, *91*(6), 532–539. doi:10.1161/01.RES.0000035242.96310.45

Sadoshima, J., & Izumo, S. (1993). Molecular characterization of angiotensin II--induced hypertrophy of cardiac myocytes and hyperplasia of cardiac fibroblasts. Critical role of the AT1 receptor subtype. *Circ Res*, *73*(3), 413–423.

Samuel, C. S., Unemori, E. N., Mookerjee, I., Bathgate, R. a D., Layfield, S. L., Mak, J., … Du, X.-J. (2004). Relaxin modulates cardiac fibroblast proliferation, differentiation, and collagen production and reverses cardiac fibrosis in vivo. *Endocrinology*, *145*(9), 4125–33. doi:10.1210/en.2004-0209

Santiago, J.-J., Dangerfield, A. L., Rattan, S. G., Bathe, K. L., Cunnington, R. H., Raizman, J. E., … Dixon, I. M. C. (2010). Cardiac fibroblast to myofibroblast differentiation in vivo and in vitro: expression of focal adhesion components in neonatal and adult rat ventricular myofibroblasts. *Developmental Dynamics : An Official Publication of the American Association of Anatomists*, *239*(6), 1573–84. doi:10.1002/dvdy.22280

Santibañez, J. F., Quintanilla, M., & Bernabeu, C. (2011). TGF-β/TGF-β receptor system and its role in physiological and pathological conditions. *Clinical Science (London, England : 1979)*, *121*(6), 233–51. doi:10.1042/CS20110086

Satyanarayana, a, & Kaldis, P. (2009). Mammalian cell-cycle regulation: several Cdks, numerous cyclins and diverse compensatory mechanisms. *Oncogene*, *28*(33), 2925–39. doi:10.1038/onc.2009.170

Schlaich, M. P., Kaye, D. M., Lambert, E., Sommerville, M., Socratous, F., & Esler, M. D. (2003). Relation between cardiac sympathetic activity and hypertensive left ventricular hypertrophy. *Circulation*, *108*(5), 560–5. doi:10.1161/01.CIR.0000081775.72651.B6

Scobioala, S., Klocke, R., Kuhlmann, M., Tian, W., Hasib, L., Milting, H., … Nikol, S. (2008). Up-regulation of nestin in the infarcted myocardium potentially indicates differentiation of resident cardiac stem cells into various lineages including cardiomyocytes. *Faseb J*, *22*(4), 1021–1031.

Senderowicz, a M. (1999). Flavopiridol: the first cyclin-dependent kinase inhibitor in human clinical trials. *Investigational New Drugs*, *17*(3), 313–20.

Senderowicz, A. M. (2002). The Cell Cycle as a Target for Cancer Therapy : Basic and Clinical Findings with the Small Molecule. *The Oncologist*, *7*(Suppl 3), 12–19. doi:10.1634/theoncologist.7-suppl

Serini, G., Bochaton-Piallat, M. L., Ropraz, P., Geinoz, a, Borsi, L., Zardi, L., & Gabbiani, G. (1998). The fibronectin domain ED-A is crucial for myofibroblastic phenotype induction by transforming growth factor-beta1. *The Journal of Cell Biology*, *142*(3), 873–81.

Shankland, S. J., & Wolf, G. (2000). Cell cycle regulatory proteins in renal disease: role in hypertrophy, proliferation, and apoptosis. *American Journal of Physiology: Renal Physiology*, *278*, F515–F529.

SHeng, M., Thompson, M., & Greenberg, M. (1991). CREB: a Ca(2+)-regulated transcription factor phosphorylated by calmodulin-dependent kinases. *Science*, *252*, 1427–1430.

Shi, Y., Li, D., Tardif, J.-C., & Nattel, S. (2002). Enalapril effects on atrial remodeling and atrial fibrillation in experimental congestive heart failure. *Cardiovascular Research*, *54*(2), 456–61.

Shiojima, I., Aikawa, M., Suzuki, J., Yazaki, Y., & Nagai, R. (1999). Embryonic Smooth Muscle Myosin Heavy Chain SMemb is Expressed in Pressure-Overloaded Cardiac Fibroblasts. *Japanese Heart Journal*, *40*(6), 803–818.

Shi-wen, X., Parapuram, S. K., Pala, D., Chen, Y., Carter, D. E., Eastwood, M., … Leask, A. (2009). Requirement of transforming growth factor beta-activated kinase 1 for transforming growth factor beta-induced alpha-smooth muscle actin expression and extracellular matrix contraction in fibroblasts. *Arthritis and Rheumatism*, *60*(1), 234–41. doi:10.1002/art.24223

Simm, a, Nestler, M., & Hoppe, V. (1997). PDGF-AA, a potent mitogen for cardiac fibroblasts from adult rats. *Journal of Molecular and Cellular Cardiology*, *29*(1), 357–68. doi:10.1006/jmcc.1996.0280

Sopel, M. J., Rosin, N. L., Lee, T. D. G., & Légaré, J.-F. (2011). Myocardial fibrosis in response to Angiotensin II is preceded by the recruitment of mesenchymal progenitor cells. *Laboratory Investigation; a Journal of Technical Methods and Pathology*, *91*(4), 565–78. doi:10.1038/labinvest.2010.190

Souders, C. A., Bowers, S. L., & Baudino, T. A. (2009). Cardiac fibroblast: the renaissance cell. *Circ Res*, *105*(12), 1164–1176.

Sun, Y., Zhang, J. Q., Zhang, J., & Lamparter, S. (2000). Cardiac remodeling by fibrous tissue after infarction in rats. *The Journal of Laboratory and Clinical Medicine*, *135*(4), 316–23. doi:10.1067/mlc.2000.105971

Swaney, J. S., Roth, D. M., Olson, E. R., Naugle, J. E., Meszaros, J. G., & Insel, P. a. (2005). Inhibition of cardiac myofibroblast formation and collagen synthesis by activation and overexpression of adenylyl cyclase. *Proceedings of the National Academy of Sciences of the United States of America*, *102*(2), 437–42. doi:10.1073/pnas.0408704102

Takeda, N., & Manabe, I. (2011). Cellular Interplay between Cardiomyocytes and Nonmyocytes in Cardiac Remodeling. *Int J Inflam*, *Epub*, 535241.

Takeshita, K., Hayashi, M., Iino, S., Kondo, T., Inden, Y., Iwase, M., … Yamamoto, K. (2004). Increased expression of plasminogen activator inhibitor-1 in cardiomyocytes contributes to cardiac fibrosis after myocardial infarction. *The American Journal of Pathology*, *164*(2), 449–56. doi:10.1016/S0002-9440(10)63135-5

Tamura, N., Ogawa, Y., Chusho, H., Nakamura, K., Nakao, K., Suda, M., … Katsuki, M. (2000). Cardiac fibrosis in mice lacking brain natriuretic peptide. *Proc Natl Acad Sci U S A*, *97*(8), 4239–4244.

Teunissen, B. E., Smeets, P. J., Willemsen, P. H., De Windt, L. J., Van der Vusse, G. J., & Van Bilsen, M. (2007). Activation of PPARdelta inhibits cardiac fibroblast proliferation and the transdifferentiation into myofibroblasts. *Cardiovasc Res*, *75*(3), 519–529.

Tomasek, J. J., Gabbiani, G., Hinz, B., Chaponnier, C., & Brown, R. a. (2002). Myofibroblasts and mechano-regulation of connective tissue remodelling. *Nature Reviews. Molecular Cell Biology*, *3*(5), 349–63. doi:10.1038/nrm809

Tsuruda, T., Jougasaki, M., Boerrigter, G., Huntley, B. K., Chen, H. H., D'Assoro, A. B., … Burnett Jr., J. C. (2002). Cardiotrophin-1 stimulation of cardiac fibroblast growth: roles for glycoprotein 130/leukemia inhibitory factor receptor and the endothelin type A receptor. *Circ Res*, *90*(2), 128–134.

Turner, N. a, O'regan, D. J., Ball, S. G., & Porter, K. E. (2004). Endothelin-1 is an essential co-factor for beta2-adrenergic receptor-induced proliferation of human cardiac fibroblasts. *FEBS Letters*, *576*(1-2), 156–60. doi:10.1016/j.febslet.2004.08.080

Turner, N. A., Porter, K. E., Smith, W. H., White, H. L., Ball, S. G., & Balmforth, A. J. (2003). Chronic beta2-adrenergic receptor stimulation increases proliferation of human cardiac fibroblasts via an autocrine mechanism. *Cardiovasc Res*, *57*(3), 784–792.

Ungerer, M., Bohm, M., Elce, J. S., Erdmann, E., & Lohse, M. J. (1993). Altered expression of beta-adrenergic receptor kinase and beta 1- adrenergic receptors in the failing human heart. *Circulation*, *87*(2), 454–463. doi:10.1161/01.CIR.87.2.454

Van Amerongen, M. J., Harmsen, M. C., van Rooijen, N., Petersen, A. H., & van Luyn, M. J. a. (2007). Macrophage depletion impairs wound healing and increases left ventricular remodeling after myocardial injury in mice. *The American Journal of Pathology*, *170*(3), 818–29. doi:10.2353/ajpath.2007.060547

Van Amerongen, MJ, Bou-Gharios, G, Popa, ER, van Ark, J, Petersen, AH, van Dma, GM, van Luyn MJA, H. M. (2008). Bone marrow-derived myofibroblasts contribute functionally to scar formation after myocardial infarction. *The Journal of Pathology*, *214*(3), 377–386.

Vassilev, L. T., Tovar, C., Chen, S., Knezevic, D., Zhao, X., Sun, H., … Chen, L. (2006). Selective small-molecule inhibitor reveals critical mitotic functions of human CDK1. *Proc Natl Acad Sci U S A*, *103*(28), 10660–10665.

Wang, J., Chen, H., Seth, a, & McCulloch, C. a. (2003). Mechanical force regulation of myofibroblast differentiation in cardiac fibroblasts. *American Journal of Physiology. Heart and Circulatory Physiology*, *285*(5), H1871–81. doi:10.1152/ajpheart.00387.2003

Wayman, N. S., Ellis, B. L., & Thiemermann, C. (2002). Ligands of the peroxisome proliferator-activated receptor-PPAR-a reduce myocardial infarct size. *Med Sci Monit*, *8*(7), BR243–7.

Weber, K. T., Pick, R., Jalil, J. E., Janicki, J. S., Carroll, E. P., & Anonymous. (1989). Patterns of myocardial fibrosis. *Journal of Molecular and Cellular Cardiology*, *21 Suppl 5*, 121–131.

Wei, S., Chow, L. T., & Sanderson, J. E. (2000). Effect of carvedilol in comparison with metoprolol on myocardial collagen postinfarction. *Journal of the American College of Cardiology*, *36*(1), 276–81.

Weisberg, A. D., Albornoz, F., Griffin, J. P., Crandall, D. L., Elokdah, H., Fogo, A. B., … Brown, N. J. (2005). Pharmacological inhibition and genetic deficiency of plasminogen activator inhibitor-1 attenuates angiotensin II/salt-induced aortic remodeling. *Arteriosclerosis, Thrombosis, and Vascular Biology*, *25*(2), 365–71. doi:10.1161/01.ATV.0000152356.85791.52

Widyantoro, B., Emoto, N., Nakayama, K., Anggrahini, D. W., Adiarto, S., Iwasa, N., … Hirata, K.-I. (2010). Endothelial cell-derived endothelin-1 promotes cardiac fibrosis in diabetic hearts through stimulation of endothelial-to-mesenchymal transition. *Circulation*, *121*(22), 2407–18. doi:10.1161/CIRCULATIONAHA.110.938217

Yu, C. M., Tipoe, G. L., Wing-Hon Lai, K., & Lau, C. P. (2001). Effects of combination of angiotensin-converting enzyme inhibitor and angiotensin receptor antagonist on inflammatory cellular infiltration and myocardial interstitial fibrosis after acute myocardial infarction. *Journal of the American College of Cardiology*, *38*(4), 1207–15.

Zeisberg, E. M., Tarnavski, O., Zeisberg, M., Dorfman, A. L., McMullen, J. R., Gustafsson, E., … Kalluri, R. (2007). Endothelial-to-mesenchymal transition contributes to cardiac fibrosis. *Nature Medicine*, *13*(8), 952–61. doi:10.1038/nm1613

Zeng, T., Yamamoto, H., Bowen, E., Broverman, R. L., Nguyen, K. H., & Humphreys-Beher, M. G. (1996). Cell cycle control in isoproterenol-induced murine salivary acinar cell proliferation. *Comp Biochem Physiol C Pharmacol Toxicol Endocrinol*, *115*(3), 271–279.

Zile, M. R., & Baicu, C. F. (2013). Biomarkers of diastolic dysfunction and myocardial fibrosis: application to heart failure with a preserved ejection fraction. *Journal of Cardiovascular Translational Research*, *6*(4), 501–15. doi:10.1007/s12265-013-9472-1

Zou, Y., Komuro, I., Yamazaki, T., Kudoh, S., Aikawa, R., Zhu, W., … Yazaki, Y. (1998). Cell type-specific angiotensin II-evoked signal transduction pathways: critical roles of Gbetagamma subunit, Src family, and Ras in cardiac fibroblasts. *Circ Res*, *82*(3), 337–345.